UNIVERSITY OF KWAZULU-NATAL

SPATIAL MODELING AND DYNAMICS OF A PHOTOVOLTAIC GENERATOR FOR RENEWABLE ENERGY APPLICATION

by

Mashood Mobolaji Bello
B.Eng. (Hons) Electrical

Submitted in fulfillment of the academic requirements for the degree of Master of Science in Engineering in the School of Electrical, Electronic and Computer Engineering, University of KwaZulu-Natal, Durban, South Africa

Dr. Innocent Davidson (Supervisor)

April, 2006

I hereby declare that all the material incorporated into this thesis is my own original unaided work except where specific reference is made by name or in the form of a numbered reference. The work contained herein has not been submitted for a degree at any other University.

Signed: 

M.M. Bello

As the candidate's Supervisor I have approved this thesis for submission.

Signature:	Name:	Date:
	DR. T. E. DAVIDSON.	13th April 2006.

To GOD.

ACKNOWLEDGMENTS

I am greatly indebted to my thesis advisor, Dr. Innocent E. Davidson for introducing me to the field of distributed generation and for his guidance and mentoring throughout my time with the Electric Power Engineering Research Group. Dr. Davidson always gave me time to discuss ideas and help resolve problems. The strength of this thesis is due to his insight and patience. Throughout the year, he has been patiently monitoring my progress and guided me in the right direction and offering encouragement. He has also supported me both morally and financially. Obviously the progress I had now will be uncertain without his assistance. His emphasis on the importance of writing technical papers and gaining practical experience as a student will greatly enhance my skill as a practicing engineer.

I would like to thank all of the other lecturers in the power group for providing such a great opportunity to the students to learn the field of power engineering in general. I also want to thank Mrs. Beverly Bennett who has ensured that my Research grants are paid well on time. A big thank you also goes to Mr. Bruce Harrison, who has promptly provided IT support. My special appreciation and thanks to my fellow office mates at the Motion Control lab; Messrs Sen Wang, Benn Lance, James Ireland and Rao Singupuram. They made the time I spent there fun and memorable. I would like to thank the following list of students for their insight and friendship: Ogundare Olukoyejo, Ugendrin Govender, Rudy Pillay, Jayesh Pillay, Oludare Sokoya, Feyi Adeoye, Clement Nyirenda, Mukesh Bisram, Narisha Harilal and Vilemseni Zikhali, and many other whose names are not listed, as you all contributed to my experience working in the School of Electrical, Electronic and Computer Engineering.

I am infinitely grateful to my parents for all of their unfailing encouragement, financial support and love given me over the years. They have been behind me throughout my extended academic career. All of my successes have been a result of their guidance throughout my life. My sincere gratitude also goes to my brothers Tunde and Kolawole; my sisters Adenike and Mopelola. They provided crucial suggestions and critical analysis in the home stretch, when I needed it the most. I love you. Thank you! The effort of my niece, Oluwatoyin is also appreciated.
I also wish to thank Oladayo Salami for all of her constant encouragement, love and support, during my time at UKZN. Finally, and most importantly I wish to thank God for guiding me through and giving me the strength to write this thesis.

ABSTRACT

Photovoltaic systems alongside energy storage systems are a recognized distributed generation (DG) technology deployed in stand-alone and grid connected system for urban and rural applications. DG system ranging in size from a few kilowatts up to 50 MW refers to a variety of small, modular power-generating technologies connected to the electric grid, and combined with energy management and storage systems to improve the operation of electricity delivery systems. DG provides solutions to two long standing problems of power system operation: non-availability at all times of sufficient power generation to meet peak demands and the lack of capacity of existing transmission lines to carry all the electricity needed by consumers. Installing DG at or near a customer load can eliminate the need to upgrade existing transmission/distribution networks to handle the extra power requirement. Since these distributed energy systems are inertia-less and possess large time constants (response times), there are significant interactions between these systems, the power converters and the distribution networks. This precipitates new dynamics and control limitations, which are unknown in the conventional electric power distribution networks. To perform effective load scheduling, high performance control and optimal operation of these energy systems require an understanding of the dynamic and steady state characteristics of the DG system. This thesis report presents a mathematical model for a Photovoltaic (PVG) generator system, including the energy-storage system. Laboratory test results for steady state performance analysis using various loads are presented and discussed. It concludes with a fundamental economic evaluation of system.

TABLE OF CONTENTS

LIST OF FIGURES

LIST OF TABLES

LIST OF ABBREVIATIONS

American Society of Testing Materials	(ASTM)
Annual Cost	(AC)
Artificial intelligence	(AI)
Balance of System	(BOS)
Combined cycle gas turbine	(CCGT)
Combined Heat and Power	(CHP)
Demand side management	(DSM)
Depth of discharge	(DOD)
Digital Visual Fortran	(DVF)
Direct Current	(DC)
Distributed Generators	(DG)
Electricity Supply Industry	(ESI)
ElectroMotiveForce	(EMF)
Fill factor	(FF)
FORmula TRANslator	(FORTRAN)
Green House Gas	(GHG)
Initial Cost	(IC)
Insulated Gate Bipolar Transistors	(IGBTs)
Internal Combustion Engines	(ICE)
Kilowatt	(KW)
Lead	(Pb)
Life Cycle Analysis	(LCA)
Life cycle costs	(LCC)
matrix laboratory	MATLAB®
Maximum Power Point	(MPP)
Maximum Power Point Tracker	(MPPT)
Metal Oxide Semiconductor Field effect Transistors	(MOSFETs)
Minimum Peak Power	(Pmpp min)
Open Circuit Voltage	(Voc)
Operating and maintenance	(O&M)
Peak power	(Pmpp)
Peak Power Voltage	(Vmpp)

Pebble bed Modular Reactor	(PMR)
Photovoltaic	(PV)
Poly Vinyl Chloride	(PVC)
Present worth	(PW)
Pulse Width Modulation	(PWM)
Revolutions per minute	(RPM)
Standalone Power Systems	(SPS)
Standard Test Conditions	(STC)
State of charge	(SOC)
Watts	(W)
Year	(yr)

LIST OF SYMBOLS

C_n	Battery capacity
I_L	Photovoltaic current across the junction
R_s	Cell series resistance
R_{SH}	Shunt resistance
k	Boltzman constant
k_o	Coefficient of the exponential
e	Electronic charge
A	Completion factor
T	Absolute temperature
I_o	Cell reverse saturation current
I_o	Diode saturation current
I_{sc}	Module short circuit current
I_{mpp}	Module maximum power current
I	Module current
G (Wm^2)	Irradiance
P	Cell output power
$f(S)$	Irradiance probability density function
S	Total tilt insolation
S_{ref}	Reference insolation
α	Current change temperature coefficient at reference insolation
E_g	Energy band gap
L	Thickness of the cell
$G(x)$	Generation rate of charge carriers at a point x
q	Electron charge= $1\text{-}602 \times 10^{-19} C$
J	Current density
φ	Intensity of light,
N	Number of photons
ξ	Photon energy
h	Planck's constant = $6\text{-}625 \times 10^{-34} Js$
c	Velocity of light $2\text{-}99 \times 10^{8}$ m/s

$N(\lambda)$	Number of incident photons
$\alpha(\lambda)$	Average absorption coefficient =4-5 x $10^{-3}cm^{-1}$
$R(\lambda)$	Reflection coefficient ≈ 0-313(average)
ω	Angular frequency
η	Efficiency
f_S	Switching frequency
T_S.	Period
Φ_i	Angular frequency
SO_x	Sulphur oxide
NO_x	Nitrogen Oxide
CO_2	Carbon dioxide
CH_4	Methane

CHAPTER ONE

INTRODUCTION

1.1 Background

The generation of electricity, historically in the regulated environment, was driven by the economies of scale, using generating plants as large as possible to reduce the cost per unit of output. In the past 20 years, several driving forces such as deregulation, have contributed to the reversal of this trend and stimulated interest in decentralized power generation. Technological advances, such as the combined cycle gas turbine (CCGT), have made possible the efficient production of electricity on a much smaller scale at marginal generation costs lower than those of the traditional large power plants. Utility industry restructuring has brought increased competition. Costs and reliability concerns associated with large power plants have made them even less appealing. Furthermore, increased customer awareness and new societal trends toward "green" generating technologies, have promoted an interest in cleaner, sustainable generators that may be safely installed in the distribution system [1].

The distributed generators are defined as small, modular electric energy generators or storage systems located relatively close to the customer. Distributed generators (DG) span a variety of operating technologies and sizes, ranging from several kW to hundreds of MW [1]. Distributed resources include DGs, pumped storage schemes, electricity storage technologies like superconducting coils and chemical storage systems. Distributed generation includes conventional technologies, such as electromechanical energy converters, powered by natural gas or diesel fuel, or from renewable technologies, such as solar photovoltaic cells. They may be interconnected with a grid, or operate in "stand alone" mode. Conventional DG technologies, dependent on the fuel supply, include industrial gas turbines, gas-fired reciprocating turbines (also called internal combustion engines), micro turbines, and fuel cells [1].

Over the past two decades, declines in the costs of small-scale electricity generation, increases in the reliability needs of many customers, and the partial deregulation of electricity markets have made distributed generation more attractive to businesses and households as a supplement to utility-supplied electric power. Distributed generation, the small-scale production of electricity at or near customers' homes and businesses, has the

potential to improve the reliability of the power supply, reduce the cost of electricity, and lower emissions of air pollutants. DG provides improved reactive power and system voltage control and also reduces system losses [2]. The high prices of electricity in sub-Saharan Africa and problems associated with emissions from older power plants have stimulated interest in alternatives to traditional electric utility-supplied electricity hence distributed generation is expected to provide significant benefits and alternatives in a number of these areas.

Renewable DG technologies include photovoltaic (PV) generators, wind generators, biomass, ocean waves, tidal flows and small hydro turbines. The operating principles for all these technologies have been known for quite some time, but only recent technology breakthroughs have made them interesting as conventional energy generators. They may allow renewable generators to be used more effectively, while also reducing the spinning reserve requirements or effectively creating avoided capacity in the bulk power market, which may be useful when the prices are high [1].

The internal combustion engine is the workhorse of the electric power industry and smaller installations maybe used for DG. They are readily available in a wide range of sizes, with proven reliability and competitive price to performance ratio. However, as they are fueled by natural gas or diesel, they face increased environmental concerns when placed in the distribution system. Table 1-1[3, 4, 5] shows examples of power conversion technologies.

Table 1-1: Power Conversion Technologies.

Item	Description
1.	Coal fired steam plant
2.	Oil fired steam plant
3.	Combined cycle gas turbine (CCGT)
4.	Micro combined heat and power
5.	Hydropower
6.	Micro hydro
7.	Hydro pumped storage
8.	Tidal power
9.	Conventional nuclear (AGR and PWR)
10.	Pebble bed Modular Reactor (PMR)
11.	Onshore and Offshore wind
12.	Land-fill gases
13.	Municipal incineration
14.	Biomass (waste organic matter)
15.	Diesel (Standby engine driven generator sets)
16.	Photovoltaic
17.	Electrochemical storage
18.	Hydrogen Fusion

1.2 Motivation

Across the world, in sub-Saharan Africa and in South Africa, the demand of electricity for commercial, industrial and domestic loads in rural, semi-urban and urban areas has grown tremendously over the years. These loads and settlements require more efficient load control and energy management techniques to minimize energy costs. With the global trend of liberalization of the electricity supply industry (ESI), new approaches to electricity delivery and demand side management (DSM) need to be investigated to satisfy customer demand for localized control of energy services (for domestic purposes e.g. heating, cooling, drying, etc.) in an efficient and environmentally friendly manner.

Electric power can be generated from a number of primary resources, such as solar, wind, nuclear and water (hydro). These energy resources are able to supply the electricity needs of homes, communities reliably when accessed and designed correctly. Renewable technologies offer a free and clean source of long-term power. Demand for the use of renewable technologies is increasing as costs decrease, system efficiency increase and environmental impacts are brought into consideration [5]. However, one of the suggested energy systems for such communities in South Africa is the photovoltaic generator energy system (PV). The purpose of this research investigation is to carry out a performance analysis of the PV system and to determine its dynamics under different steady state operating (load) conditions. A detailed mathematical model of the system was carried out using different analytical tools (MATLAB, Digital Visual Fortran and C++). The simulation results were compared to practical measurements and the results are presented and discussed.

1.3 Objectives

The objectives of this research investigation are the following;

- Modeling of a micro PV-Generating System and load,
- Mathematical Modeling a single- machine and load system,
- Steady state performance analysis,
- Time and Spatial Modeling of PV Generator,
- Determination of reduced order models that are adequate for system control studies and steady-state scheduling,
- Economic evaluation of the system.

1.4 Literature Review

A number of authors have discussed various aspects of the steady-state performance of PV systems. Bernhard Michael Jatzeck [6] examined the application of the Luus-Jaakola direct search method to the optimization of stand-alone hybrid energy systems consisting of wind turbine generators, photovoltaic (W) modules, batteries and an auxiliary generator. The loads for these systems were for agricultural applications, with the optimization conducted on the basis of minimum capital, operating, and maintenance costs. Rajesh Karki [7] presented an evaluation model for small isolated systems containing renewable energy sources. Leonard G. Leslie, Jr [8] proposed a control method for a system that provides approximately 1.0kW of solar generation as well as up to 10kVA of harmonic and reactive compensation simultaneously. Magnus Gustafsson and Niclas Krantz, [9] gave a physical approach to the problem of voltage instability and collapse using a PV model. Joseph N. Wolete [10] developed an interactive menu driven design tool that addresses the technical and economic aspects of a stand-alone photovoltaic system. David C. Cherus, [11] worked on the modeling, simulation and performance analysis of a hybrid power system to supply equipment onboard an omnibus. The concept of a high-efficiency hybrid energy system consisting of a photovoltaic and a battery is not new but the dynamics of such a system have not been thoroughly studied.

A localized PV-generator scheme for localized load management and connected in hybrid notation for a standalone system is proposed and presented as a viable solution to some domestic and commercial load services requirements. It also compliments the present centralized network-wide area load control approach and is proven to be cost-effective. It further serves as a stand-by power supply in the event of major utility outages.

The PV system is a hybrid generator which uses batteries to store energy harnessed from the sun using the photovoltaic sub-system, producing an unsteady dc power. The battery serves as an energy storage device and processing unit to provide a standard residential ac voltage for such loads through an inverter unit. Photovoltaic is the technology that generates direct current (DC) electrical power measured in watts (W) or kilowatts (kW) from semiconductors when they are illuminated by photons. As long as light is shining on the solar cell, it generates electrical power. When the light stops, electricity generation stops [12]. The process is illustrated in figure 1-1.

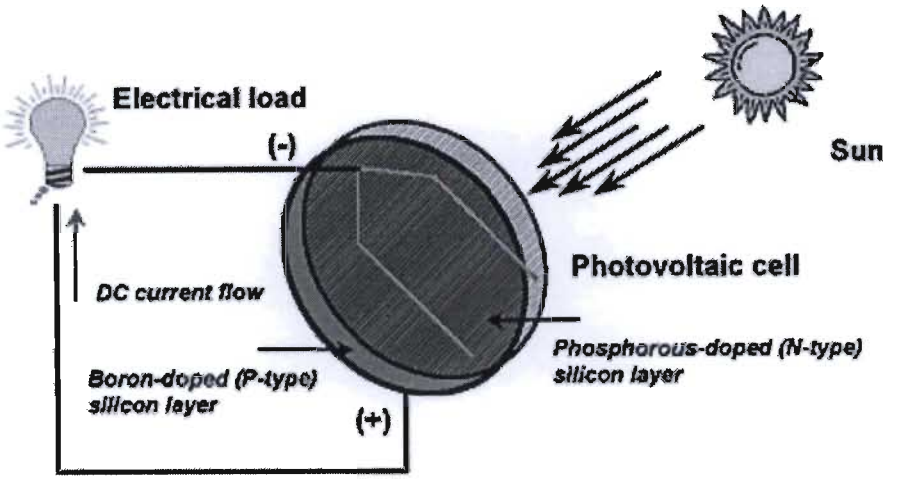

Figure 1-1: Diagram of Photovoltaic Cell [12].

Solar cells are made of semiconductors, which have weakly bonded electrons occupying a band of energy called the valence band. A semiconductor may be described as silicon combined with phosphorous to make negative type silicon and boron to make positive type silicon, which can be combined to produce an electric field. A typical silicon PV cell is composed of a thin wafer consisting of an ultra-thin layer of phosphorus-doped (N-type) silicon on top of a thicker layer of boron-doped (P-type) silicon. An electrical field is created near the top surface of the cell where these two materials are in contact, called the P-N junction. When energy exceeding a certain threshold, called the band gap energy, is applied to a valence electron, the bonds are broken and the electron is somewhat "free" to move around in a new energy band called the conduction band where it can "conduct" electricity through the material. Thus, the free electrons in the conduction band are separated from the valence band by the band gap (measured in units of electron volts or eV) [13]. This energy needed to free the electron can be supplied by photons, which are particles of light. Figure 1-2 shows the idealized relation between energy (vertical axis) and the spatial boundaries (horizontal axis).

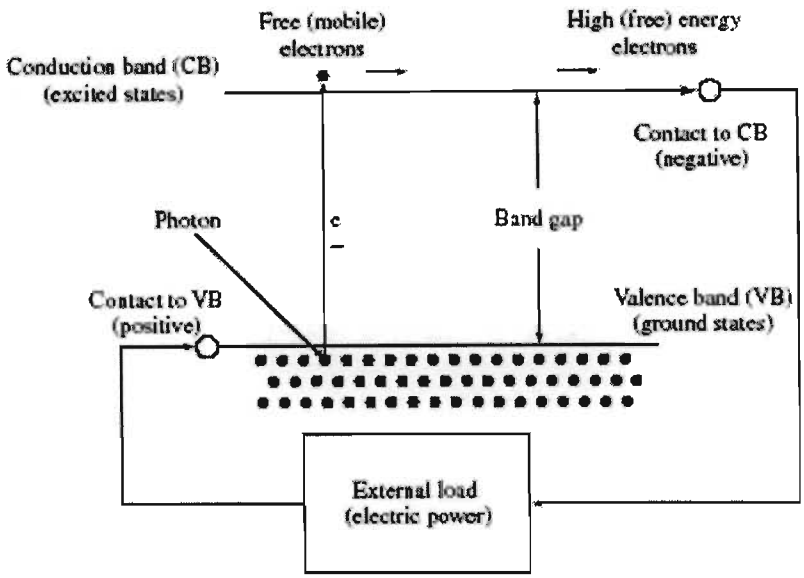

Figure 1-2: Relation Between Energy and the Spatial Boundaries [13].

When the solar cell is exposed to sunlight, photons strike at valence electrons, breaking the bonds and propelling them to the conduction band. There, a specially made selective contact that collects conduction-band electrons drives such electrons to the external circuit [14, 15]. The potential at which the electrons are delivered to the external world is slightly less than the threshold energy that excited the electrons; that is, the band gap. Thus, in a material with a 1.0 eV band gap, electrons excited by a 2.0 eV photon or by a 3.0 eV photon will both have a potential slightly less than 1.0 V (i.e. the electrons are delivered with an energy of 1.0 eV) [16].

PV systems can be classified into two general categories: flat-plate systems or concentrator systems [16]. Connected cells are encapsulated between a transparent window and a reflective backing which is moisture proof to insulate the cells and protect them from the weather and accidental damage. Fixing holes or clamps are provided for securing the module to a supporting structure. The string of cells is connected to a terminal box for wiring the module to a load or to other modules. Commonly, the module consists of 33 to 36 cells and the module edges are sealed against moisture ingress and protected by a metal frame [17, 18].

Photovoltaic devices can be made from various types of semiconductor materials, deposited or arranged in various structures, to produce optimal performance solar cells. There are three main types of materials used for solar cells. The first type is silicon, which can be used in

various forms, including single-crystalline, multi-crystalline, and amorphous. The second type is polycrystalline thin films, with different grades of copper indium diselenide (CIS), cadmium telluride (CdTe), and thin-film silicon. [19]. The third type of material is single-crystalline thin-film, focusing essentially on cells made with gallium arsenide [20]. These materials are then arranged to make solar devices in different ways. The four basic structures include homojunction, heterojunction, p-i-n and n-i-p, and multijunction devices. Multijunctional cells represents attempts to broaden the limited band of solar wavelengths that can be absorbed and converted photovoltaically in a single p-n-junction [21]. Single crystal silicon is one material used but is not the only material in photovoltaic (PV) cells. Polycrystalline silicon is also used in an attempt to minimize manufacturing costs. Unfortunately, the resulting cells are not as efficient as single crystal silicon cells. Amorphous silicon, which has no crystalline structure, is also used, again in an attempt to reduce production costs. Other materials used include gallium arsenide, copper indium diselenide and cadmium telluride. Since different materials have different band gaps, which define the amount of energy that can be absorbed by a single cell, they seem to be "tuned" to different wavelengths, or photons of different energies. A method by which efficiency has been improved in PV arrays has been to use two or more layers of different materials with different band gaps. The higher band gap material is on the surface, absorbing high-energy photons while allowing lower-energy photons to be absorbed by the lower band gap material beneath. This technique can result in much higher efficiencies and can have more than one electric field [12].

A PV system comprises of the following components, namely: PV arrays, storage batteries, charge controller, inverter, safety disconnects and fuses, a grounding circuit, wiring and a utility switch.

Photovoltaic Solar Panels

A photovoltaic (PV) or solar cell is the basic building block of a PV (or solar electric) system. Single PV cells (also known as "solar cells") are connected electrically to form PV modules, which are the building blocks of PV systems [22]. The basic photovoltaic or solar cell typically produces only a small amount of power. To produce more power, cells can be interconnected to form modules, which can in turn be connected to form PV arrays of different sizes and power output. This is illustrated in Fig 1-3. The size of an array depends on several factors, such as the needs of the consumer, the amount of sunlight available in a particular location, space constraints and cost to mention a few.

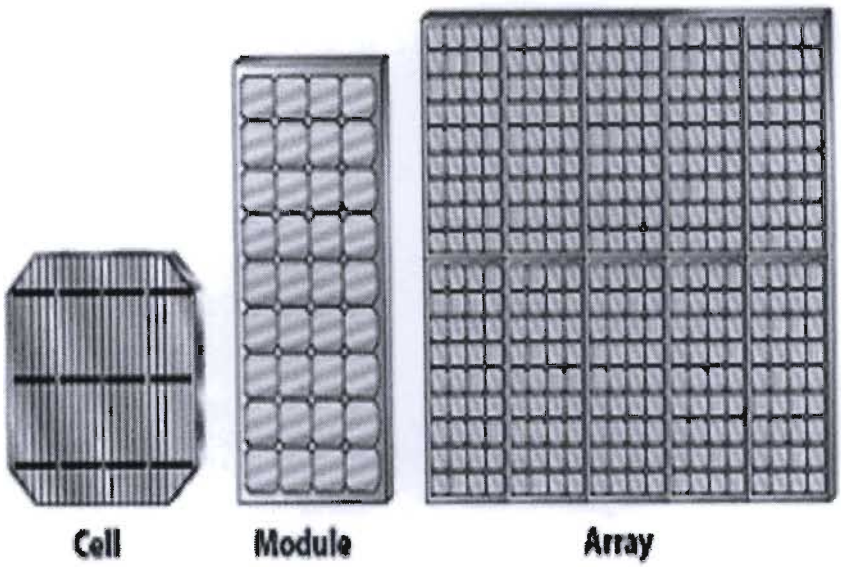

Figure 1-3: Diagram of a Cell, Module and an Array [12].

Fuses and Cables

The PV system can be wired with weather proof cable, resistant to degradation from ultra-violet radiation and wide variation in temperature. The cable should be 'robust' in terms of the voltage and current handling capability. The cable should be rated adequately to continuously carry the expected peak (short-circuit) current. Fuses are generally used to protect electrical appliances from passing short circuit current in the event of a malfunction and are sized to allow a reasonable margin above the expected peak current. A PV cell/module is designed to operate from open circuit to short circuit and its peak power is delivered at approximately 90% of its short circuit current. A PV system cannot provide more than its short circuit current and most of the time delivers much less than this. Although a fuse is not required to directly protect the module, whole strings or the whole array usually have fuses installed to protect them from abnormal operation. In addition, separate fuses are used for each of the other components of the PV system. In particular, batteries, because of their very low internal resistance can cause very high short circuit currents [18]. referenced.

Batteries

Since photovoltaic are intermittent power sources, they cannot meet the load demand all times, 24hrs a day, 365 days a year. The energy storage therefore, is a desired feature to incorporate with renewable power systems, particularly in stand alone systems. Considering the cost and performance requirements a balance is made between the average generating capacity of the PV, the battery storage capacity and the average load demand. It can

significantly improve the load availability, a key requirement for any power system. The battery stores energy in the electrochemical form, and is the most widely used device for energy storage in a variety of applications. It has one-way conversion efficiency of 85 to 90% [23, 24].

Stand-alone PV systems require energy storage to compensate for periods without or with insufficient solar irradiation, such as during the night or during cloudy weather. In all cases in which electric energy storage is required, the classical electrochemical accumulator battery is the most convenient form of energy storage for a PV system. The DC (direct current) characteristic allows for direct connection between the PV generator and the battery, without a need for any conversion or transformation of the supplied PV. Energy provides three main functions in PV systems namely;

Autonomy: The system can meet the load at all times even at night or overcast periods

Surge Current: The system can supply short term surges in current higher than the array output current to start industrial loads e.g. motors and heavy equipment

Leveling voltage: System can provide a constant voltage by eliminating wide swings in array voltage [25].

The two most common types of rechargeable batteries in use are lead-acid and alkaline. Lead acid batteries have plates made of lead (Pb.) mixed with other materials, and submerged in a sulfuric acid solution. Alkaline batteries are either nickel-cadmium or nickel-iron batteries. They have plates made of nickel submerged in a solution of potassium hydroxide. After a discharge, it can be recharged by injecting direct current from external source. This type of battery converts the chemical energy to electrical energy in the discharge mode. In the charge mode, it converts the electrical energy to chemical energy. In both cases, a small amount of energy is converted into heat, which is dissipated around the surrounding medium. Although a variety of storage technologies are under development, the lead-acid battery remains the prime energy resource for electricity supplies in remote areas. Lead-acid batteries are the most common in PV systems because their initial cost is lower and because they are readily available nearly everywhere in the world. There are many different sizes and designs of lead-acid batteries, but the most important designation is whether they are deep cycle batteries or shallow cycle batteries.

Shallow cycle batteries, like the type used as starting batteries in automobiles, are designed to supply a large amount of current for a short time and stand mild overcharge without losing electrolyte. Unfortunately, they cannot tolerate being deeply discharged. If they are repeatedly discharged more than 20 percent, their lifespan will be grossly reduced. These batteries are not a suitable choice for a PV system [16]. Deep cycle batteries are designed to be repeatedly discharged by as much as 80 percent of their capacity so they are a good choice for power systems. Even though they are designed to withstand deep cycling, these batteries will have a longer life if the cycles are shallower. All lead-acid batteries will fail prematurely if they are not recharged completely after each cycle. Allowing a lead-acid battery stay in a discharged condition for many days at a time will cause sulfation of the positive plate and a permanent loss of capacity.

Sealed deep-cycle lead-acid batteries are maintenance free. They never need watering or an equalization charge. They cannot freeze or spill, so they can be mounted in any position. Sealed batteries require very accurate regulation to prevent overcharge and over discharge. Either of these conditions will drastically shorten their lives. Sealed batteries are recommended for remote, unattended power systems [25, 26].

The lead acid battery uses a combination of lead plates or grids and an electrolyte consisting of a dilute sulfuric acid to convert electrical energy into chemical energy and vice versa.

Anode: Sponge metallic lead

$$Pb + SO_4^{2-} \longrightarrow PbSO_4 + 2e^-$$

Cathode: Lead dioxide (PbO_2)

$$PbO_2 + SO_4^{2-} + 4H^+ + 2e^- \longrightarrow PbSO_4 + 2H_2O$$

The water formed in this process and the loss of sulfate ions causes the density of the electrolyte to decrease. Therefore the value of this density can be used to measure the state of charge of the battery.

Electrolyte: Dilute mixture of aqueous sulfuric acid

Applications: Motive power in cars, trucks, forklifts, construction equipment, recreational water craft, standby/backup systems

Advantages

- Low cost
- Ability to provide wide current range

- Long life cycles
- Ability to withstand a harsh environment
- The performance is good in low and high temperatures and in high-drain applications
- It has a high degree of recycling potential at relatively low temperatures
- Maintenance free batteries
- Comprisable good shelf life

Disadvantages

- For voltages above 2.39V per cell the battery's water breaks down into hydrogen and oxygen (called gassing voltage). This requires replacement of the cell's water
- When battery is in use, hydrogen and oxygen are released from the cells. A very high concentration of this mixture can cause an explosion.
- Fumes from the acid or hydroxide solution may have a corrosive effect on the area surrounding the battery.
- The electrolyte of lead-acid batteries is hazardous to you health and may produce burns and other permanent damage if handled carelessly.

Inverter

A semiconductor-based device known as a power inverter is used to convert the DC power to AC power. Some loads (such as induction motors) may have significantly high starting currents. It is therefore important to provide adequate surge current capacity in the inverters, to meet load surge requirements. Other loads either overheat or introduce unwanted noise if the harmonic distortion of their power supply is not below specific level [27].

Charge Controller

The charge controller regulates the flow of electricity from the PV modules to the battery and the load. The controller keeps the battery fully charged without overcharging it. When the load is drawing power, the controller allows charge to flow from the modules into the battery, the load, or both. When the controller senses that the battery is fully charged, it stops the flow of charge from the modules. Many controllers will also sense when loads have taken too much electricity from batteries and will stop the flow until sufficient charge is restored to the batteries. This can greatly extend the battery's lifespan [28].

The fundamental task of a charge controller is to operate the battery within the safe limits defined with respect to overcharging and deep discharging by the battery manufacturer or by

the operation mode. Compared to conventional battery chargers powered by the public grid, the situation is much more complex in PV systems. Here, charging power and energy are limited and depend on the varying insolation and load demand [13]. The charge controller must shutdown the load when the battery reaches a prescribed state of discharge and must shut down the PV array when the battery is fully charged [27]. The main reasons for this interest are reduced operating cost and increased system efficiency [29].

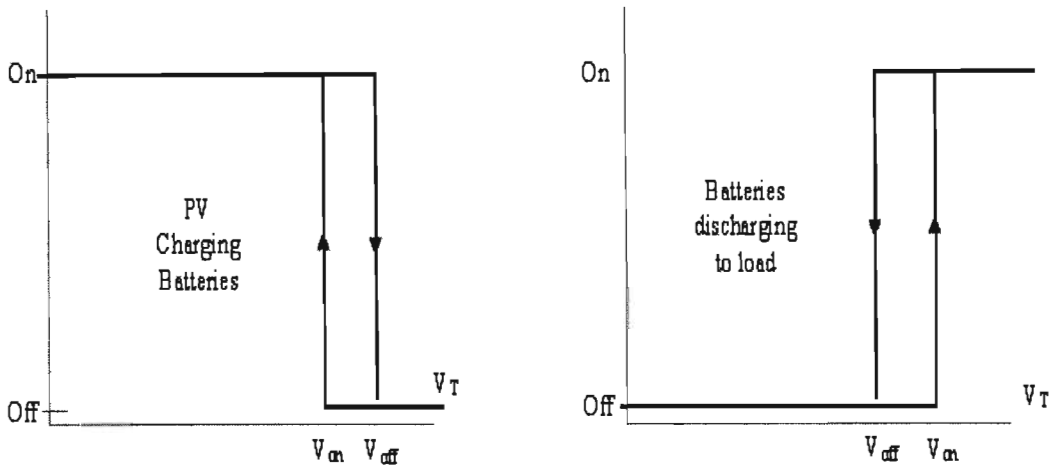

Figure 1-4: Hysteresis Loops in a Charge Controller using Regenerative Comparator for Voltage Sensing [27].

In a stand alone system, to prolong battery life, over-charge and over-discharge of the battery should be avoided. Battery state of charge (SOC) can be roughly determined by measuring the terminal voltage to determine the battery's condition. In the case of over-charge, the rise in voltage is used to control the charging by shunt regulation or by series regulation. With over-discharge, the drop in voltage is used to disconnect loads from the battery using a low voltage disconnect circuit [18].

Factors Affecting Output

Some factors affecting the output of a typical PV are;

- **Standard Test Conditions**: Solar modules produce dc electricity. The dc output of solar modules is rated by manufacturers under Standard Test Conditions (STC). These conditions are easily recreated in a factory, and allow for consistent comparisons of products, but need to be modified to estimate output under common outdoor operating conditions. STC conditions are:

  Solar cell temperature = 25°C;

  Solar irradiance (intensity) = 1000 W/m^2 (often referred to as peak sunlight intensity)

Solar spectrum as filtered by passing through 1.5 thickness of atmosphere (ASTM Standard Spectrum [25]).

- **Temperature**: Module output power reduces as module temperature increases. When operating on a roof, a solar module will heat up substantially, reaching inner temperatures of 50-75°C.
- **Dirt and Dust**: Dirt and dust can accumulate on the solar module surface, blocking some of the sunlight and reducing output.
- **Mismatch and Wiring Losses**: The maximum power output of the total PV array is always less than the sum of the maximum output of the individual modules. This difference is a result of slight inconsistencies in performance from one module to the next and is called module mismatch and amounts to at least a 2% loss in system power. Power is also lost to resistance in the system wiring. These losses should be kept to a minimum but it is difficult to keep these losses below 3% for the system. A reasonable reduction factor for these losses is 95% or 0.95.
- **DC to AC conversion losses**: The dc power generated by the solar module must be converted into common household ac power using an inverter. Some power is lost in the conversion process, and there are additional losses in the wires from the rooftop array down to the inverter and out to the house panel [30].

CHAPTER TWO

PHOTOVOLTAIC SYSTEM: DESIGN METHODOLOGY AND CONSTRUCTION

2.1 Methodology

The general assembly of the PV System test facility is shown in figure 2-1. It comprises of the following components: a 550W solar panel, a 30A, 24V charge controller, a variac, battery banks, isolation switches, a 3.0KW, 24V DC/220V, 50Hz, AC inverter and test loads (Universal motor, light bulbs, fractional horse power induction motors)

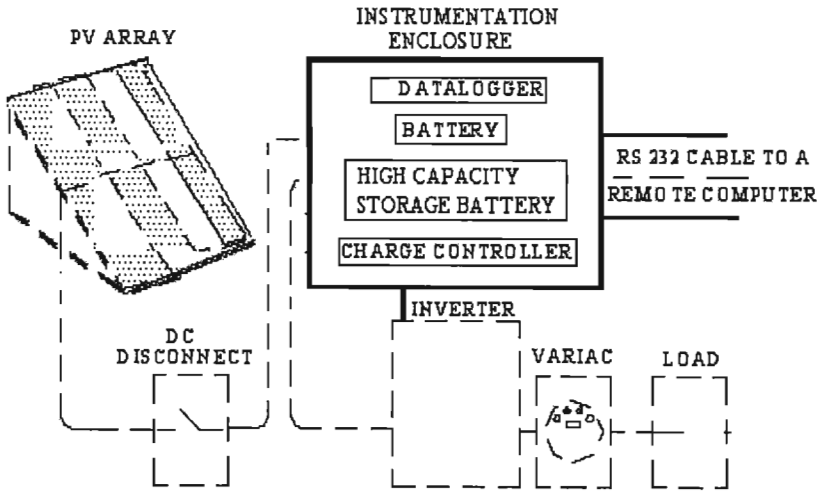

Figure 2-1: Experimental Set-up of the Photovoltaic System.

A description of the function and technical specification of each of these components and sub systems is discussed.

2.1.1 Photovoltaic (PV) Panels

Figure 2-2 shows the Photovoltaic system consisting of six panels which was mounted on the roof of the School of Electrical, Electronic and Computer Engineering Building at the University of KwaZulu-Natal, Howard College Campus. These panels utilize sunlight to produce DC electricity.

Figure 2-2: PV Solar Panels

The PV panels utilized for this experiment consists of five Shell SM 110-24 110W panels solar panels [31]. The smallest solar panel seen in the picture was not connected due to some broken compartments. These panels consist of mono-crystalline silicon solar cells which convert sunlight energy to electrical energy. The solar array has the following Standard Test Conditions (STC): irradiance level 1000W/m^2, spectrum AM 1.5 and cell temperature 25 ^{0}C specification data.

Table 2-1: Illustrating the data sheet of the PV array

Rated Power	Pr	110W
Peak power	Pmpp	110W
Peak Power Voltage	Vmpp	35V
Open Circuit Voltage	Voc	43.5V
Minimum Peak Power	Pmpp min	104.5W
Tolerance on Peak Power		+/-5%

These panels have been arranged in a flexible support structure, for maximum insolation, ease of mobility for experimentation and dismantling for on-site deployment.

2.1.2 Battery Bank

A total of ten, 12V, 102Ah batteries (connected back to back in pairs) were connected in parallel, with their output terminals connected in series to give 24V DC supply as shown in figure 2-3. The DC bus is directly connected to the inverter. A battery bank is used for storing the electric energy produced by the PV cells. The battery bank then delivers power to the load whenever the PV output from the solar panel falls below the threshold voltage due

to poor or zero insolation. Furthermore, when a load needs more current such as during motor starting, the battery bank supplies sufficient current during that time.

Figure 2-3: Illustrating the battery arrangement in the laboratory

The configuration of the battery bank depends on the loading applications. Each load can require a certain amount of power and thus a specified power capacity will then be needed from the battery bank.

2.1.3 Wiring Cables and Accessories

$4mm^2$ single core PVC cables (a red and a black) were used for all the wiring connections, linking the PV panels to the auxiliary systems in the laboratory. The accessories include cable lugs, racks, glands, plugs and masking tapes.

2.1.4 Inverter

A 3.0kW, 24VDC / 220VAC inverter was used for conducting AC load tests. It converts direct current to alternative current in the circuit setup. The inverter is supplied dc current from the charge controller depending on the load and converts direct current to alternative current.

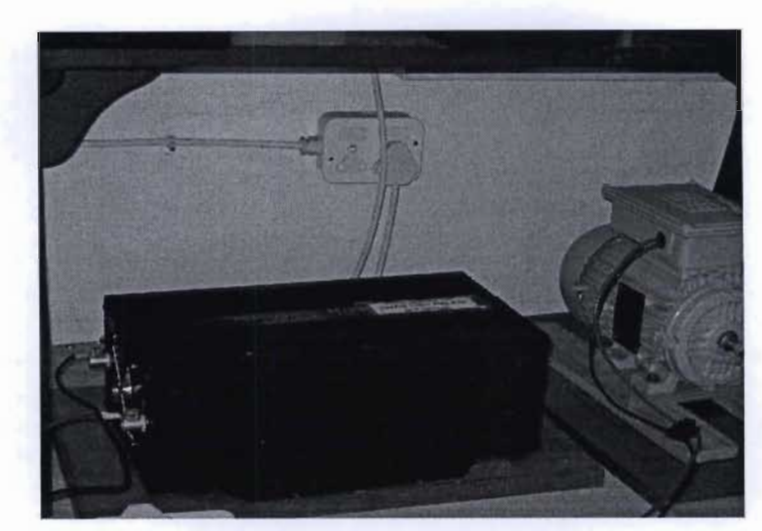

Figure 2-4: Illustrating the inverter arrangement in the laboratory

2.1.5 Variac

A variac (range 0 – 250V) was used to provide variable voltage output from the inverter to the load. Thus the variac acts like a step-down transformer that can give a wide range of output voltage from the input on the inverter.

2.1.6 Data Acquisition System

A data acquisition system was implemented to capture solar insolation data from the PV test facility. The data points were taken every five minutes from 1st February 2005 to 12th December 2005 and stored using Lutron 801 software as shown in figure 2-5. It is capable of visually displaying all readings both on the multimeter and on the Personal Computer (PC). It records and stores all the data acquired in real-time.

Figure 2-5: Lutron-based Data Acquisition System

The data acquisition system consists of an ISO–TECH IDM 203 digital multimeter; a lutron DM 9093 multimeter along with a 232serial cable was connected to a computer system to record all the readings of the PV and to store all test results. The computer system used was an Hewlett Packard, Intel(R) Pentium(R) 1.5GHz, 512MB of RAM, 80Gb hard drive.

2.1.7 Fuse

A 30A, 500V, Gewiss, GW 70434 switch fuse was also used. This was meant to isolate the circuit from over-current. Hence it was used to prevent fault currents in the system.

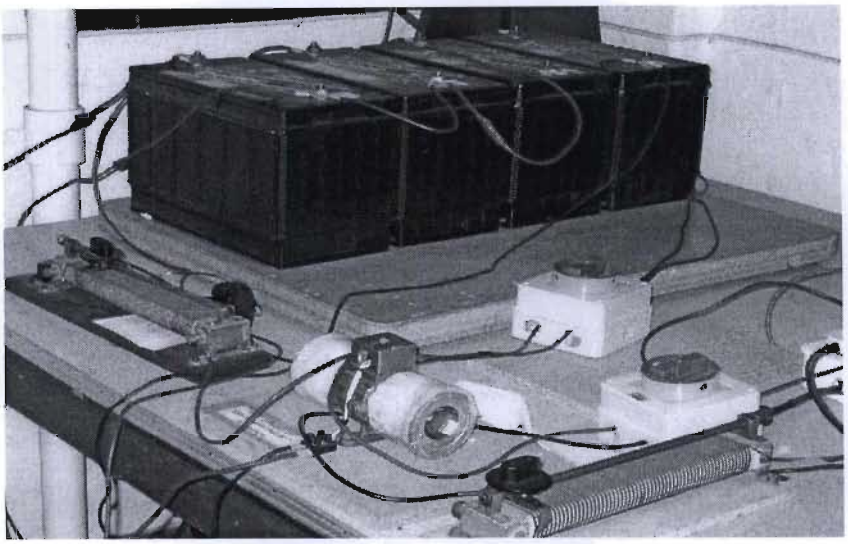

Figure 2-6: Switch Fuses used for the test facility

2.1.8 Charge Controller

A 30A, 24V Isoler charge controller, was used to control the charge state of the battery bank from the PV Generator. The charge controller is also used to provide an output of 24VDC to the inverter to effectively manage the power from the PV cells and the Battery bank so that they can work efficiently and provide the required load current. It also serves as a meter to measure the voltage on the battery bank, such that when the battery bank is discharged below a threshold, it can then charge the battery bank.

During faults in the system, the charge controller can be used to detect the faults and thus cuts the power from being distributed to that specific fault using its AI (artificial intelligence) capabilities. During the day when there is enough sunlight the charge controller switches the batteries off from being discharged but recharges them instead. During the night the charge controller can detect the insufficient supply from the PV cells and thus use the battery bank to supply power to the load.

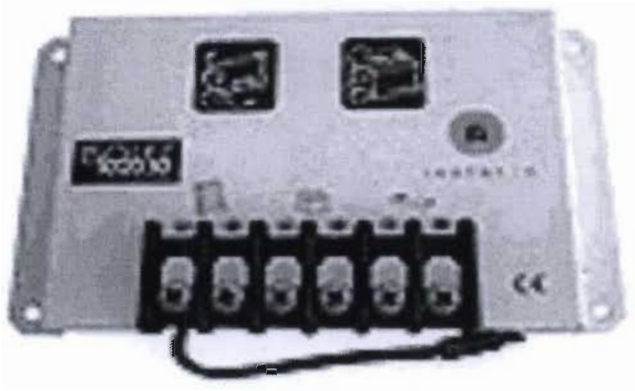

Figure 2-7: Illustrating the Charge controller used in the laboratory

2.2 Inverter Design and Testing

Preliminary laboratory design of the inverter unit was carried out

The design of the inverter was carried out using a full bridge circuit topology using MOSFETs switches and a 50 Hz transformer. The circuit has the robustness to provide the required output power, but problems relating to the correct firing of the MOSFETs were experienced, the conclusion was to experiment with other topologies namely the push pull configuration.

Table 2-2: Design Specifications

Parameter	Design Specifications
Output Power	1.5 kW
Output Voltage	220 V ac, 50 Hz, suitable for domestic applications. Semi sine wave output.
Input Source	12 V dc battery (Fed from PV System)
Safety	System to be used domestically, thus provide ease of use to non-technical individuals.

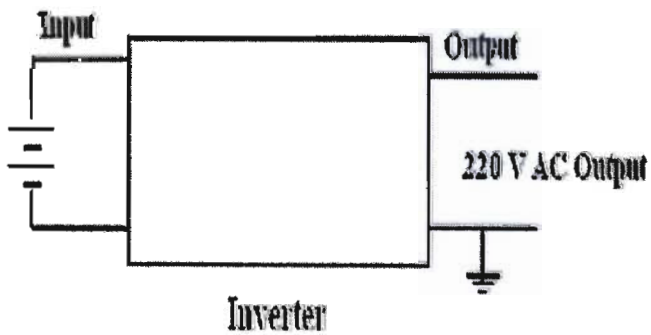

Figure 2-8: Block Diagram of Inverter

The design of the push-pull configuration relies on the use of a centre-tapped transformer. In this case the transformer is a 50Hz type. The circuit configuration shown in figure 2-9 is that of the push-pull inverter circuit. The inverter is a voltage source inverter with the source in this case being the 12V battery fed from the PV system. Power is fed directly to the centre of the transformer through a fuse. This voltage is then switched through the transformer via the MOSFET switches thus producing the desired alternating current at the output. The choice of the switches (MOSFET/IGBT) was determined from the maximum current on full load, as well as the voltage at the input of the inverter. It can be seen that there are fuses at each of the drains of the MOSFETs. This was used to prevent over-current of the switching devices. The transient voltage spikes at the output are reduced via an R-C snubber across the drain and source of the devices. It must be stated that the switches in the network are controlled via a PWM (pulse width modulation) circuit.

2.2.1 Control Circuitry

The purpose of the circuit was to produce the desired output frequency of 50Hz, while maintaining an output voltage of 12V, enough to properly turn on the MOSFETs. The circuit uses a PWM generator chip from Motorola. During the design of the circuit, problems were encountered regarding the amplitude of the output signals. This problem was solved using an inverter chip as well as a MOSFET driver.

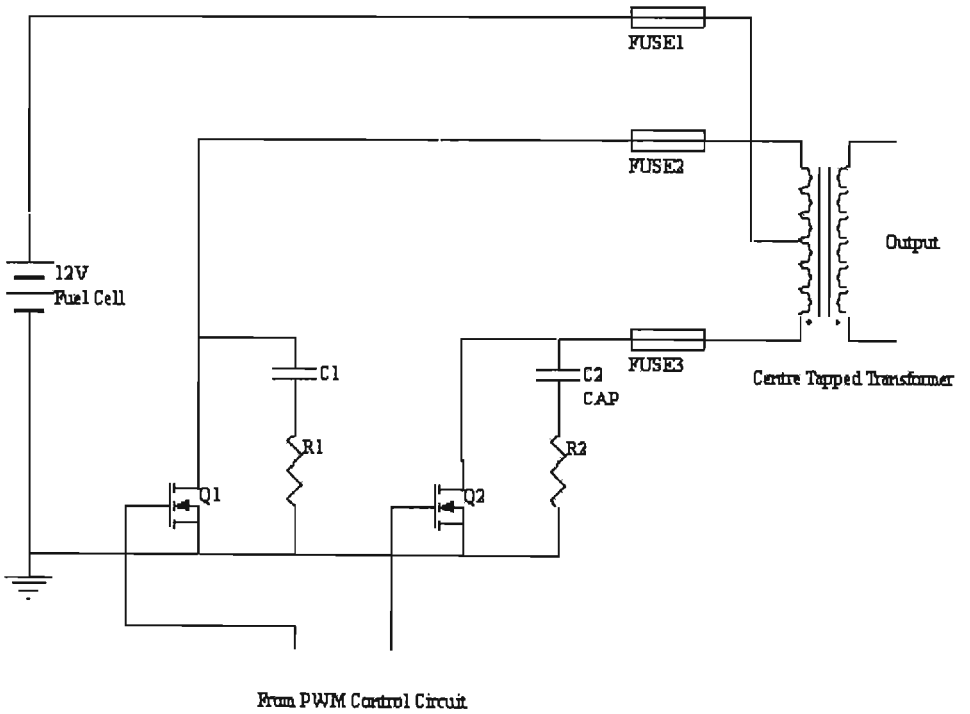

Figure 2-9: Inverter Schematic Diagram

2.2.2 Snubber Network

The snubber network was needed to compensate for the drastic voltage spikes at each transition of the output signal. The voltage spikes were reduced to a respectable level on the addition of the snubber network. The calculation of the R and C values were achieved using the turn off, turn on and voltage and current ratings of the MOSFETs.

2.2.3 Heatsinking

The heat sink is an important aspect of the inverter as it protects and aids the switching device on higher loads, thus it ultimately increases the lifespan of the device. The heat-sink was designed using the values obtained from the data sheet of the MOSFET, as well as heat-sink manufacturer's handbooks. The final heat-sink implemented was that of an extrusion type aluminum heat-sink, this dissipated heat efficiently [32-37].

2.2.4 Testing of the Inverter

Three low-power inverter topologies were utilized. The first two inverters were designed and constructed for different topologies and tested using MOSFET, while the third inverter was designed and constructed using IGBT switches. The specifications of the first two inverters were:

Power Output: 1.5kW

Input dc voltage: 24V and

Output ac voltage: 220V.

Operating Output frequency: 50Hz

The first inverter was built using two MOSFET switches for single-phase application with a centre-tapped transformer. After testing this inverter with several loads, the performance was not satisfactory because the output voltage of the inverter was far less than 220V, necessitating replacement with a better inverter topology. Hence a four MOSFET switched inverter was considered. The second inverter consisted of four MOSFET switches for single-phase but without a centre-tapped transformer [38]. However on implementation, the output voltage was still very small. In the MOSFET switched inverter, the output voltages shown in figures below are in the range of 250 V for an input voltage of 13.5V.

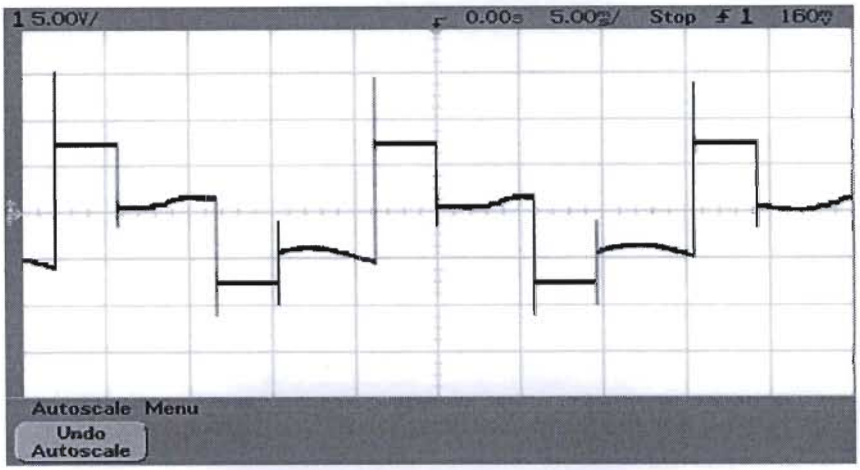

Figure 2-10: Inverter waveform using MOSFET switches

The MOSFET configuration diagram is shown in figure 2-10. The inverter was tested with a 100W light bulb, a universal motor (see specification in table 5-2), and both a light bulb and a universal motor combined.

The load voltage remained close to theoretical expectations for the resistive case, while the waveform changed significantly during inductive loading. The output voltage and current waveform for each type of load are shown in figures 2-10 to 2-16. The current waveform shows a semi-sine wave output for the resistive load, while the other two cases shows a domination in inductive characteristics as would be expected of inductive loads. The light bulb was light for a long time throughout testing, with no visible signs of inadequate supply. The motor on the other hand did not perform to optimal levels. The speed of the motor was very small. However, when resistive and inductive loads were combined and tested using the inverter, the results of the output voltage was 129V. This is still far lesser than the anticipated value of 220V.

Figure 2-11: Inverter output voltage on resistive load waveform using MOSFET switches

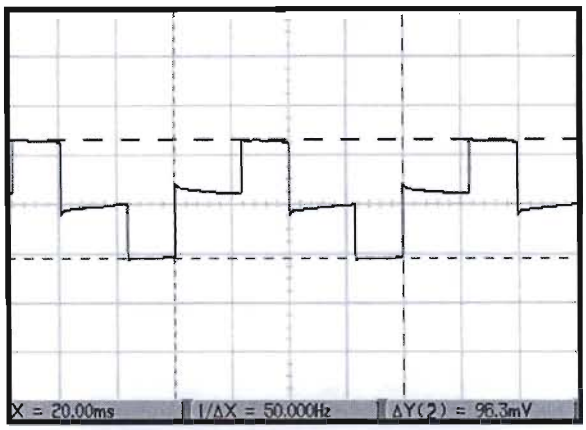

Figure 2-12: Inverter output current on resistive load waveform using MOSFET switches

Figure 2-13. Inverter output voltage on inductive load waveform using MOSFET switches

Figure 2-14: Inverter output current on inductive load waveform using MOSFET switches

Figure 2-15. Inverter output voltage on both resistive and inductive load waveform using MOSFET switches

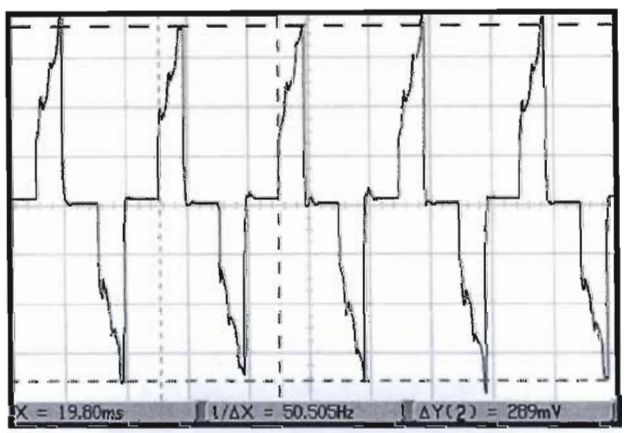

Figure 2-16. Inverter output current on both resistive and inductive load waveform using MOSFET switches

Nevertheless, these two topologies did not meet the voltage requirements of 220V of the test facility so they were replaced by an IGBT switched inverter. The specifications of the IGBT inverter used include an output single phase power of 1.5kilowatts, input source of 48 volts DC and output was 220volts. The frequency was maintained at 50Hz and fuses were used for the over current protection devices.

The IGBT switched inverter was also tested with a 100W light bulb, a universal motors (see specifications in table 5-2), and both a light bulb and a universal motor together. The load voltage remained close to theoretical expectations for the resistive case, while the waveform changed rather drastically during inductive loading. The waveform of the output voltage is shown in figure 2-17.

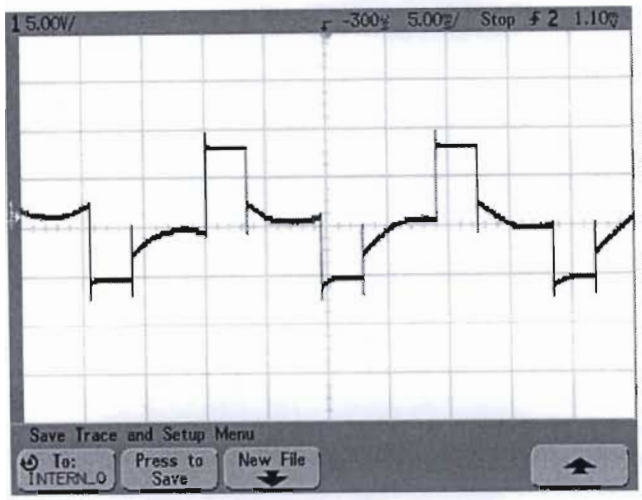

Figure 2-17: Inverter waveform using IGBT switches

The voltage and current waveforms for each of the test loads are shown in figures 2-18 to 2-23.

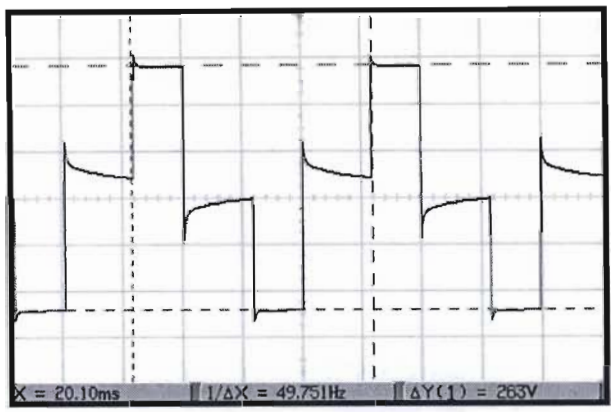

Figure 2-18: Inverter output voltage on resistive load waveform using IGBT switches

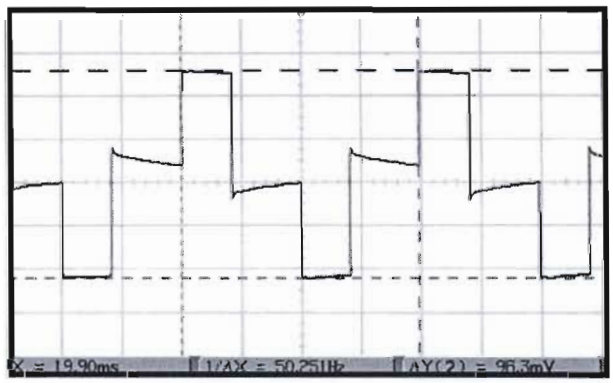

Figure 2-19: Inverter output current on resistive load waveform using IGBT switches

Figure 2-20: Inverter output voltage on inductive load waveform using IGBT switches

Figure 2-21: Inverter output current on inductive load waveform using IGBT switches

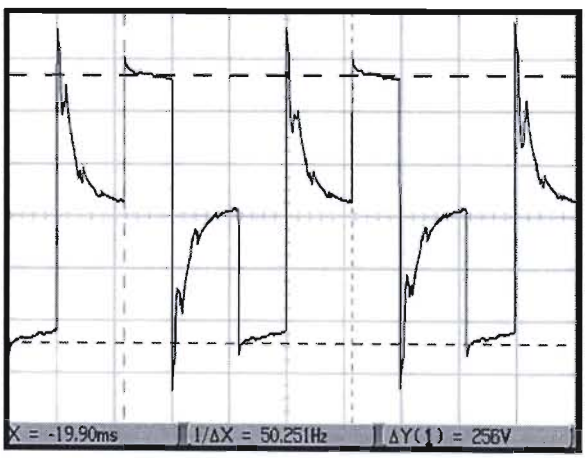

Figure 2-22: Inverter output voltage on both resistive and inductive load waveform using IGBT switches

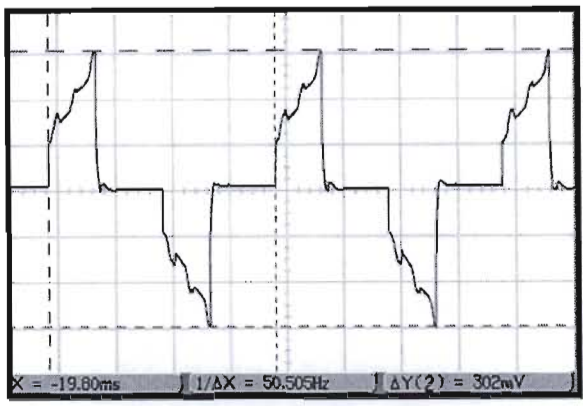

Figure 2-23: Inverter output current on both resistive and inductive load waveform using IGBT switches

2.2.5 Inverter Development

In the process of testing, three temporary setbacks occurred, namely: (i.) a malfunctioning of the regulator, and (ii.) loss of two MOSFET switches, which at this stage was attributed to switching surges. (iii.) the four switch inverter topology gave poor results with the upper two firing switches giving far less than the desired secondary voltage [38].

To mitigate the third problem temporarily, the centre-tapped transformer topology was adopted, while the regulator was replaced. The secondary voltage of the third inverter was still far less than 220V, hence a 3.0kW commercial inverter was procured for the PV test facility

CHAPTER THREE

MATHEMATICAL MODELING OF THE PV SYSTEM

The PV generator is a semiconductor device that converts the solar insolation directly to electrical energy [39]. The PV generator is a nonlinear device with an electrical cell of low-level voltage and power; therefore the cells are connected in series and parallel combinations in order to form an array of desired voltage and current rating [40]. Figure 3-1 shows the commonly used equivalent circuit of a PV cell [41]. It is made up of a current source in parallel with a p-n junction diode. The shunt resistance R_{SH} is introduced in the equivalent circuit to absorb the leakage around the edge of the cell, while the series resistance R_s takes account of the contact resistance between the metallic contacts, semiconductors and the resistance of the semiconductor material of the solar cell [42-45]. The output of the current source is directly proportional to the amount of light rays incident on the cell. The diode determines the I-V characteristics of the cell.

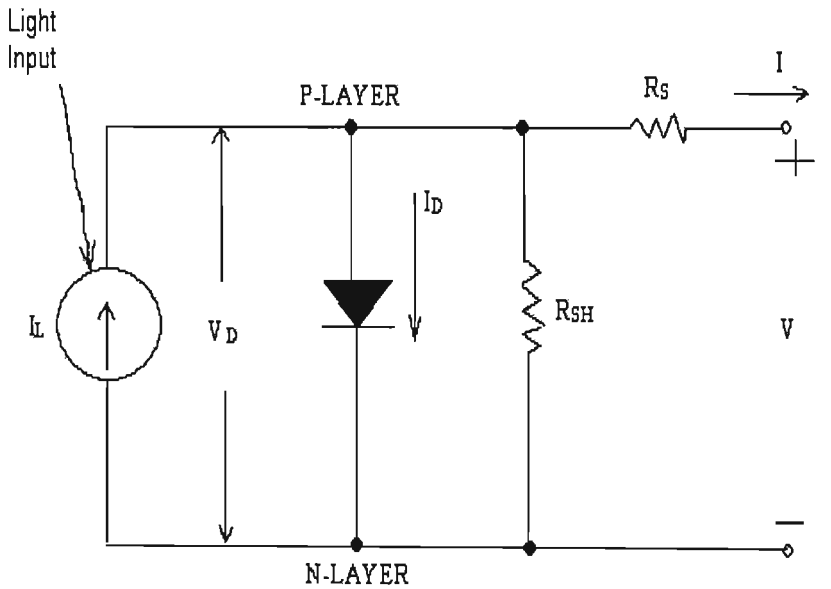

Figure 3-1: Equivalent Circuit of a Solar Cell Generator

The single solar cell model is given by the equation [41]:

$$V = R_{SH}\left\{I_L - I - I_O\left[\ell^{K_o(V+R_sI)} - 1\right]\right\} \tag{3.1}$$

where

I is the current through the load,

I_L is the photovoltaic current across the junction,

R_s is cell series resistance,

R_{SH} is the shunt resistance,

k is Boltzman constant.

$k_o = e/AkT$ is the coefficient of the exponential, where e is the electronic charge, A is completion factor, T is absolute temperature and I_o is cell reverse saturation current.

However, solving for I in equation (3.1) gives;

$$I = I_L - I_0 \left\{ \left[\ell^{K_o (V + R_s I)} - 1 \right] \right\} - \frac{V}{R_{SH}} \tag{3.2}$$

where

I_L is the light generated current, and

I_o is the diode saturation current.

The term $(-V/R_{SH})$ is considered to be very small and may be neglected.

Equation (3.2) becomes;

$$I = I_{sc} \left\{ 1 - C_1 \left[\ell^{\left(\frac{V}{C_2 V_{oc}} \right)} - 1 \right] \right\} \tag{3.3}$$

where;

$$C_1 = \left(1 - \left[\frac{I_{mpp}}{I_{sc}} \right] \ell^{\frac{-V_{mpp}}{C_2 V_{oc}}} \right) \tag{3.4}$$

$$C_2 = \left[\left(\frac{V_{mpp}}{V_{oc}} \right) - 1 \right] \left\{ \ln \left[1 - \left(\frac{I_{mpp}}{I_{sc}} \right) \right] \right\}^{-1} \tag{3.5}$$

V_{oc} is module open circuit voltage, V_{mpp} is module maximum power voltage, I_{sc} is module short circuit current, I_{mpp} is module maximum power current and I is the module current [46,47].

In order to have a coherent agreement between the calculated and actual characteristics of the solar cell at higher intensities, equation (3.3) can be solved to form;

$$I = K_6 - \left\{ \ell^{K_4 V^m - K_5} \right\} \tag{3.6}$$

Expressing the constants in terms of the three characteristic cell points, results in equation (3.7) below.

$$I = I_{sc}\left\{1 - C_3\left(\ell^{C_4 V} - 1\right)\right\} \tag{3.7}$$

The constants are defined in equations 3.8,3. 9, 3.10 and 3.11.

$$m = \frac{\left[\ln\left(\frac{C_5}{C_6}\right)\right]}{\left[\ln\left(\frac{V_{mpp}}{V_{oc}}\right)\right]} \tag{3.8}$$

$$C_4 = C_6 / \left(V_{oc}\right)^m \tag{3.9}$$

$$C_5 = In\left[\frac{\left(I_{sc}\left(1 + C_3\right) - I_{mpp}\right)}{C_3 I_{sc}}\right] \tag{3.10}$$

$$C_6 = \ln\frac{1 + C_3}{C_3} \tag{3.11}$$

The constant C_3 has a value of 0.01175. This value would give the least number of errors over the different ranges of illumination and temperatures. When 0.01175 is substituted for C_3, the other constants are reduced as shown in equations 3.12, 3.13, 3.14 and 3.15[41].

$$m = \frac{\ln\frac{C_5}{4.46}}{\ln\frac{V_{mpp}}{V_{oc}}} \tag{3.12}$$

$$C_4 = \frac{4.46}{\left(V_{oc}\right)^m} \tag{3.13}$$

$$C_5 = \ln\frac{1.01175\, I_{sc} - I_{mpp}}{0.01175\, I_{sc}} \tag{3.14}$$

$C_6 = 4.46$ (3.15)

The photo-current I_L (A) is directly proportional to irradiance G (Wm^2). When the cell is short-circuited, negligible current flows in the diode. When the cell is not illuminated, the relationship between the cell's terminal voltage and current is linear. When the cell is open

circuited and illuminated, the photo-current flows entirely in the diode. The I-V curve is offset from the origin by the photo generated current I_L [[48].

3.1 Mean Power Output of PV Model

The power output of the PV module, *P(S)* is the product of the module output voltage and output current. Information on temperature, reference irradiance, maximum power point voltage and current are supplied in the manufacturer's data sheet [31]. The output power of a solar cell is dc power which can be expressed in terms of the cell current ***I*** and cell terminal voltage ***V*** as:

$$P_{dc} = V.\ I \tag{3.16}$$

Recall from equation (3.3) that the cell current may be expressed in terms of solar cell parameters as:

$$I = I_L - I_o\left[\ell^{\left(\frac{t(V+IR_s)}{AKT}\right)} - 1\right] - 1 \tag{3.17}$$

Where $k_1V_{oc} = AKT/e$, $k_2I_{sc} = I_o$, and $I_L = I_{sc}$. Then the equivalent circuit output current I of the module is [51].

$$I = I_{sc} - I_{sc}K_2\left[\ell^{\left(\frac{V+IR_s}{K_1V_{oc}}\right)} - 1\right] \tag{3.18}$$

Referring to equation (3.18) the cell output power P can be written as:

$$P = IV = VI_{sc}\left[1 - K_2\left(\ell^{\frac{V+IR_s}{K_1+V_{oc}}} - 1\right)\right] \tag{3.19}$$

The mean power output from the PV module is calculated using the integral expression [46] [53];

$$P_{pv(mean)} = \int P(S).f(S)ds \tag{3.20}$$

Where $f(S)$ is irradiance probability density function

$$I = \alpha\left(\frac{S}{S_{ref}}\right)T + \left[\left(\frac{S}{S_{ref}}\right) - 1\right]I_{sc} \tag{3.21}$$

Where S is the total tilt insolation, S_{ref} is reference insolation, T is cell temperature in °C, α is the current change temperature coefficient at reference insolation.

The minimum value of I_D is approximately [46]:

$$I_D = 1.5*10^{5} * \ell^{\frac{-E_g}{KI}} \tag{3.22}$$

where E_g is the energy band gap.

For the semi conductor, E_g is given by ≈ 1.1eV = 1.76 * 10^{-19}J.

According to [46], I_D is the function of temperature only which is $I_D = f_1\ (T)$. The light generated current I_{ph} may be expressed as $I_{ph} = A * J$. the current density is given by:

$$J = q\int_{o}^{L} G(x)dx \tag{3.23}$$

Where L is the thickness of the cell, $G(x)$ is the generation rate of charge carriers at a point x, and $q = 1.602 \times 10^{-19} C$ is the electron charge.

The generation term is a function of wavelength given by the expression [46]:

$$G(\lambda) = [1 - R(\lambda)]\alpha(\lambda)N(\lambda)e^{(-\alpha(\lambda)x)} \tag{3.24}$$

The solar insolation, φ which is the intensity of light, corresponding to the solar cell is expressed in terms of number of photons N and its energy ξ is given as [46].

$$\varphi = N * \xi \tag{3.25}$$

$$\text{where} \quad \xi = h * \nu \quad \text{and} \quad \nu = c/\lambda. \tag{3.26, 3.27}$$

Thus,

$$\varphi = N*h*(c/\lambda) \tag{3.28}$$

h is Planck's constant = 6.625×10^{-34} J-s,

c is the velocity of light 2.99×10^{8} m/s.

$N(\lambda)$ is the number of incident photons with energies greater than the band gap, and

$\alpha(\lambda) = 4.5 \times 10^{-3} cm^{-1}$ is the average absorption coefficient, and

$R(\lambda) \approx 0.313$(average) is the reflection coefficient [46].

3.2 Open Circuit Voltage and Short Circuit Current

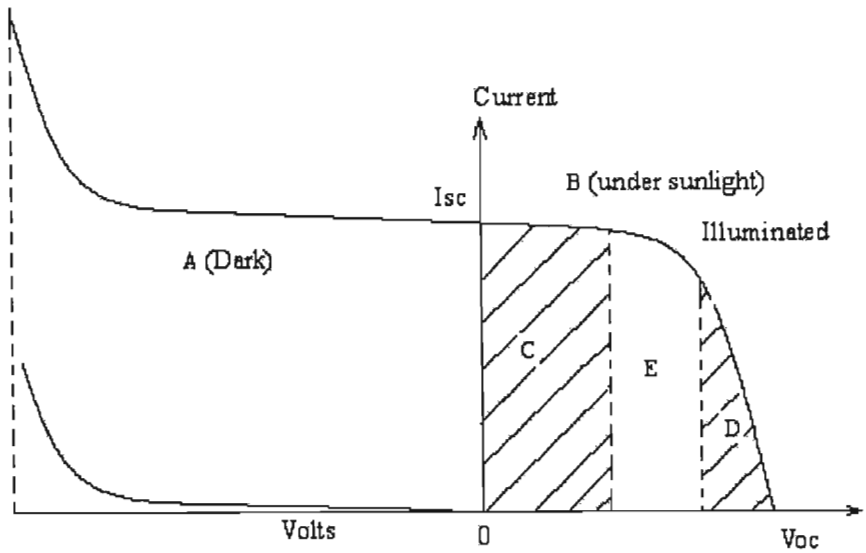

Figure 3-2: I-V characteristics of the PV module in sunlight and in the dark [49].

The electrical characteristic is generally represented by the current versus voltage (I-V) curve. Figure 3-2 shows the I-V characteristic of a PV module under two conditions, in sunlight and in the dark. In the first quadrant, i.e. region A of the I-V curve at zero voltage is called the short circuit current. This is the current that is measured with the output terminals shorted (zero voltage), that is, $I_{SC} = I_{Ph}$. It is produced under short circuit condition: $V = 0$

In region B of the curve at zero current is called the open circuit voltage. This is the voltage that is measured with the output terminals open (zero current). It corresponds to the voltage drop across the diode (p-n junction) when it is traversed by the photo current. It reflects the voltage of the cell in the night.

In region C, the cell works like a constant current source, generating voltage to match the load resistance. In region D, the current drops rapidly with a small rise in voltage. In this region, the cell works like a constant voltage source with an internal resistance. In between regions C and D, the curve has a knee point. If a voltage is externally applied in the reverse direction, (e.g. during a system fault transient), the current remains flat and the power is absorbed by the cell.

In the dark, the current is zero for voltage up to the breakdown voltage which is the same as in the illumination condition. The power output of the panel is the product of the voltage and the current outputs as illustrated in figure 3-3.

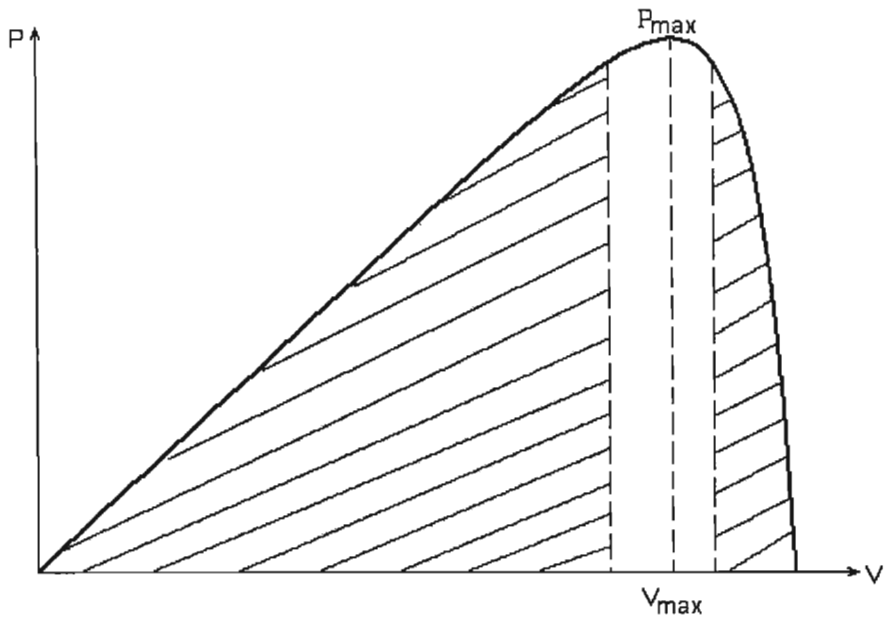

Figure 3-3: Power Vs Voltage characteristics of the PV module in sunlight [49]

It should be noted that the cell produces no power at zero voltage or zero current, and produces the maximum power at voltage corresponding to the knee point of the I-V curve. Hence, PV power circuits are designed such that the modules operate closed to the knee point, slightly on the left hand side. The PV modules are modeled approximately as a constant current source in the electrical analysis of the system [49].

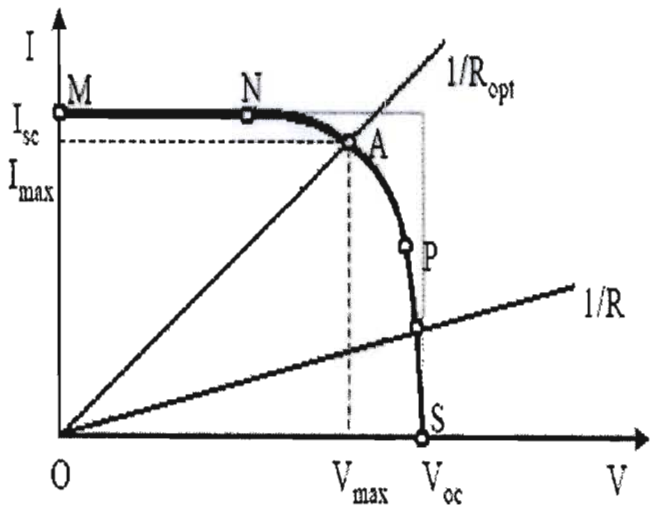

Figure 3-4: Typical Current Voltage I-V Curve of a Solar Cell connected to a load [49].

The operating point is determined from the intersection of the I-V characteristic of the solar cell with the load I-V characteristic; this holds true only if the cells terminals are connected to a variable resistance R. If the load R is relatively small, the cell operates in the region M-N of the curve. In this region the cell behaves very similarly to a current source with a current value nearly equal to the short circuit current. However if the load R, is large, the cell operates in the P-S region of the curve. In this region of the curve, it is apparent that the cell would behave more like a constant voltage source, and the voltage value would be nearly equal to the open circuit voltage.

3.3 System Architecture Flowchart of the PV Generator Test Facility

The system architecture used in the laboratory is simplified using a flow chart. This is illustrated in Figure 3-5.

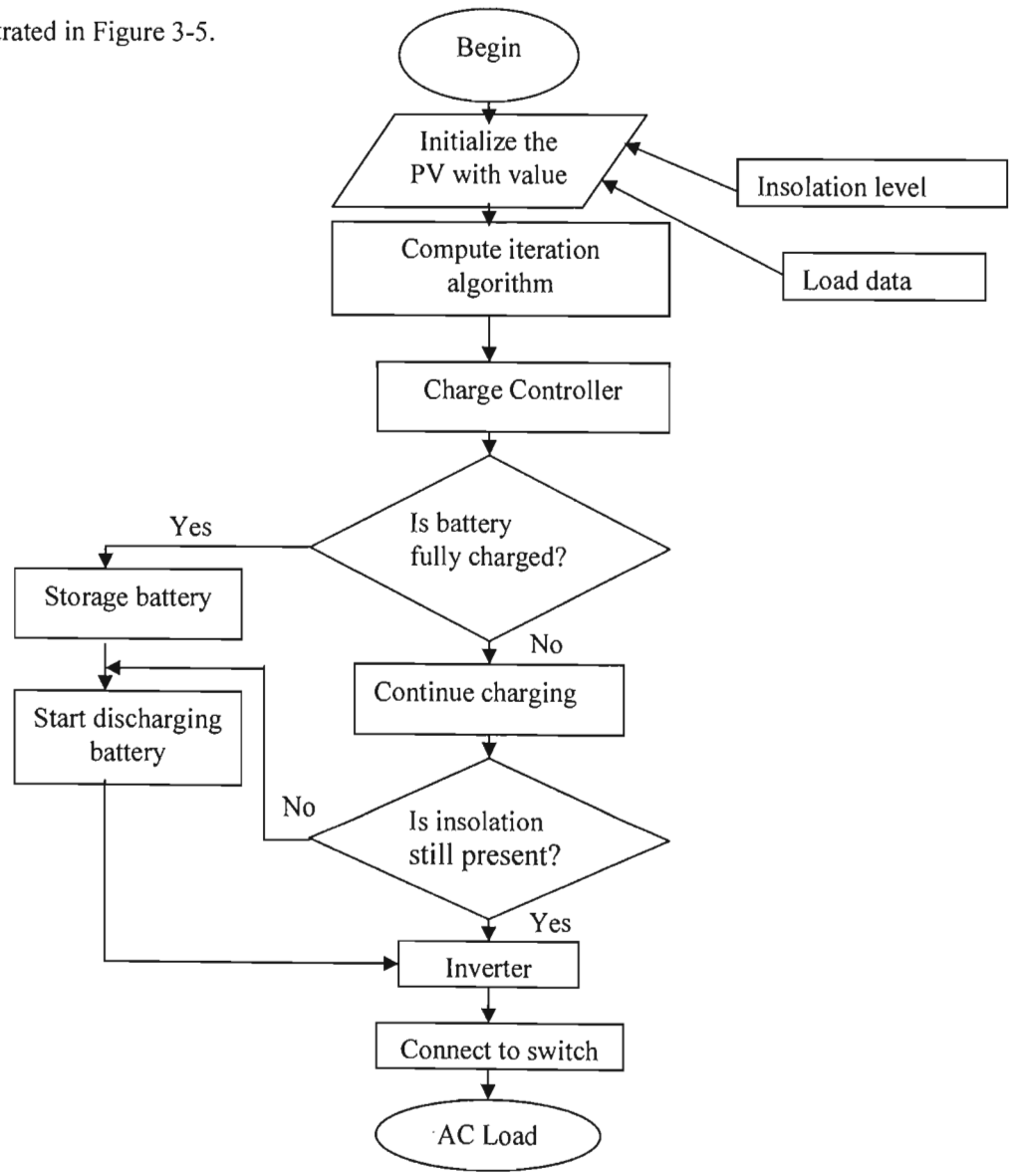

Figure 3-5: Illustration of the system architecture of the PV test facility modeled.

3.4 Insolation Data

The insolation data used was from the PV test facility mounted on the roof of the School of Electrical, Electronic and Computer Engineering, University of KwaZulu Natal, Durban. The data points were taken every five minutes from 1st February 2005 to 12th December 2005 and stored using Lutron 801 software. The curves used in these simulations were for the best day in October 2005, based on cumulative insolation. Usually, insolation data is presumed to follow a daily sinusoidal curve from dawn to dusk, with the peak value set to the value calculated for that day of the year. This averaged data removes the rapid peaks and troughs caused by passing clouds. The daily average power per time of a typical summertime situation of the PV is presented in the Figure 3-6.

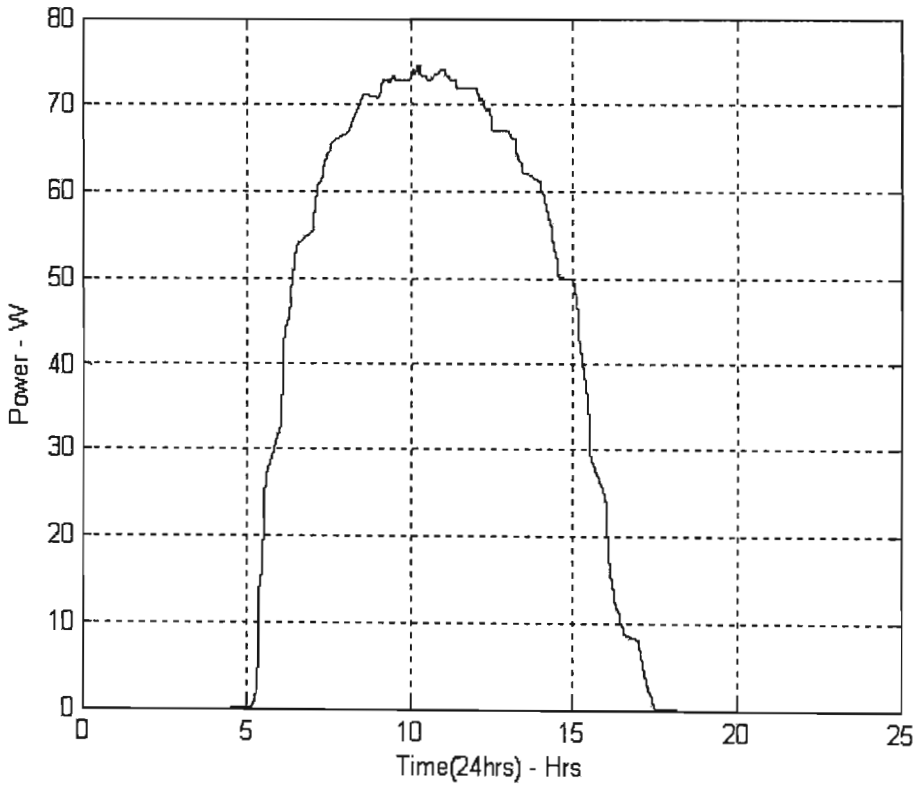

Figure 3-6: Typical hourly average values of consumption and PV generation during a summer day.

3.5 Discussion

From of the literature review, a mathematical model of the PV system was developed. The simulation was implemented using three techniques namely MATLAB, DVF and C++. The results were compared with practical measurements.

CHAPTER FOUR

SIMULATION OF THE PV SYSTEM USING MATLAB, DIGITAL VISUAL FORTRAN AND C++

Software codes were developed for each of the mathematical analysis used. The pseudocode for developing the software codes are illustrated in section 4.1

4.1 Development Procedure

Step 1 Function v (j) must be programmed as a function subprogram, to make the program as general as possible.

Step 2 Enter initial values of all the constants to solve the equations

Step 3 Break long equations down into smaller forms so that computation can be easy and understandable

Step 4 Compute the values of transformation constants and multiplying constants

Step 5 Set an array for the values of the voltage and set iteration value from 0 to 50

Step 6 Write out and proceed to compute the value of the current.

Step 7 Iterate many values of current I, from the array declared using Voltage V, since there are two unknowns in the equation.

Step 8 Check if convergence condition, i.e., voltage value is greater than 50, is satisfied. If it is so, end program.

Step 9 If convergence solution is not satisfied, go back and compute the next current value and corresponding power value

Step 10 Repeat procedure from step 5 on. Stop if the number of iterations is more than 50.

Step 11 Write out current and power values.

Step 12 Plot graphs of current –Voltage and power –Voltage.

4.2 Flowchart

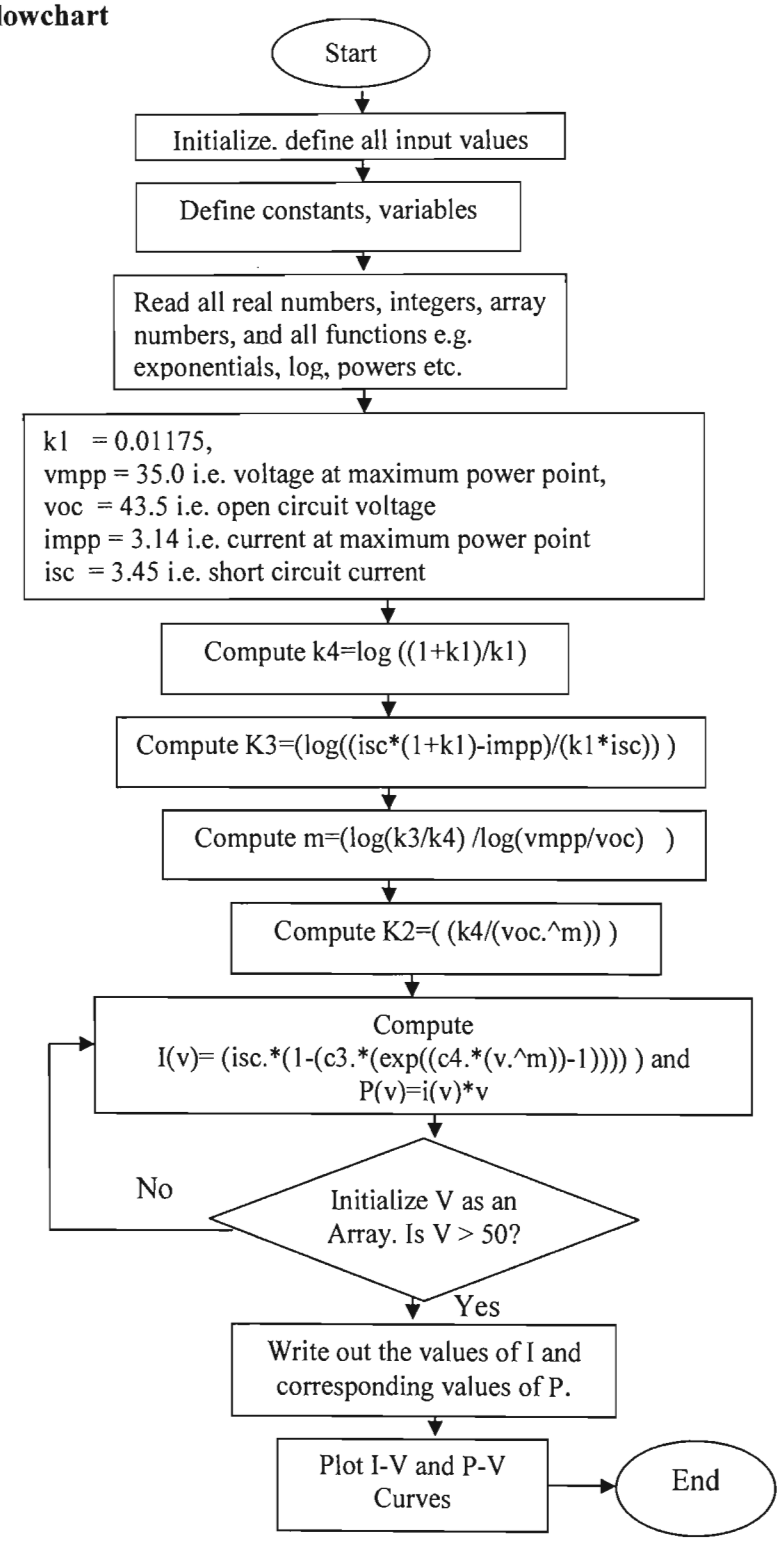

Figure 4-1: Pseudocode of the Mathematical Model.

4.3 MATLAB Model of the PV Generator

MATLAB® *(matrix laboratory)* is a high-performance language for technical computing. It integrates computation, visualization, and programming in an easy-to-use environment where problems and solutions are expressed in familiar mathematical notation [50]. MATLAB was used because it has always been known as a good software for Modeling, Analysis Tools (Existing, Custom), data Acquisition, Multi-platform, Multi Format data importing, Statistics and graphing [51, 52].

Equations 3.1 to 3.19 in chapter three were used in MATLAB to model a 550W, Shell SM110-24 solar panels. Module manufacturers normally provide I_{sc} , V_{oc} , V_{mpp} , I_{mpp} , and I-V characteristic parameters at Standard Test Conditions (STC) of AM 1.5 , irradiance 1000W/m^2 and 25°C. Table 4-1 shows at STC for the 110W Shell SM110-24 solar panel used. Data are obtained from the module datasheet [31].

Table 4-1: Parameters for Shell SM110-24 Solar Panel at STC

PARAMETER	VALUE
Maximum Power Rating, P_{mpp}	110W
Minimum Power Rating , P_{min}	104.5W
Current at MPP , I_{mpp}	3.142A
Voltage at MPP , V_{mpp}	35V
Short Circuit Current, I_{sc}	3.45A
Open Circuit Voltage , V_{oc}	35V
Short circuit current temperature coefficient , α_{scT}	1.4mA/ °C
Open circuit voltage temperature coefficient , β_{ocT}	-152mV/ °C
NOCT (Normal Operating Cell Temperature)	
Insolation , G=800W/m2 , Ta= 20°, wind velocity = 1m/s	

The model parameters are evaluated during execution using the mathematical modeling equations contained in the script. The current ***I*** is then evaluated using these parameters, and the variables namely voltage and electric power. If one of the input variables is a vector, the output variable (current) is also a vector. The inclusion of a series resistance in the model makes the solution for current a recurrent equation (refer to equations 3.1-3.24 in chapter three). A simple iterative technique converged for all currents values. A listing of the MATLAB script which was used to implement the equations is shown in Appendix A.

4.3.1 MATLAB Simulation Results

The output of the MATLAB function is shown for various irradiation levels using different current values Figures. 4.2 and 4.3. A number of discrete data points are shown on the curves in figures 4.2 and 4.3. These are points taken directly from the manufacturer's published curves, and shows excellent correspondence to the model. The I-V characteristic from the model is shown in figure 4.2.

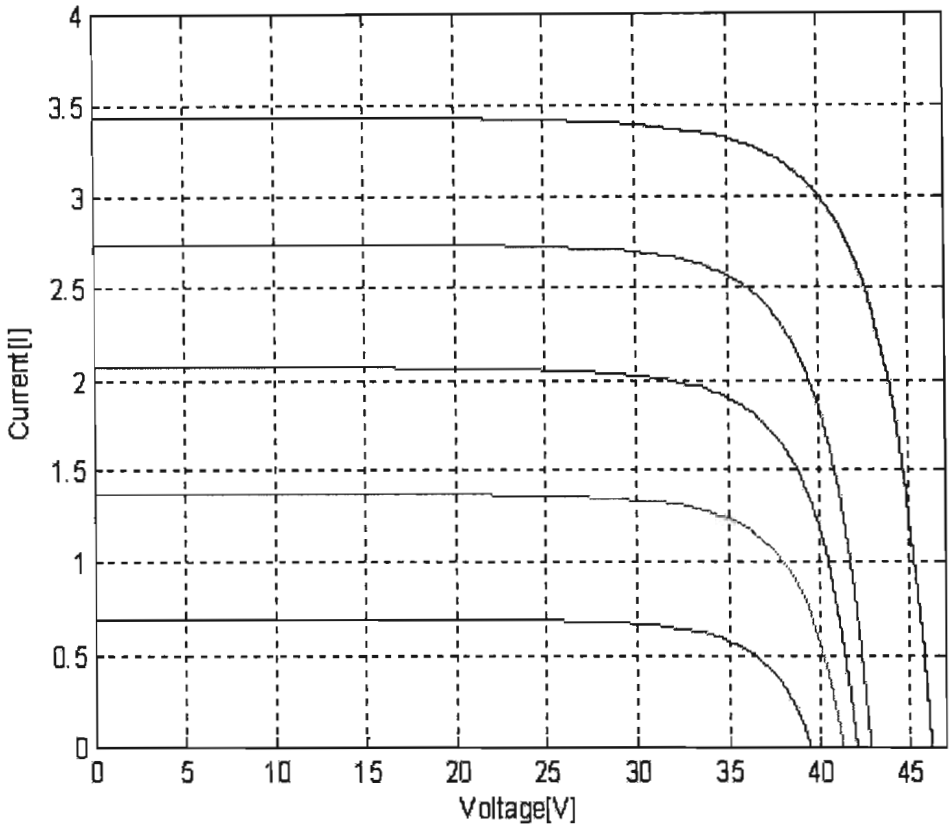

Figure 4-2: Current-voltage Characteristics of the PV Generator.

Figure 4.3 shows the power-voltage relationship of the solar panel. The power curves are obtained from the product of the I-V curves as shown in figure 4.2. The maximum power obtained for an insolation of 100% can be seen from the figure to be very close to 110W. This validates the maximum power value (P_{mpp}) as stated on the solar panel data sheet.

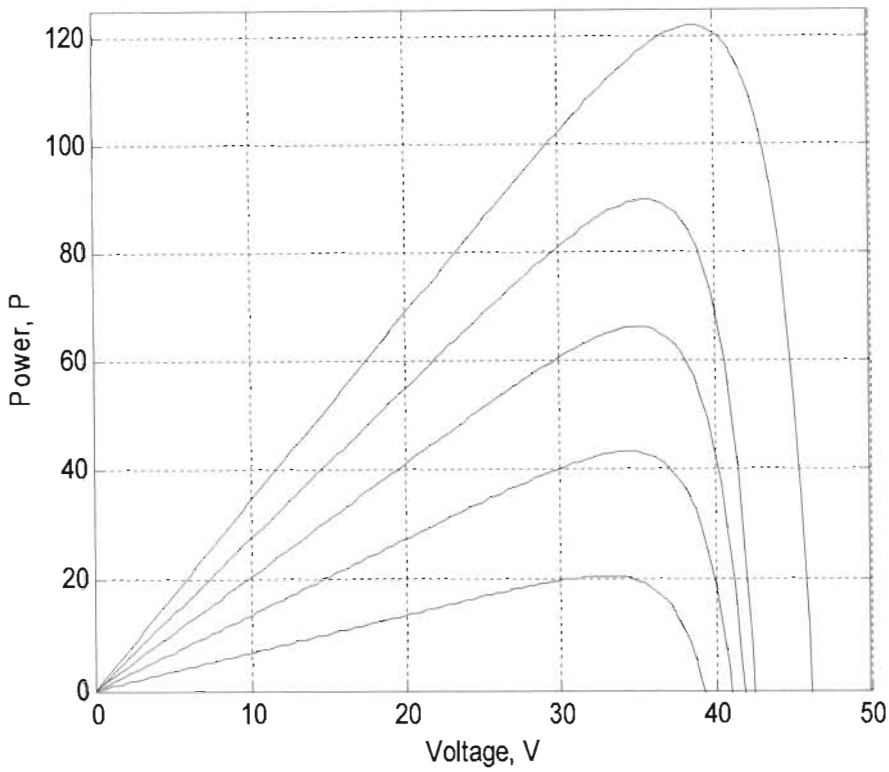

Figure 4.3: P-V characteristics of the PV Generator for five different levels of insolation.

4.4 Digital Visual Fortran (DVF) Model of the PV Generator

Digital Visual Fortran (DVF) was developed basically for science and engineering applications. Historically, the Engineering community has used FORTRAN to communicate algorithms in scientific literature and to build mathematical and statistical software[53]. FORTRAN remains strongly supported for writing and optimally compiling numerical algorithms. The programme provides an interface between high performance data parallel computing model and other models such as message passing and scalar models for single logical threads of control [54].

The program codes developed and used for the mathematical model of the PV system is shown in Appendix B1. Figure 4-4 shows the screen view of the Visual Digital Fortran programme which was used to analyze the mathematical model of the PV generator system

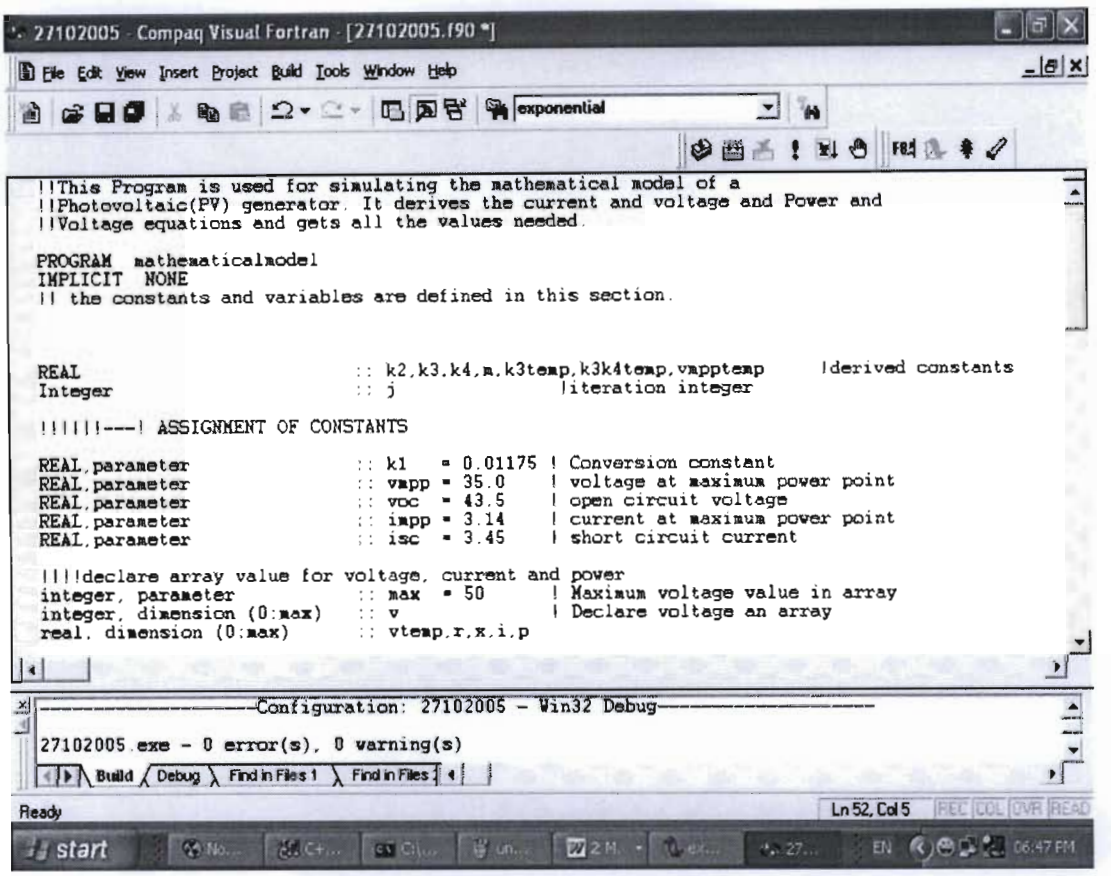

Figure 4-4: Screen view of the Digital Visual Fortran Program.

4.4.1 DVF Simulation Results

The simulation results are shown in figures 4-5 and 4-6. The I-V and P-V curves follow the same trends as seen using MATLAB graph output. This written code in FORTRAN was used to validate the mathematical modeling of the PV using MATLAB. The shapes of the I-V and P-V curves are exactly the same as those obtained when MATLAB was used for the modeling.

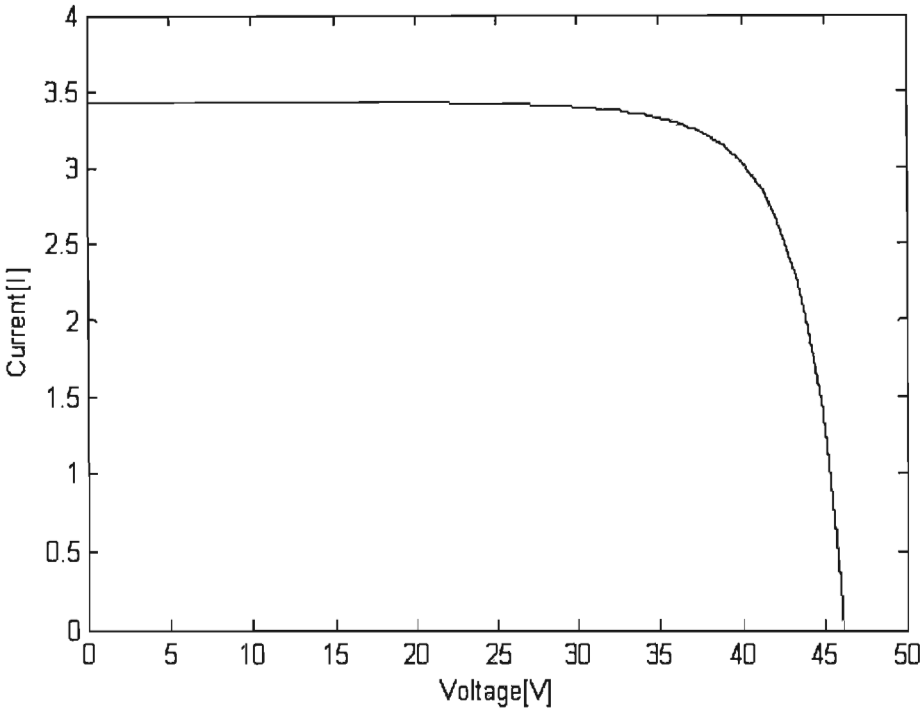

Figure 4-5: P-V characteristics of the PV Generator using Digital Visual Fortran.

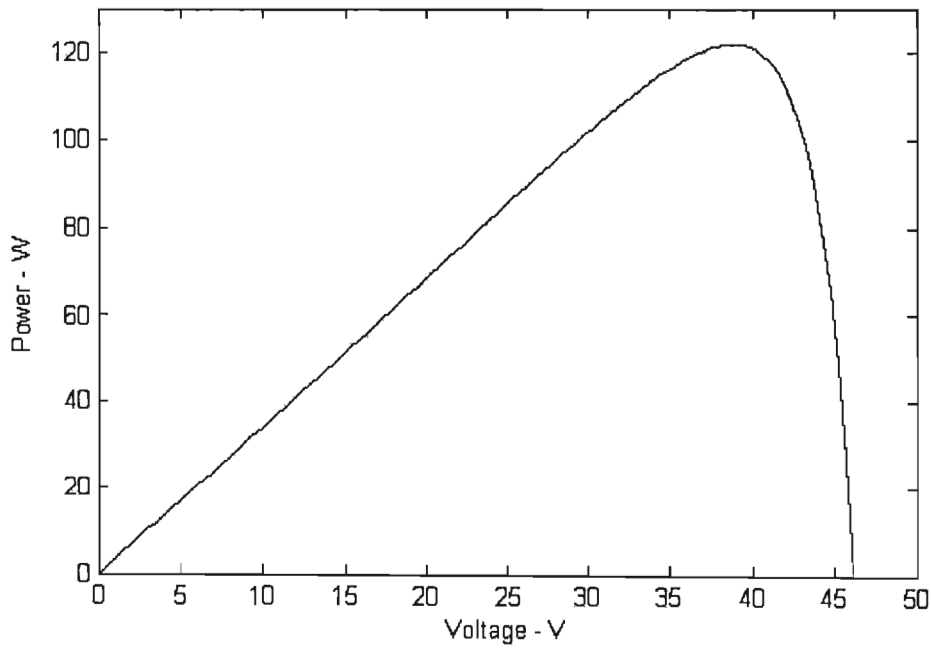

Figure 4-6: P-V characteristics of the PV Generator using Digital Visual Fortran.

4.5 C++ Model of the PV Generator

The C++ programming language is used to create a wide variety of modern computer programs. Program analysis can assist in improving human understanding of code, generating specifications and improving software quality and security. Hence, it is one of the programming languages used for communications data systems, simulation and modeling [55]. The C++ codes used for the mathematical modeling are shown in appendix B2. Figure 4-7 shows the screen view of the C++ programme to solve the mathematical model of the PV generator system

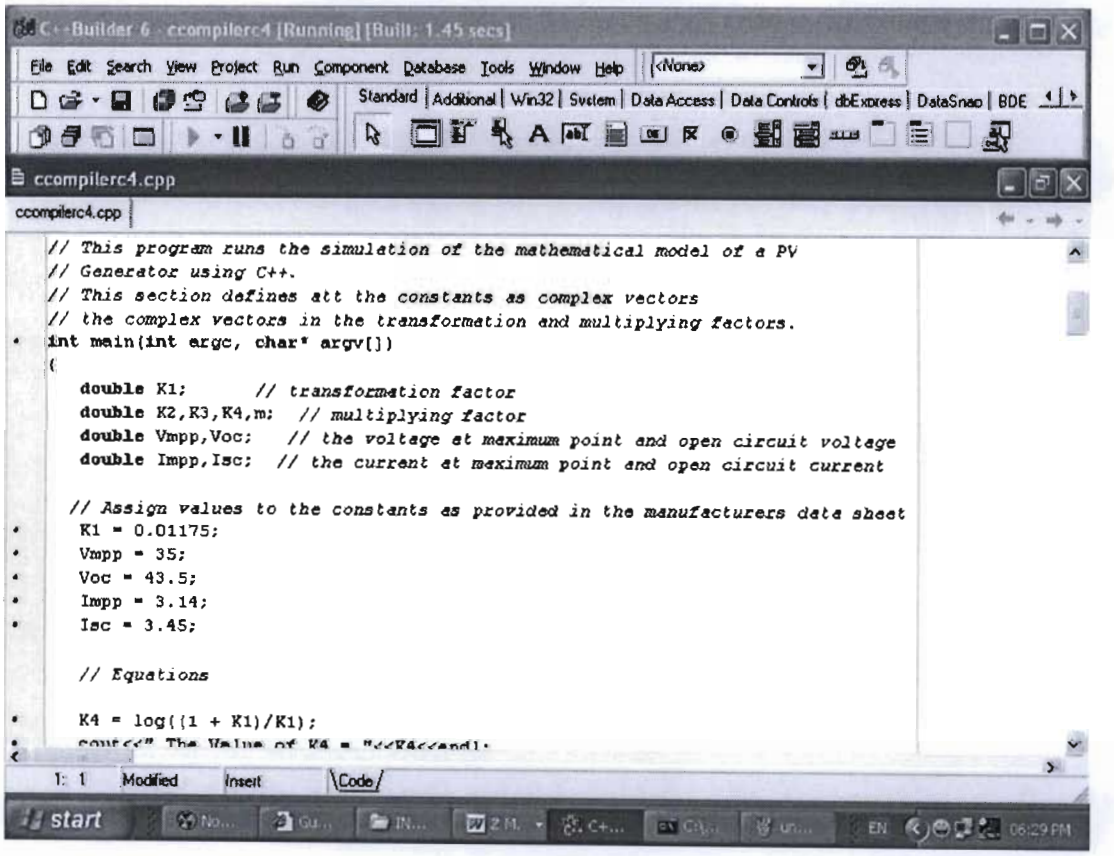

Figure 4-7: Screen view of the C++ Program.

4.5.1 C++ Simulation Results

Similarly, results from the software code written in C++ were compared and also used to validate the mathematical modeling of the PV using MATLAB and DVF. The C++ simulation results are shown in figures 4-8 and Figure 4-9. The I-V and P-V curves follow the same trends as seen using MATLAB and Visual Digital Fortran graphical output.

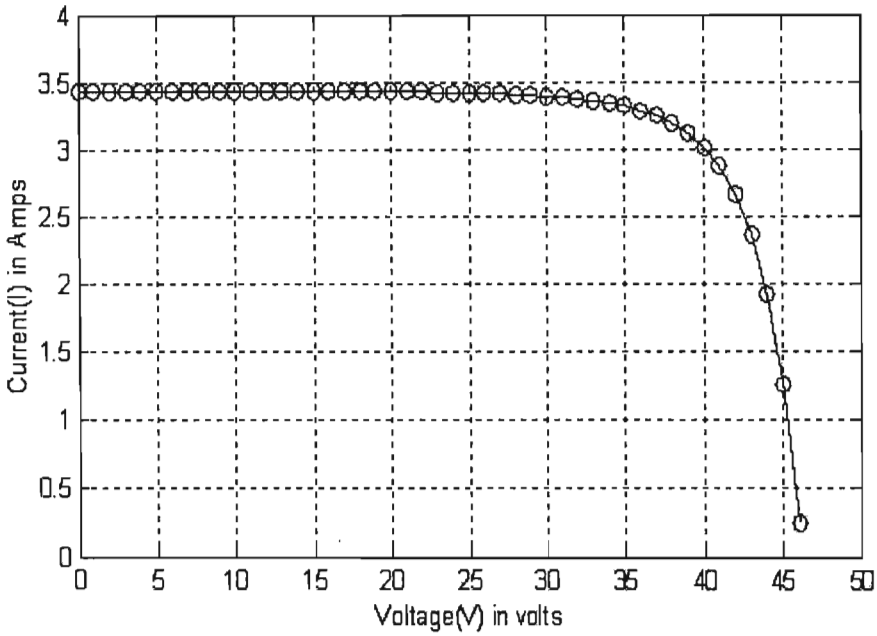

Figure 4-8: I-V characteristics of the PV Generator using C++.

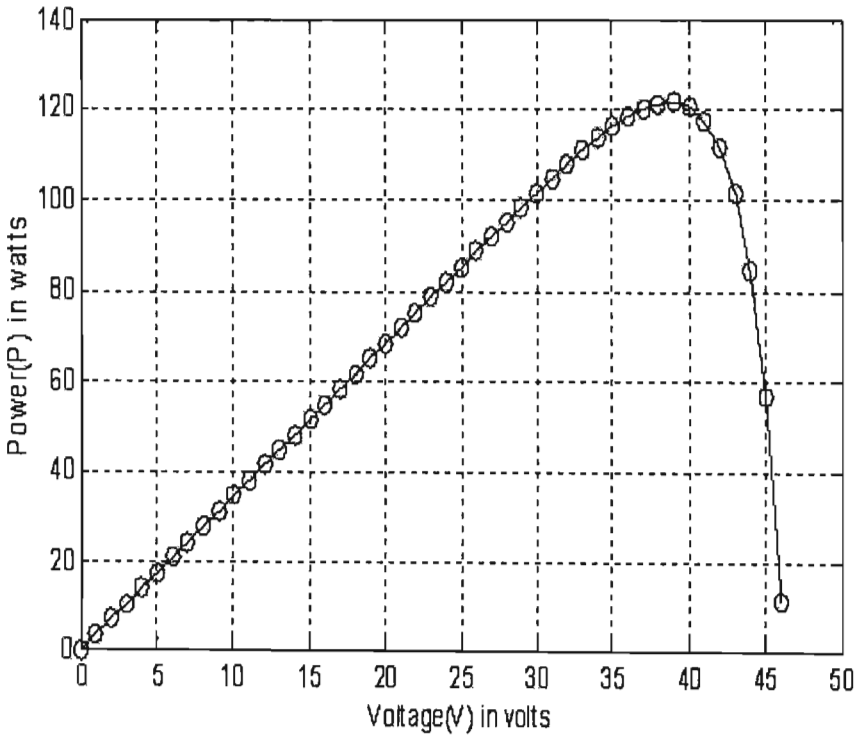

Figure 4-9: P-V characteristics of the PV Generator using C++.

4.6 Deductions from MATLAB, DVF and C++ models

An accurate PV module, electrical model is presented and demonstrated in MATLAB, DVF and C++ for a typical 550W solar panel. Given solar insolation and temperature, the models returns a current vector for a given voltage vector.

This model is used to compare the mathematical analysis of the PV under test conditions with the manufacturer's specification. It validates the mathematical model from the graphs of the I-V and P-V under different conditions of insolation and temperature. The MATLAB, DVF and C++ models also shows that there is a sufficient accuracy in the manipulation of the I-V Curves because with different current values, the curves still followed a similar trend (shape). Hence, it is capable of predicting the array performance under specified array operating conditions e.g. temperature and illumination levels. It can be concluded that the MATLAB, DVF and C++ models can be used to verify the Shell SM 110-24 array [31] specifications because all the simulation results using these software tools are similar with no deviations from the results obtained.

CHAPTER FIVE

EXPERIMENTAL TESTING OF THE PVG SYSTEM

Figure 5-1 shows the assembly of the PVG system, with AC and DC loads being fed concurrently.

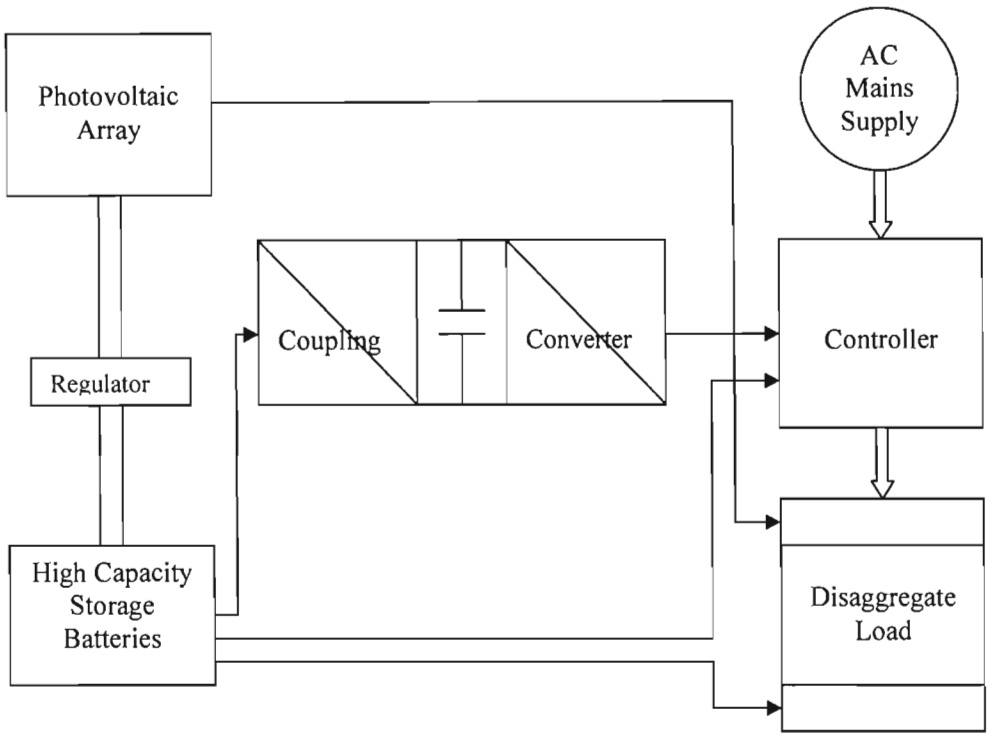

Figure 5-1: PVG System

Although the testing of individual units and components of the PVG system were very successful providing good results as reported in chapter two, the testing of the complete PVG system was challenging, which is not unusual for typical systems. To further reinforce the existing system, two major steps have been taken, first, to implement a robust monitoring system proposed in Figure 5-2, and procurement of six more high-energy storage battery units, to increase the power capacity of the system.

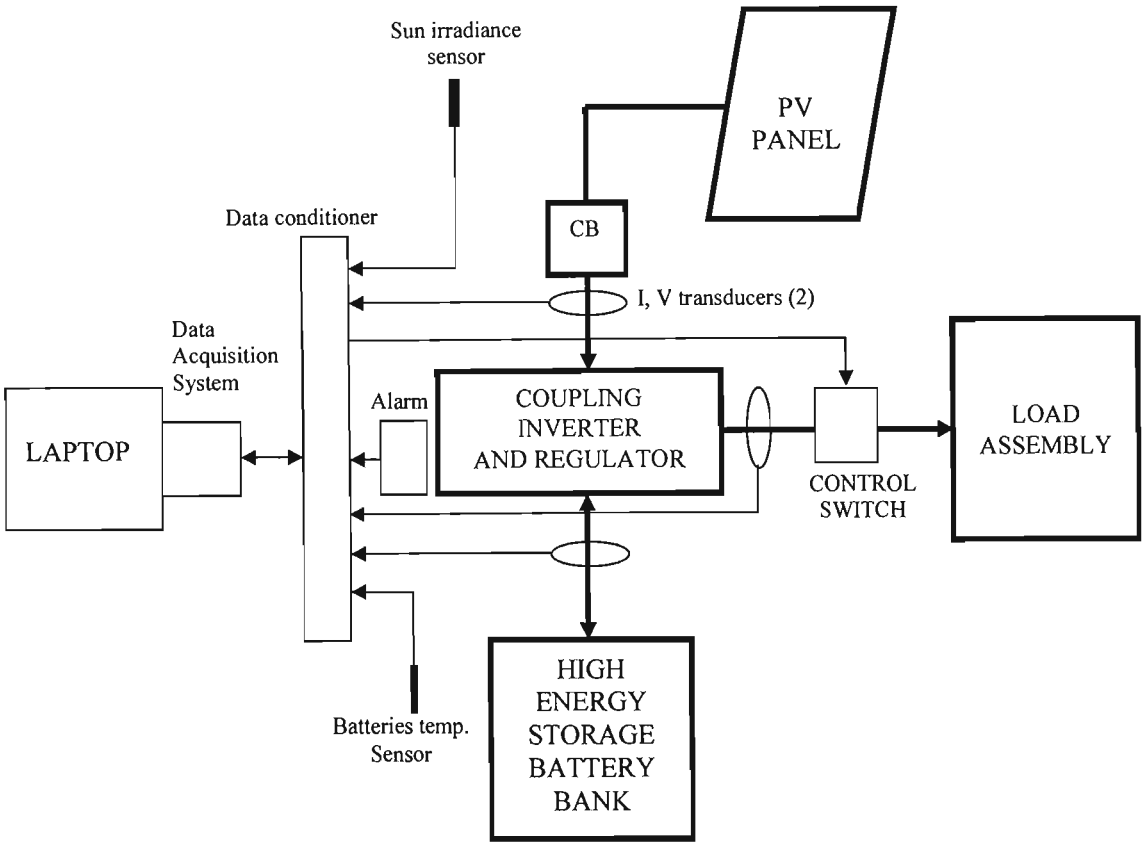

Figure 5-2: PVG Monitoring System Layout [38]

5.1 Dynamics of the solar panel

The dynamic performance analysis of the PV was carried out when directly coupled to different types of load and loading level. The first load type is a battery load. The graph in Figure 5-4 shows the behaviour of an ideal battery situation and a realistic battery performance. During the daytime, solar panel voltage is greater than the load voltage and in the night, the load voltage is greater than the solar panel voltage. The diode is added to the system to prevent the battery from discharging.

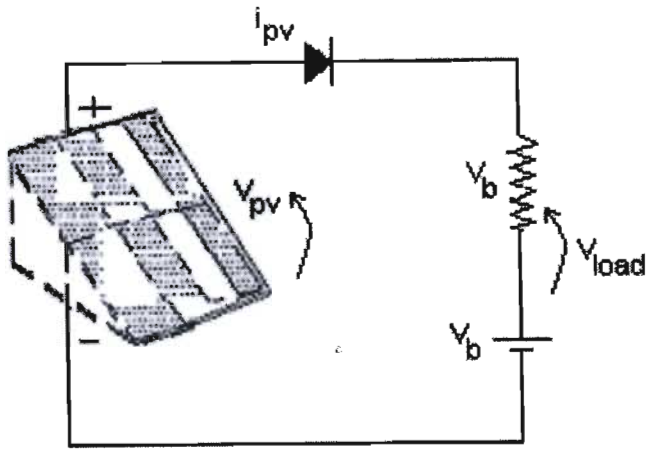

Figure 5-3: PV array connected directly to a battery load.

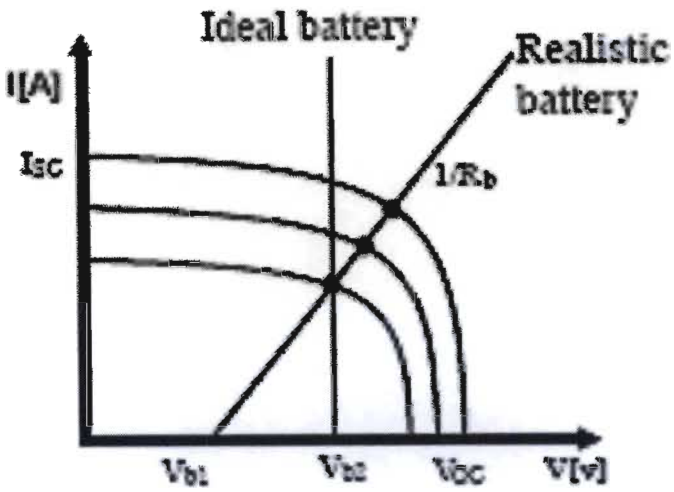

Figure 5-4: I-V Curve for an ideal battery and a practical / realistic situation.

5.2 Battery Testing and Specification

The capacity of the battery is a measure of how much energy can be extracted from the battery. It is often quoted in terms of amp-hours (Ah).

To supply 5A for 10hrs from a battery for example, it requires a capacity of: 5 x 10 = 50Ah.

The capacity of a battery depends on how quickly/slowly it is discharged or charged. It is generally measured in Ampere-hours and is denoted by C_n. This is defined as follows. If a battery has a capacity of x Ah at the C_n rate, then it will supply a constant current of (x/n) amps for n hours before being classed as flat, or fully discharged. The flat or fully

discharged condition is generally taken as being when the battery voltage falls to a value between 1.75 to 1.85 volts per cell [56].

For example, a battery has a C_{100} rating of 366 Ah and a C_{10} rating of 240 Ah, as given on manufacturer's specification sheets. This means that the battery will supply $(366/100)$ amps or 3.66 amps for 100 hours before it is flat (in this case, before it reaches a voltage of 1.85 volts per cell). It will also supply $(240/10)$ amps or 24 amps for 10 hours before reaching the same low voltage cut-off point. This is clear evidence that the faster the battery is discharged, the lower the capacity that is available from the battery.

It should be noted that the data supplied by manufacturers is generally for ambient temperatures of 25°C. In practice, batteries will experience quite a range of temperatures, and the capacity varies with temperature. As a general rule the battery capacity will decrease as the temperature decreases. The effect of very low temperatures is more severe for higher rates of discharge.

5.2.1 Methodology for Sizing a Battery Bank

For our renewable energy application, sizing of the energy-storage unit is essential to the overall performance of the system. A battery bank consists of a string of batteries in series to obtain the required system voltage and a number of strings in parallel (if required), to obtain the required battery capacity. The actual capacity of a battery bank required depends on the number of days of the load required to be met from the bank, the depth of discharge to which the battery is allowed to fall, and the efficiency of any power conversion equipment between the battery and the load [56].

$$E_c = \frac{n \times P_{LD}}{D_{OD} \times \eta_{PC}} \qquad (5.1)$$

where E_c is the required battery capacity (kWh), P_{LD} is the daily load or average daily load supplied by the system in kWh, D_{OD} is the maximum allowed depth of discharge for the battery, n is the period (or number of days the load is supplied), and η_{PC} is the efficiency of any power conditioning equipment between the battery and the load.

The battery capacity in Ah is then calculated by dividing the battery capacity in kWh by the system voltage. This will be Ah required from all the strings of different batteries in parallel. It is then necessary to select a particular battery and by looking at the battery specification,

then a battery can be chosen as well as the number of strings needed. The general rule would be to select the largest viable battery size so as to reduce the number of strings in parallel. Ideally one string of batteries would provide the least number of battery connections and the least number of batteries to check during routine maintenance. In addition, different strings in parallel configurations can lead to additional problems because of slight differences in the characteristics of the batteries in each string. In assessing Ah rating, it is important to use values representative of the discharge condition that will be met in the specific application [57].

5.2.2 Battery Discharge Tests

5.2.2.1 Using a Single Unit of 12Ah battery

Discharge tests were performed on a single unit of 12Ah battery. The discharge time was measured by discharging the batteries through a resistive load as shown in table 5-1.

Table 5-1: Battery discharge test for a single unit and 10units of 12Ah batteries respectively

Battery Discharge tests						
Single unit of 12Ah Battery				10 units of 12Ah Batteries		
	Voltage	Current	Power	Voltage	Current	Power
Time(Min)	V_1(V)	I_1(A)	P_1(W)	V_2(V)	I_2(A)	P_2(W)
0	12.23	10	122.28	12.23	10	122.3
5	12.21	10	122.1	12.22	10	122.2
10	12.19	10	121.87	12.22	10	122.2
15	12.16	10	121.6	12.22	10	122.2
20	12.15	10	121.47	12.21	10	122.1
25	12.13	9.91	120.21	12.21	9.91	121.0
30	12.12	9.91	120.09	12.21	9.91	121.0
35	12.10	9.91	119.91	12.2	9.91	120.9
40	12.08	9.81	118.54	12.2	9.81	119.7
45	12.06	9.81	118.31	12.2	9.81	119.7
50	12.04	9.81	118.11	12.2	9.81	119.7
55	12.02	9.81	117.92	12.19	9.81	119.6
60	12.01	9.76	117.24	12.19	9.76	119.0
65	12.00	9.76	117.12	12.19	9.76	119.0
70	11.98	9.76	116.92	12.19	9.76	119.0
75	11.96	9.71	116.13	12.19	9.71	118.4
80	11.95	9.71	116.05	12.18	9.71	118.3
85	11.94	9.71	115.94	12.18	9.71	118.3
90	11.92	9.61	114.56	12.18	9.61	117.1
95	11.90	9.61	114.36	12.18	9.61	117.0
100	11.89	9.61	114.28	12.18	9.61	117.1
105	11.88	9.61	114.17	12.18	9.61	117.0
110	11.87	9.61	114.11	12.18	9.61	117.1
115	11.86	9.61	113.97	12.18	9.61	117.0
120	11.85	9.61	113.90	12.17	9.61	117.0

125	11.84	9.56	113.19	12.17	9.56	116.3
130	11.83	9.56	113.08	12.17	9.56	116.4
135	11.82	9.56	113.00	12.17	9.56	116.3
140	11.80	9.51	112.24	12.17	9.51	115.7
145	11.79	9.51	112.12	12.17	9.51	115.7
150	11.78	9.51	112.06	12.17	9.51	115.7
155	11.77	9.51	111.93	12.17	9.51	115.7
160	11.76	9.51	111.86	12.17	9.51	115.7
165	11.74	9.51	111.65	12.17	9.51	115.7
170	11.73	9.51	111.56	12.17	9.51	115.7
175	11.72	9.51	111.46	12.17	9.51	115.7
180	11.71	9.51	111.40	12.17	9.51	115.7
185	11.69	9.51	111.17	12.16	9.51	115.6
190	11.68	9.51	111.13	12.16	9.51	115.7
195	11.67	9.51	110.98	12.16	9.51	115.6
200	11.66	9.51	110.88	12.16	9.51	115.7
205	11.65	9.51	110.79	12.16	9.51	115.6
210	11.64	9.51	110.67	12.16	9.51	115.7
215	11.62	9.41	109.34	12.16	9.41	114.4
220	11.60	9.41	109.20	12.16	9.41	114.4
225	11.59	9.41	109.06	12.16	9.41	114.4
230	11.58	9.41	108.94	12.16	9.41	114.4
235	11.56	9.41	108.78	12.16	9.41	114.4
240	11.55	9.41	108.70	12.16	9.41	114.4
245	11.53	9.41	108.50	12.16	9.41	114.4
250	11.52	9.31	107.24	12.16	9.31	113.2
255	11.50	9.31	107.07	12.16	9.31	113.2
260	11.48	9.31	106.88	12.16	9.31	113.2
265	11.46	9.31	106.69	12.16	9.31	113.2
270	11.45	9.31	106.59	12.16	9.31	113.2
275	11.44	9.31	106.51	12.16	9.31	113.2
280	11.42	9.31	106.29	12.16	9.31	113.2
285	11.40	9.31	106.13	12.16	9.31	113.2
290	11.38	9.31	106.00	12.16	9.31	113.2
295	11.36	9.31	105.76	12.16	9.31	113.2
300	11.34	9.11	103.28	12.16	9.11	110.8
305	11.32	9.11	103.13	12.15	9.11	110.7
310	11.30	9.01	101.80	12.15	9.01	109.5
315	11.27	9.01	101.54	12.15	9.01	109.5
320	11.25	9.01	101.41	12.15	9.01	109.5
325	11.22	9.01	101.09	12.15	9.01	109.5
330	11.20	9.01	100.94	12.15	9.01	109.5
335	11.17	9.01	100.64	12.15	9.01	109.5
340	11.13	9.01	100.25	12.15	9.01	109.5
345	11.11	9.01	100.10	12.15	9.01	109.5
350	11.08	9.01	99.80	12.15	9.01	109.5
355	11.04	9.01	99.47	12.15	9.01	109.5
360	11.01	9.01	99.25	12.15	9.01	109.5

A discharge curve was plotted for the single battery.

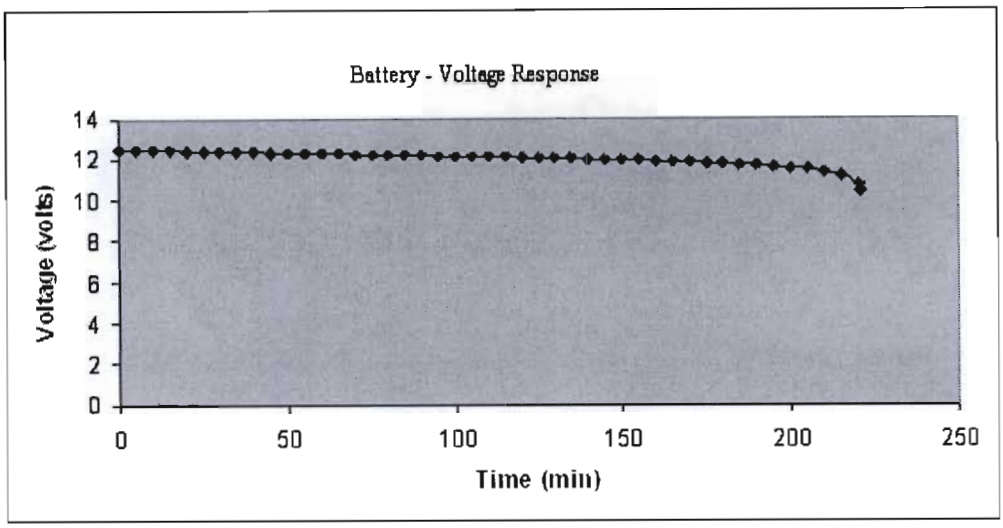

Figure 5-5: Discharge curve of a lead acid battery at 10A with capacity of 12Ah.

It can be seen that for most of the discharge curves the voltage is relatively constant, but when the battery is almost discharged, the voltage collapses suddenly. The reverse occurs during charging. For most of the charging process the battery voltage is relatively constant and then when it is getting close to being charged the voltage suddenly rises. If the charging rate is high, the battery may not be fully charged when the voltage rise occurs and so a reduction in the charging current will see more charge added to the battery.

The power/time, current / time, and voltage / time characteristic was measured and plotted. Figures 5-6, 5-7 and 5-8, show the power, voltage and current discharge durations respectively.

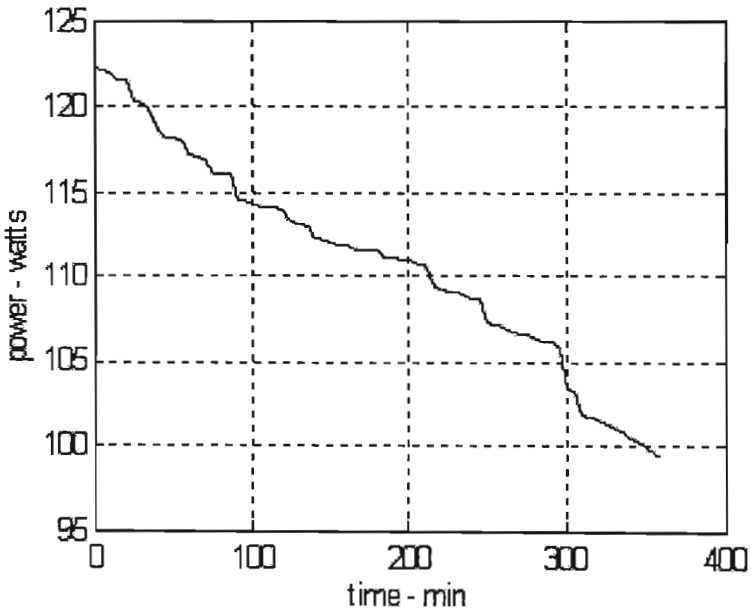

Figure 5-6: Power vs. Time for a 10-A load battery discharge on a single 12Ah battery

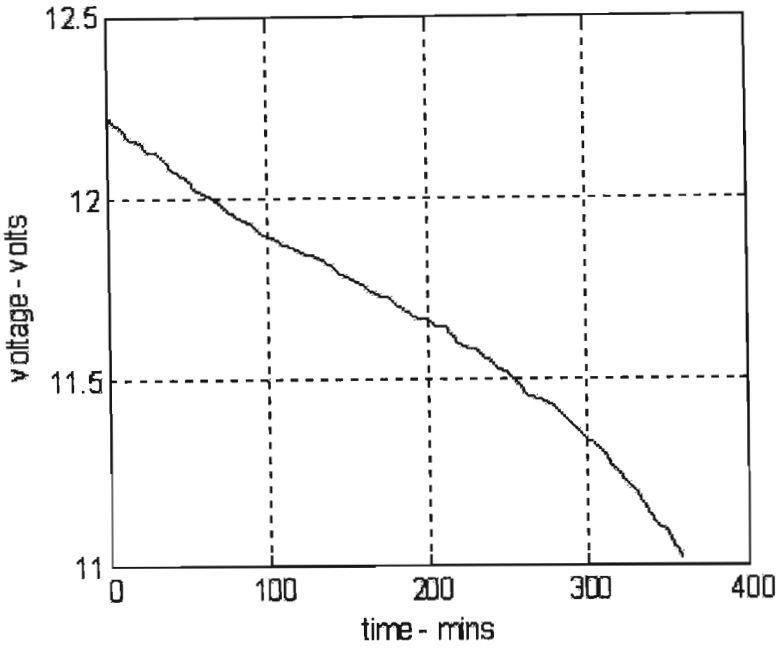

Figure 5-7: Voltage vs. Time for a 10-A load battery discharge on a single 12Ah battery

[Note: The MATLAB m-file used in plotting the graphs is shown in Appendix C1.]

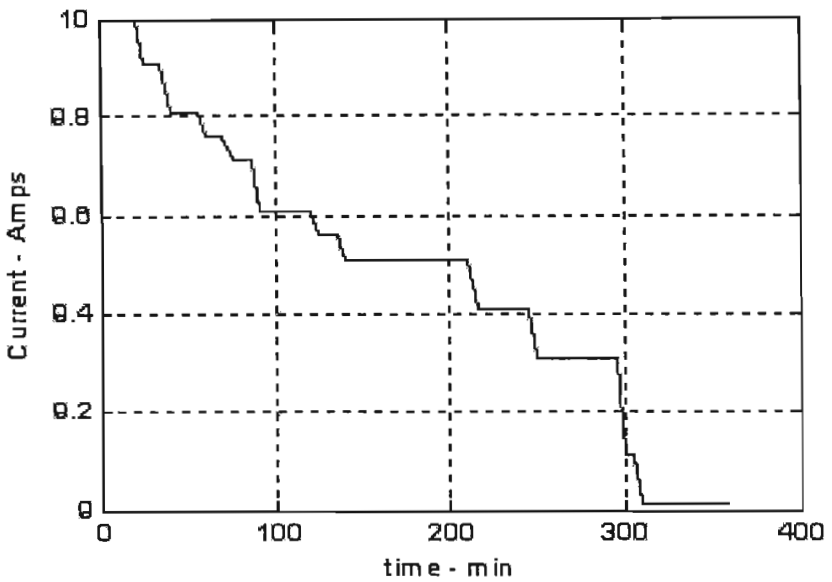

Figure 5-8: Current vs. Time for a 10-A load battery discharge on a single 12Ah battery

It can be observed from Figures 5-6 to 5-8, the discharge time for the battery was 360 minutes. The output voltage from the battery was 12V but declined gradually until it got to

11V. The resistive load that was used for the discharge had a load of 0.75 ohms. It was observed that the battery discharged as the voltage reduces. The time of discharge was much about 360 minutes before the voltage level reduced to 10-15% of its threshold value. This shows that for the battery to perform better in electric power applications, the slower the rate of voltage drop with discharge time, the better.

In order to have a better understanding of the performance of the battery as an alternative source when the PV system is not generating power, more batteries were added to the test facility.

5.2.2.2 Using a 10-unit Battery-bank Test in Parallel Back-to-Back Topology

Discharge tests were performed on 10 units of 12Ah battery. The discharge time was measured by discharging the batteries through a resistive load, and the power/time, current / time, and voltage / time characteristic were measured and plotted. Figures 5-9, 5-10 and 5-11, show the power, voltage and current discharge durations respectively.

It was however observed that the discharge time for the battery was in the order of 360 minutes. The output voltage from the battery was also 12V. The voltage was maintained at 12V because all the 10units of batteries were connected in parallel. The resistive load that was used for the discharge had a load of 75 ohms. It was observed that the battery discharge rates had almost constant resistance values, but the load currents were very high. The load current was 10A but the voltage was constant at 12.16V for a very long time allowing more load to be added to the system before the battery discharged.

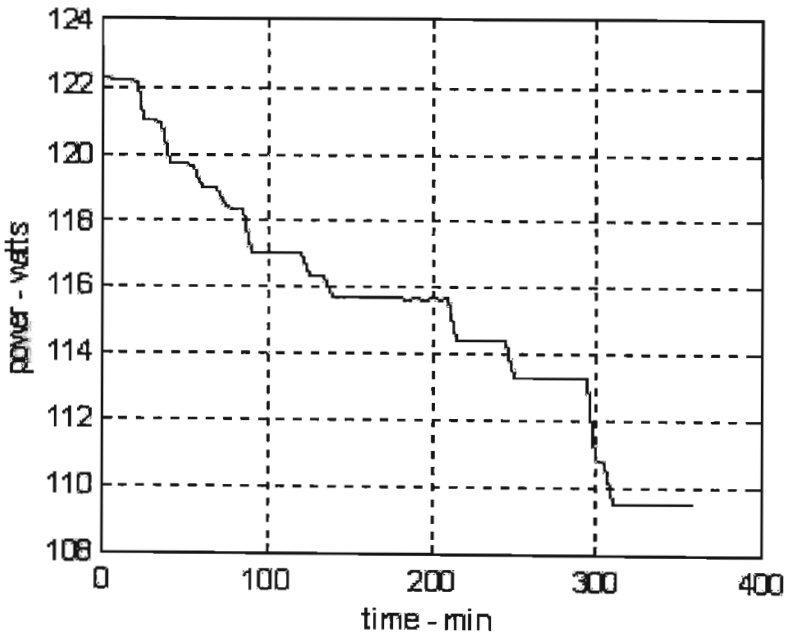

Figure 5-9: Power vs. Time for a 10-A load battery discharge on 10 Units of 12Ah battery

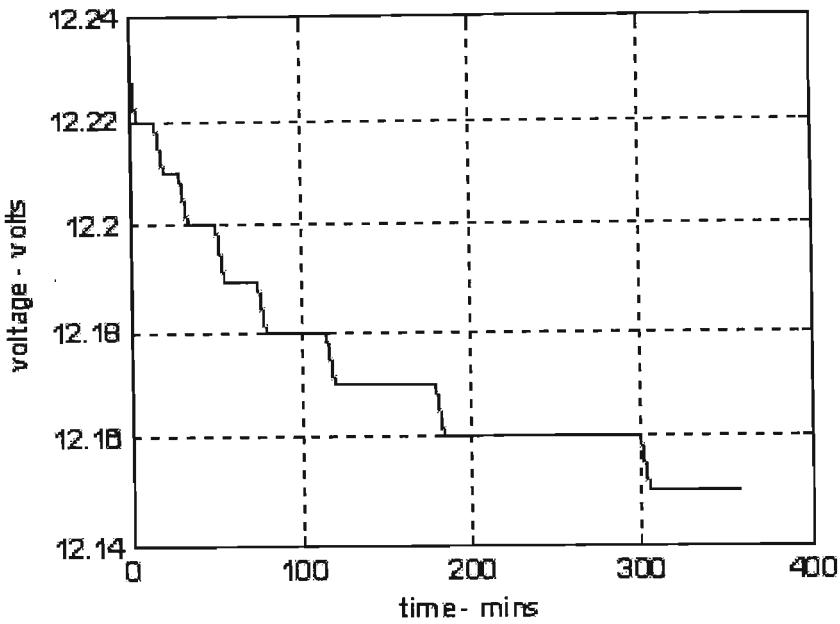

Figure 5-10: Voltage vs. Time for a 10-A load battery discharge on 10 Units of 12Ah battery

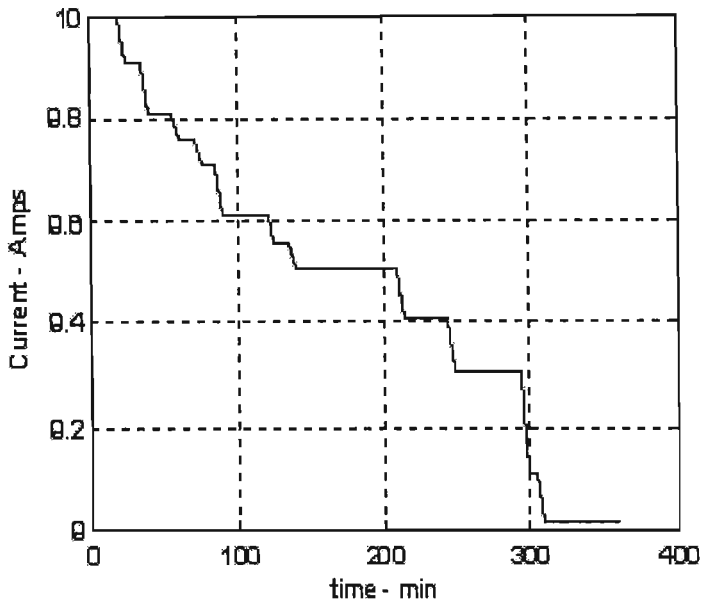

Figure 5-11: Current vs. Time for a 10-A load battery discharge on 10 Units of 12Ah battery

The relationships from these two measurements lead to two critical observations. The first was the discharge rate and duration for each batteries compared to the combined units. The second observation was the voltage drop on connection to load in both tests. Based on the statutory requirements for voltage drop ±6%, and the anticipated load to be served by the PV Generator system, an appropriate sizing and specification for the battery units was concluded

since small aggregate loads are intended for the study model in the test facility. It also showed that all the battery units should be connected in parallel configurations so that the voltage in the system can be kept constant while operating at high current.

5.3 Experimental Testing

Analytical work on the PV system model with load was carried out to establish useful relationships which will influence the control of disaggregate loads. The system is tested to assess the overall optimum performance of the existing system.

5.3.1 Experimental Test Results using a Universal Motor

Since many household and commercial loads extensively use single-phase motors, a model of the PV system coupled to a universal motor was analyzed and tested.

The universal motor presents a special case for a small-series motor that can be driven by either an AC or DC current source. The universal motor is a rotating electric machine similar to a DC motor but designed to operate either from direct current or single-phase alternating current. The stator and rotor windings of the motor are connected in series through the rotor commutator [58]. A 132W, 220V universal motor was used for modeling. (see specification in table 5-4)

Three tests were carried out in the laboratory to analyze the performance of the universal motor supplied by three different sources, which are DC supply source, AC supply source and PV supply source. The results were tabulated and the graphs were analyzed.

The PV system was used drive a universal motor with a DC source. An inverter was connected to the PV system in order to get 220V. A variac was used to increase the voltage values. The results obtained are shown in table 5-2.

Table 5-2: DC excitation tests on the PV Generator.

DC EXCITATION TEST

Voltage(V)	Current(I)	speed(rpm)	speed(rad/s)
20	0.14	365	38.23
30	0.17	1650	172.81
40	0.18	2615	273.88
50	0.19	3645	381.75
60	0.21	4535	474.97
70	0.23	5504	576.45
80	0.25	5815	609.02
90	0.27	6005	628.92
100	0.29	6634	694.80
110	0.31	7056	739.00
120	0.315	8290	868.24
130	0.315	8874	929.40
140	0.32	9610	1006.49
150	0.33	10319	1080.74
160	0.34	10885	1140.02
170	0.35	11351	1188.83
180	0.37	11873	1243.50
190	0.38	12354	1293.88
200	0.41	12785	1339.02
210	0.42	13321	1395.15
220	0.43	13781	1443.33

The PV system was used drive a universal motor with an AC source. An inverter was also connected to the PV system in order to get 220V. A variac was used to increase the voltage values to measure the corresponding speed and current at different voltage values. The results obtained are shown in table 5-3.

Table 5-3: AC Excitation Tests on the PV Generator.

AC EXCITATION TEST

Voltage(V)	Current (I)	Speed, n(rpm)	Speed, n(rad/s)
50	0.175	979	102.53
60	0.200	2065	216.27
70	0.230	3310	346.67
80	0.245	3495	366.04
90	0.255	4350	455.59
100	0.258	4780	500.63
110	0.290	5316	556.76
120	0.315	5841	611.75
130	0.335	6490	679.72
140	0.355	6860	718.47
150	0.370	7850	822.16
160	0.395	8250	864.05
170	0.420	8465	886.57
180	0.430	9680	1013.82
190	0.435	10540	1103.89
200	0.440	10850	1136.36
210	0.465	11365	1190.29
220	0.485	11946	1251.14

Both the AC and DC excitation tests were plotted together to compare the performance of the PV system when connected directly to an AC and a DC source in terms of speed and current. Tables 5-3 and 5-4 were plotted in MATLAB (See Appendix C3 for m.file for the graphs) and the AC and DC Speeds were plotted on the same graph for comparison.

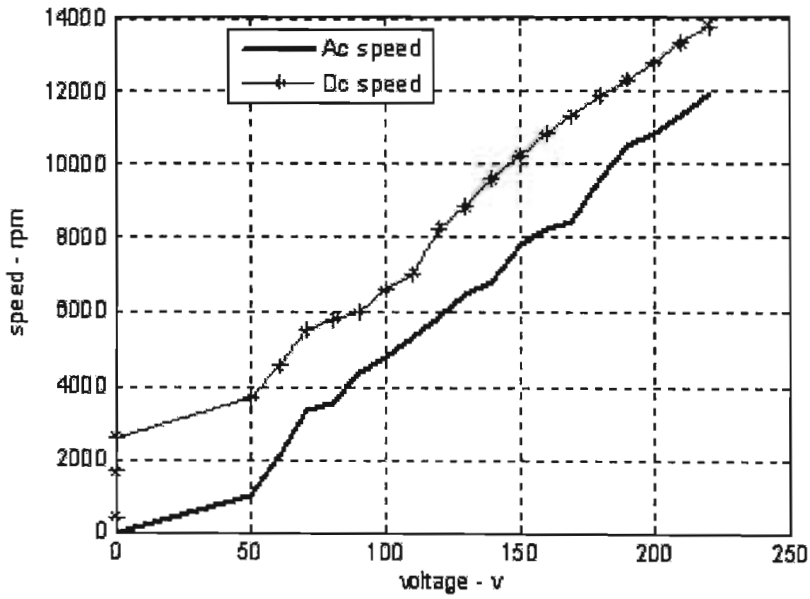

Figure 5-12: Graph comparing the AC and DC speeds of the PV Generator.

The curve above represents the AC and DC speeds of a Universal Motor coupled to an AC and a DC source respectively. The different range of voltages and currents were recorded and plotted. As seen from Figure 5-24, the speed obtained near rated voltage was 12000rpm for the ac source while the dc source had a slightly higher value of almost 14000rpm. This is quite similar to the universal motor rated speed of between 13000 – 15000rpm. The graph above shows that at nearly rated voltage, a speed of 12000rpm and almost 14000rpm were achieved for both the DC and AC sources. From the theory of the universal motor, it is clear that there is a relationship between the speed and the voltage in the universal motor; as the voltage increases, the speed also increases. However, if all the other factors in the equation are kept constant, there exists a direct relationship between the speed and voltage, but since these factors can not be assumed constant, the curve obtained is not a linear one.

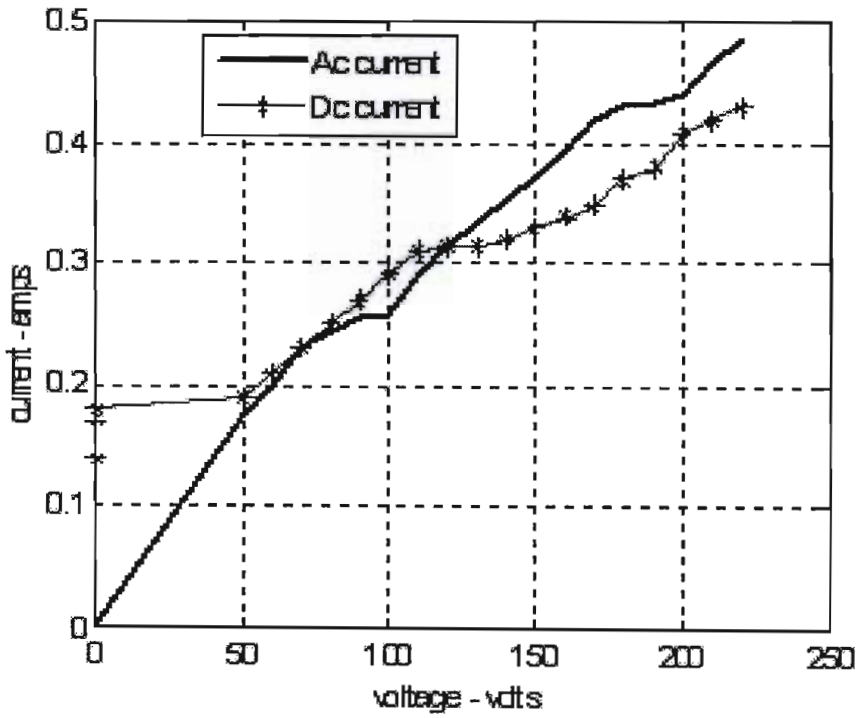

Figure 5-13: Graph comparing the AC and DC Currents of the PV Generator.

The graph above shows the AC and DC currents plotted against the voltage of a universal motor. As can be seen, at close to rated voltage, the currents drawn were very close to the actual rated speed. The values of currents drawn and recorded were between 0.4A and 0.5A, and the actual rated current of the machine was 0.6A. Due to the fact that there were some losses in the system, the performance of the motor was affected. Thus the rated current was not drawn during tests, and this is normally expected since machines will very rarely operate to its absolute maximum ratings. With an increase in voltage, the universal motor was seen

and expected to draw more current up till the rated voltage. An increase in current, proved by simple motor theory; shows that the speed will generally increase.

PV Excitation Tests were performed on the universal motor. The starting voltage was 80V and the corresponding speed of the universal motor was measured. The results obtained are shown in table 5-4.

Table 5-4: Illustrating the PV excitation test on the PV Generator.

PV Excitation Tests			
voltage (V)	current (A)	Speed(rpm)	Speed(rad/sec)
80	0.29	6425	672.91
75	0.25	6001	628.50
70	0.23	5646	591.32
65	0.23	5135	537.81
60	0.225	4420	462.92
55	0.22	4020	421.03
50	0.21	3640	381.23
45	0.2	3220	337.24
40	0.19	2878	301.42
35	0.15	2165	226.75
30	0.14	1600	167.57

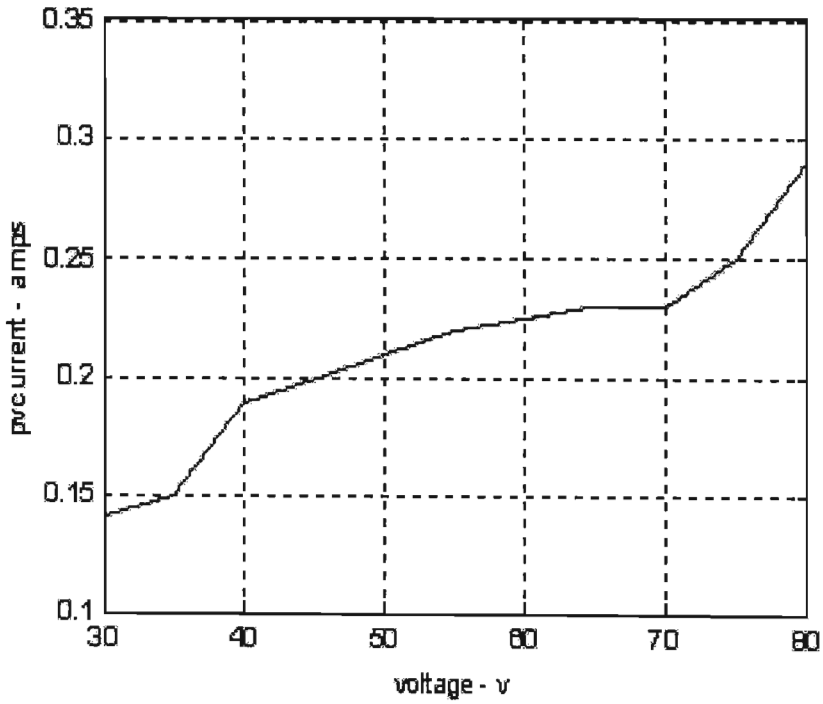

Figure 5-14: Graph illustrating the I-V curve of the PV excitation tests on the PV Generator.

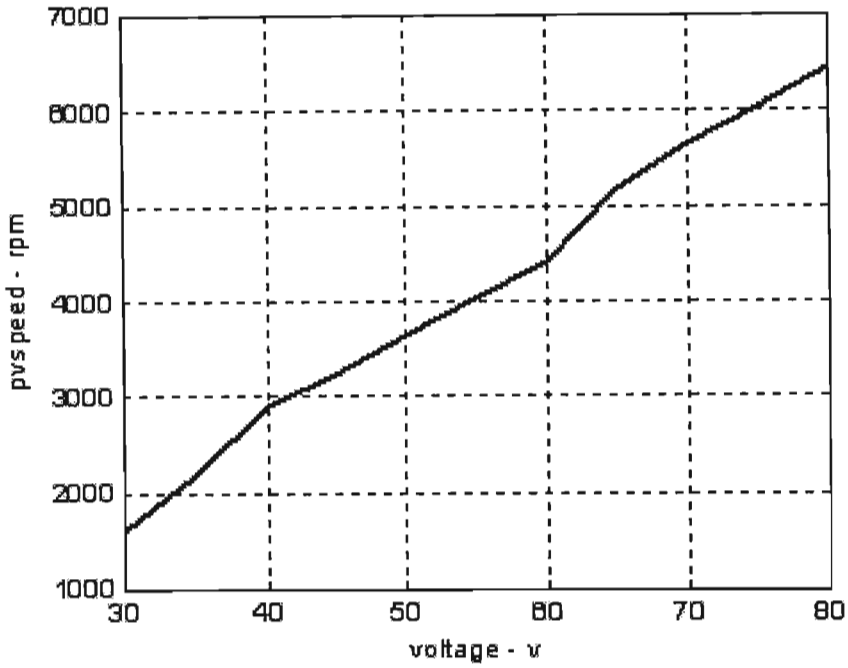

Figure 5-15: Graph illustrating the Speed-voltage curve of the PV excitation tests on the PV Generator.

From figure 5-14, the I-V plane of the motor connected directly to the generator showed that the starting current of the motor was 0.135A and the motor did not start initially. However, when the insolation increased, there was some stability in the system and the I-V curve was linear until it reached a threshold and there were some fluctuations because the insolation was not high enough to start up the motor. But, after some time, the current was proportional to the voltage following the ohm's law. For the power –voltage curve, it formed almost a linear curve because the voltage was steady against the power delivered from the PV generator.

The maximum speed the PV supply system gave was high. The ac current is higher than the dc current with high input voltages while in low input voltages, the dc current is higher than the ac current. This is due to ac circuit armature and field inductances which dc circuits don't have. The PV current of the motor behaves similarly to dc current from the dc supply source.

For the same terminal voltage and armature current the speed of the motor loaded to the PV was lower for ac excitation compared with dc excitation. This is illustrated in fig 5-12 and 5-13. AC excitation produces pulsating torque, poor power factor and lower speed. Poor power factor and lower speed are caused by the reactance voltage drop produced by field reactance, X_f and armature reactance X_a [59].

The speed-torque characteristics at steady state were modeled using MATLAB, (See Appendix C2). The motor data and results obtained from the analysis are shown in Table 5-2 [60] and Figure 5-16.

Table 5-5: Specifications of the Universal Motor Powered by the PV Generator.

Symbol	Value & units	Nomenclature
V	220 volts	Terminal Voltage
Ia	0.6 A	Armature current
R	2.2 ohms	Armature and field resistance
L	15mH	Armature and field inductance
Tm		Electromagnetic torque
Ke	0.3856	
J	0.02365 $Kg.m^2$	Moment of inertia
A	0.02N.m	Torque constant of rotational losses
B	0.00025 N.m/rpm	Viscous torque constant of rotational losses
	0.002387 N.m/rad/sec	
Km	0.0621	

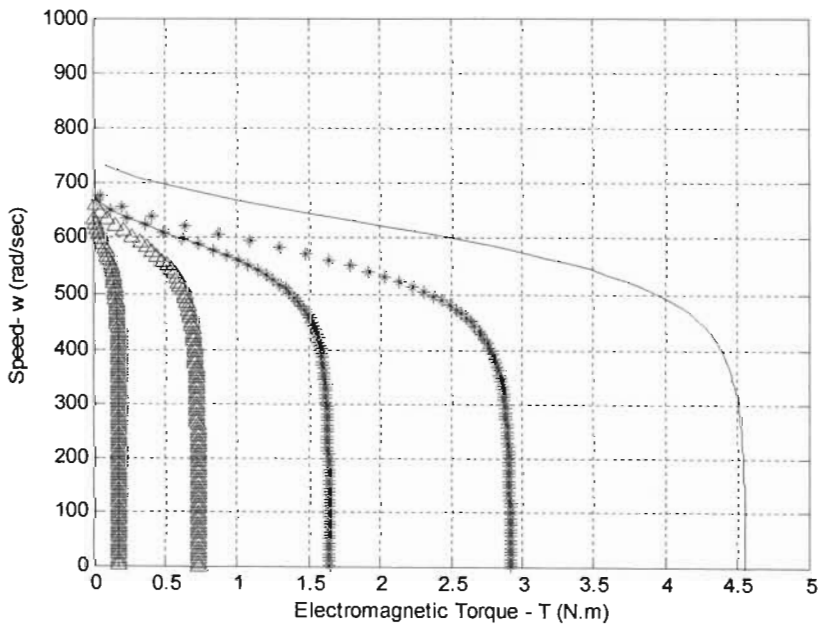

Figure 5-16: Torque-Speed Characteristic of a Universal Motor Powered by the PV Generator.

Figure 5.16 shows the universal motor speed-torque characteristics in the mechanical plane for five insolation levels. From this graph, it was observed that at low insolation, there were low speeds. However, the starting speed at low insolation can be improved if load is matched adequately with the PV system.

5.3.2 Experimental Test Results using a 60W light bulb

The second load powered by the PV system was a 60W light bulb. The light bulb was connected directly to the PV system. There was a control switch used in isolating the supply from the load (i.e. the light bulb). The light bulb was then switched on permanently until there was no longer enough power coming from the PV system. During this period, the power, current and voltage values were taken and recorded. Graphs on figures 5-17 and 5-18 (i.e. I-V and P-V) obtained from these values were both linear indicating that the experimental results authenticate the theoretical analysis of the I-V and P-V relationship of the normal conventional generators. The fact that the scaled ampere-hours generated by the PV exceeded the required load current of the household light bulb (if considered separately) proves the efficiency of solar power.

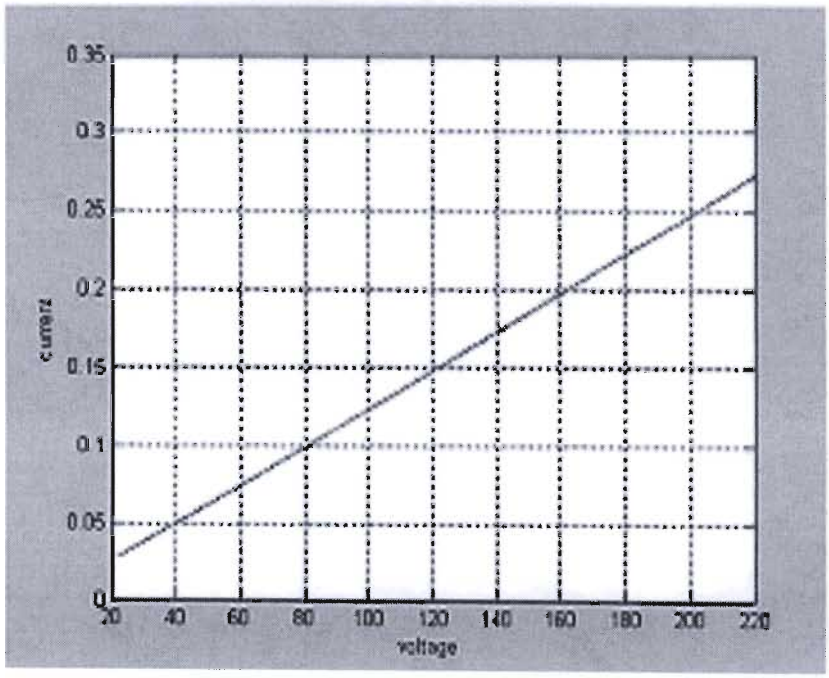

Figure 5-17: Current vs. Voltage graph for a 60W Light Bulb Load

As the load being purely resistive, the results plotted were as expected.

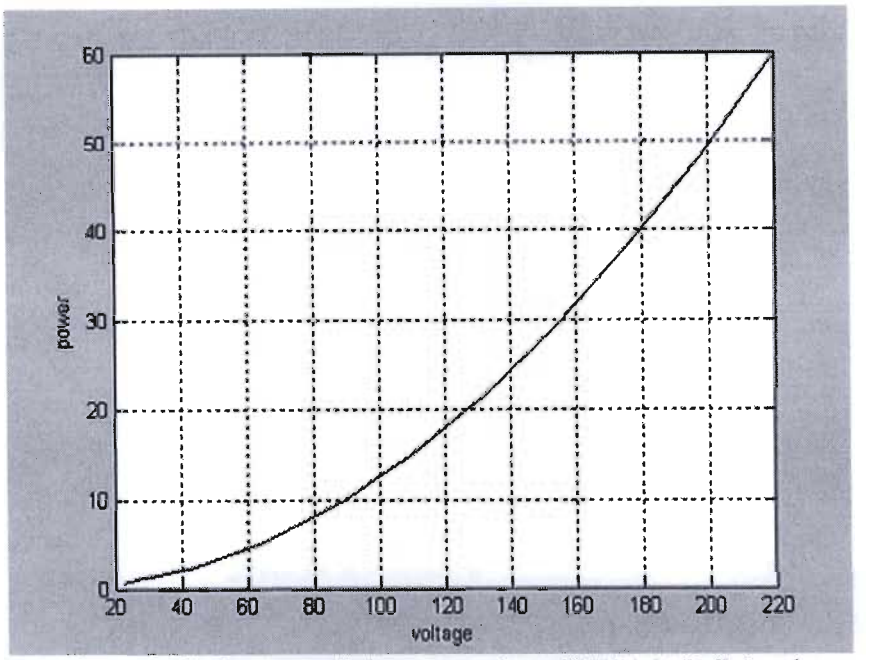

Figure 5-18: Power vs. Voltage curve for a 60W Light Bulb Load

5.3.2.1 Simulation for a Light Bulb Load using Inverter 1

The PV Generator is modeled as a single 24VDC source; ideally the PV generator supplies a constant 24VDC. The inverter was then modeled as a PWM driven universal bridge which was used to convert the 24VDC to 48VAC. The transformer was used to step up this output inverter voltage to 220VAC. The variac was modeled as a slider gain block, in which variable voltage control was achieved. Appropriately positioned displays were used to record and plot the data in Simulink [61].

Figure 5-19 details the Simulink implementation of the entire PV system with a 60W light bulb load.

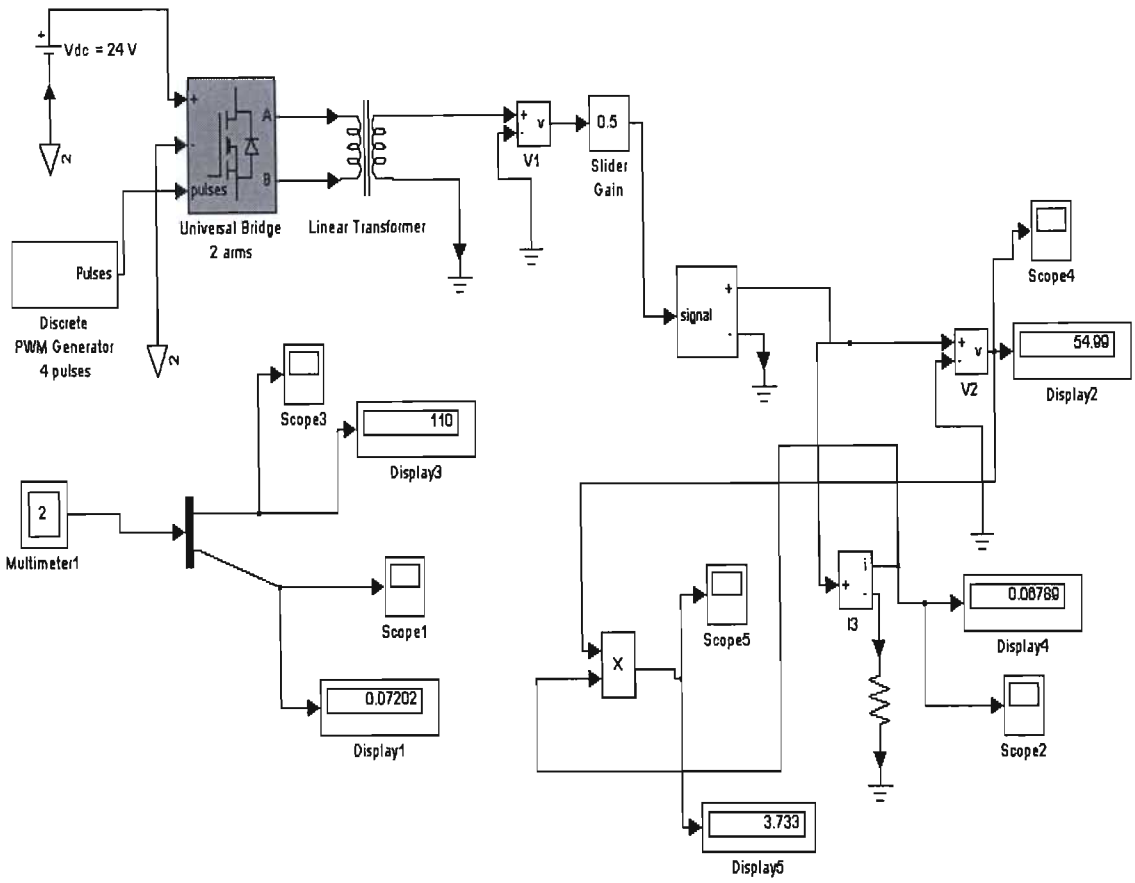

Figure 5-19: Simulink Modelling of a Light Bulb Load

5.3.3 Experimental Test Results using a 0.32kw Induction Motor

No load tests were only performed on the 0.32kW, 220V, 50Hz, induction motor using an inverter connected to the output power of the PV system. The output voltage of the inverter was varied with the use of a variac to obtain varying values of speed, current, and power. The MATLAB m-file used to generate Figures 5-21 to 5-23 can be found in Appendix C4.

Table 5-6: The results obtained for the no load test on the induction motor

Induction Motor No-Load Test			
AC Input Voltage (V)	AC Input Current (A)	Motor Speed (rpm)	Input Power (W)
220	2.05	1500	195
210	1.8	1500	170
200	1.65	1500	150
190	1.50	1500	130
180	1.35	1500	115
170	1.25	1500	100
160	1.15	1500	90
150	1.05	1450	80
140	0.85	1400	73
130	0.75	1300	65

Initially for the tests conducted on the induction machine, the motor was started up and set to steady state. The voltage that was used at the start of tests was 220V respectively. The voltage was then decreased in acceptable increments until the motor reached a voltage low enough to cut off.

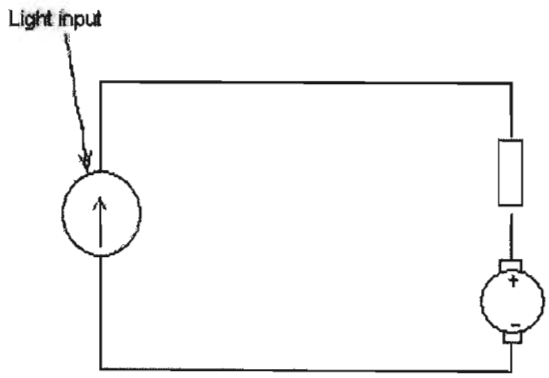

Fig 5-20: Circuit diagram of the PV array connected directly to the induction motor.

The voltage range was between the 130 – 220V region, in which the speed, current, and input power was measured. All other voltages lower than this did not run the motor at all. Upon start up, the induction motor proved to draw a large amount of current and this lead to the inverter tripping when the voltage was slowly increased from zero, so the voltage was increased immediately to allow the motor reach a steady state. The tripping of the inverter was thus averted. Figure 5-21 shows how the voltage decreased from steady state to pull out state. The graph of the input voltage against the speed is shown in Figure 5-22 while Figure 5-23 shows a graph of the input power against the voltage all at no load. No load tests were

only performed because the PV generator output power used in the test facility could not drive large loads.

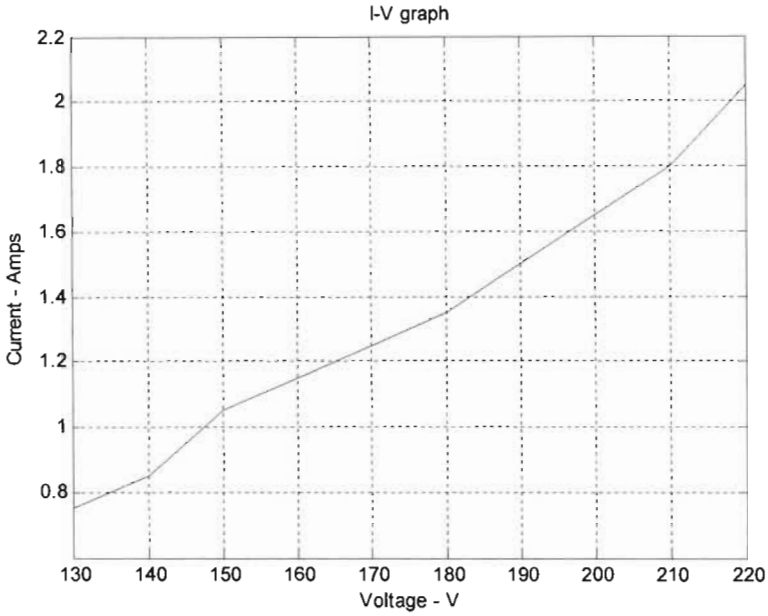

Figure 5-21: No Load Test Results for the 0.32kW Induction Motor.

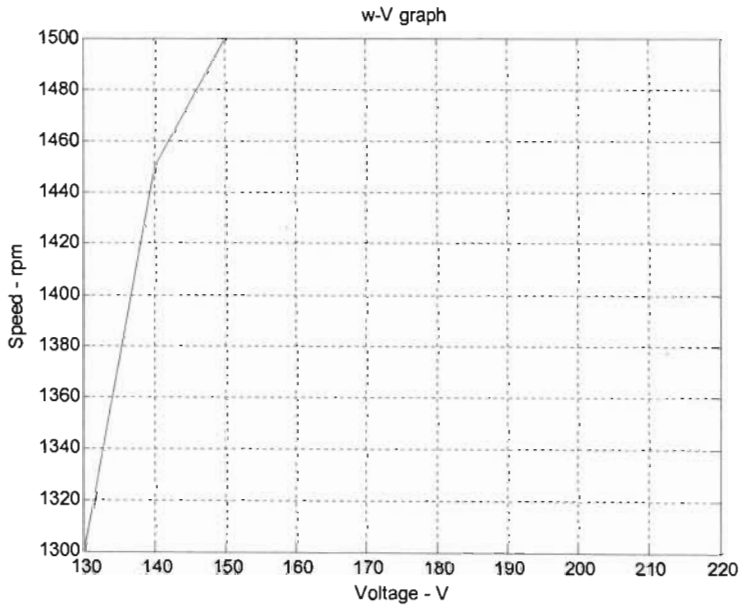

Figure 5-22: Induction Motor Input Voltage and Motor Speed at No Load.

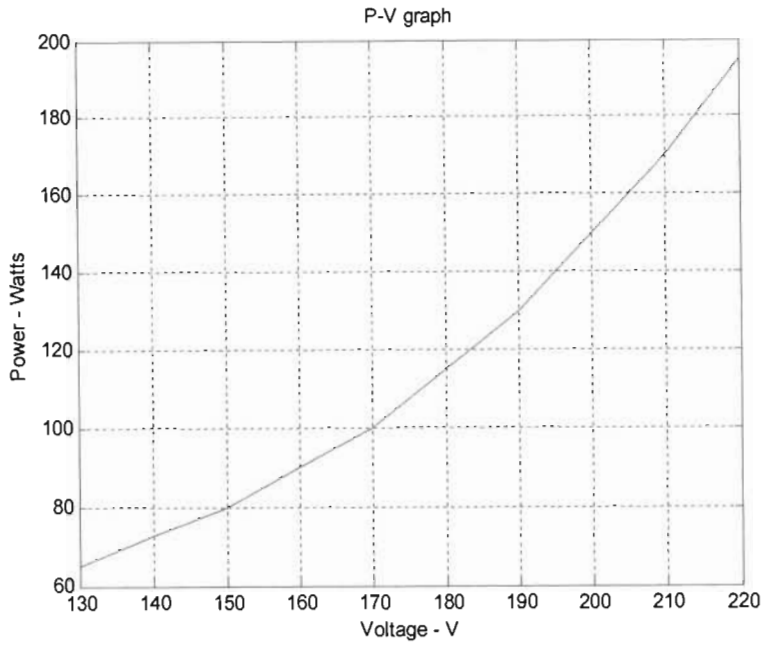

Figure 5-23: Induction Motor Input Voltage and Input Power at No Load.

5.4 Discussion on the Different Experimental Tests on Loads Analyzed

From our investigations, the performance of a PV generator and its maximum power transfer is closely related to both the environmental parameters (i.e. insolation) and load magnitude. Varying the internal resistance can change the operating point of the generator for maximum power delivery. It, therefore, follows that the amount of power produced by the PV generator does not depend only on the amount of solar radiation but also on the position of the operating point on the I-V curve. Choosing a correct system configuration corresponding to a given load can therefore optimize the power output.

The performance analyses of the directly coupled PV powered universal motor; 60W light bulb and a 0.32KW induction motor have been studied. The steady state speed torque characteristics of the universal motor are obtained at different solar intensities and corresponding cell temperature. They are shown in the mechanical plane (w-T). It is observed that the system started to operate at low value of solar intensity and performed during most of the daytime. While the short circuit current varies greatly with the solar intensity level, the open circuit voltage does not. This is because the photocurrent (Iph) and hence the short circuit current is a linear function of the solar intensity and the open circuit voltage is a logarithmic function of the solar intensity. The PV array open circuit voltage decreases with an increase in cell temperature, causes the open circuit voltage to drop,

whereas the short circuit current increases slightly with an increase in cell temperature [62]. The overall result of these variations is a reduction in the PV array efficiency with an increase in cell temperature.

It is observed that for good match between the characteristics of the PV array and the load e.g a universal motor, the load should have torque-speed characteristics that increase rapidly as rapidly as possible in the operating region. The proper matching between the components is the main issue in a directly coupled PV electromechanical system [63].

Laboratory experimental results show the steady state performance of the PV system with changing loads. Experimental results indicate that this PV is suitable as a standalone system supported with an energy storage unit. It was found out that even when there is a little cloud cover, the PV array still generated a considerable amount of power; meaning that the performance of the PV array is not limited to high insolation only. The amount of power produced by the generator does not depend only on the amount of solar radiation but also on the position of the operating point on the I-V Curve [64].

5.5 Impedance Matching

Energy reclamation by definition relates to converting any form of energy that is otherwise wasted to some form of useful power. The idea of matching load impedance to source impedance stems from a principle which a generator supplies power to its load (R_L) via its own internal or source resistance (R^1). Using R_L greater than R^1, more power will be dissipated in R_L than in R^1. As we decrease R_L, the power in both R_L and R^1 will increase up to a point where $R_L = R^1$ and equal power will be dissipated in each. Decreasing R_L further increases the power lost in R^1 but the power in R_L is decreased. Clearly, maximum possible power is dissipated in R_L where $R_L = R^1$. The problem with this matching system of $R_L = R^1$ is that half the power is lost in the source [65]. Imagine a power supply authority tolerating a system in which half the power they generate is lost in their own generating machine. The idea of impedance matching is a very simple example of an electrical generator feeding a resistive load. Generators have an internal resistance if their own (R_G) as all real power generators do, this tend to dissipate some of the generator output power as heat, wherever a load is connected at the output terminals. So the full mechanical power fed

into the generator can not be drawn from it as electrical power, because some will always be wasted in (R_G) resistance generator [65].

The generator internal resistance can be minimized. The power loss is also minimized by varying the resistance of the load. In real terms, the power transferred to the load will be a maximum; but at the same time, the actual power being dissipated in the generator's internal resistance is exactly the same as that reaching the load. In other words half the total power from the generator is now being turned into heat inside R_G (resistance generator), because its resistance is now half the total connected across the generator, the other half is the load resistance R_L .

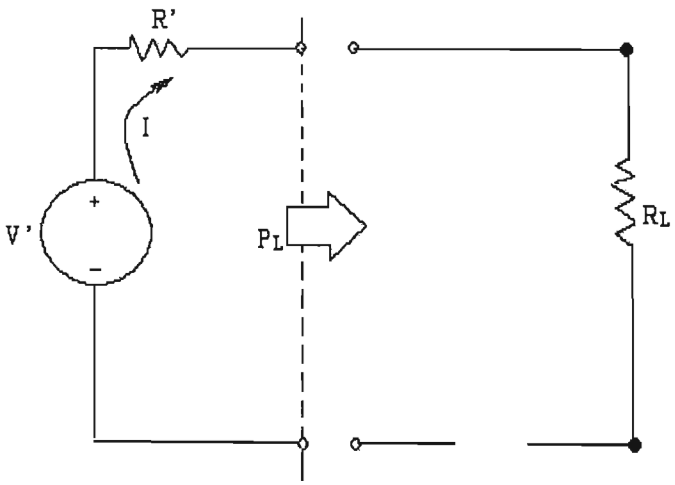

Fig.5-24: Equivalent circuit of a linear network showing the Maximum Power transfer theorem.

For a linear network, the maximum power transfer from an active network to an external load resistor R_L can be reduced to an equivalent circuit as shown in figure 5.24.

$$I = \frac{V'}{R' + R_L} \tag{5.2}$$

And so the power absorbed by the load is

$$P_L = \frac{V'^2 R_L}{(R' + R_L)^2} = \frac{V'^2}{4R'}\left[1 - \left(\frac{R' - R_L}{R' + R_L}\right)^2\right] \tag{5.3}$$

P_L attains a maximum value, V'2/ 4R', when RL=R', in which case the power in R' is also V'2 / 4R'. Consequently, when the power transferred is a maximum, the efficiency is 50% [66].

5.6 Photovoltaic Maximum Power Point Tracking

Maximum power trackers are high frequency DC to DC converters. They take the DC input from the solar panels, change it to AC, and convert it to a different DC voltage and current to exactly match the panels to the batteries [67]. It operates the Photovoltaic (PV) modules in a manner that allows the modules to produce all the power they are capable of [68]. Its purpose is to correctly couple the output from the solar array to the requirements of the battery so as to allow the solar array power to be delivered in its optimal format in terms of voltage and current [69].

Figure 5-25 shows a PV generator showing its maximum power point.

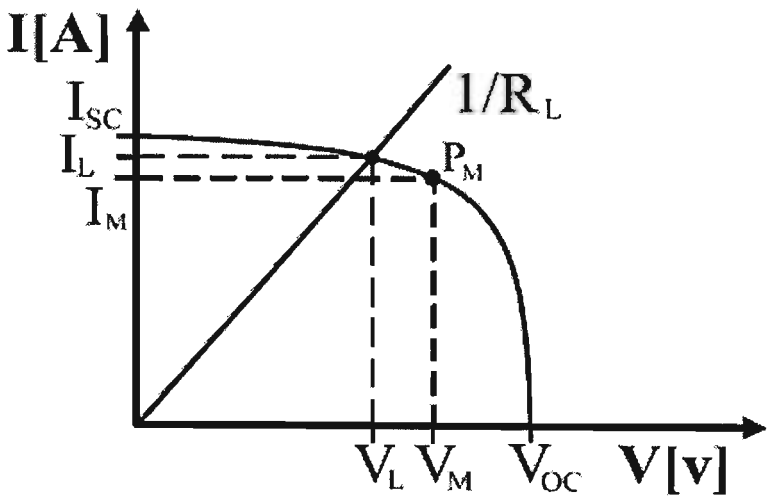

Figure 5-25: I-V curve of a PV generator showing the Maximum Power Points [70].

Where V_{oc} –open circuit voltage, I_{sc}-Short circuit current, I_M- Current at maximum power point, V_M-Voltage at maximum power point and P_M is the Power at maximum points.

The actual operation (V_L, I_L) point is defined by the intersection of the PV curve with the load line. From figure 5-26, I_L. $V_L \leq I_{MMP}.V_{MMP}$

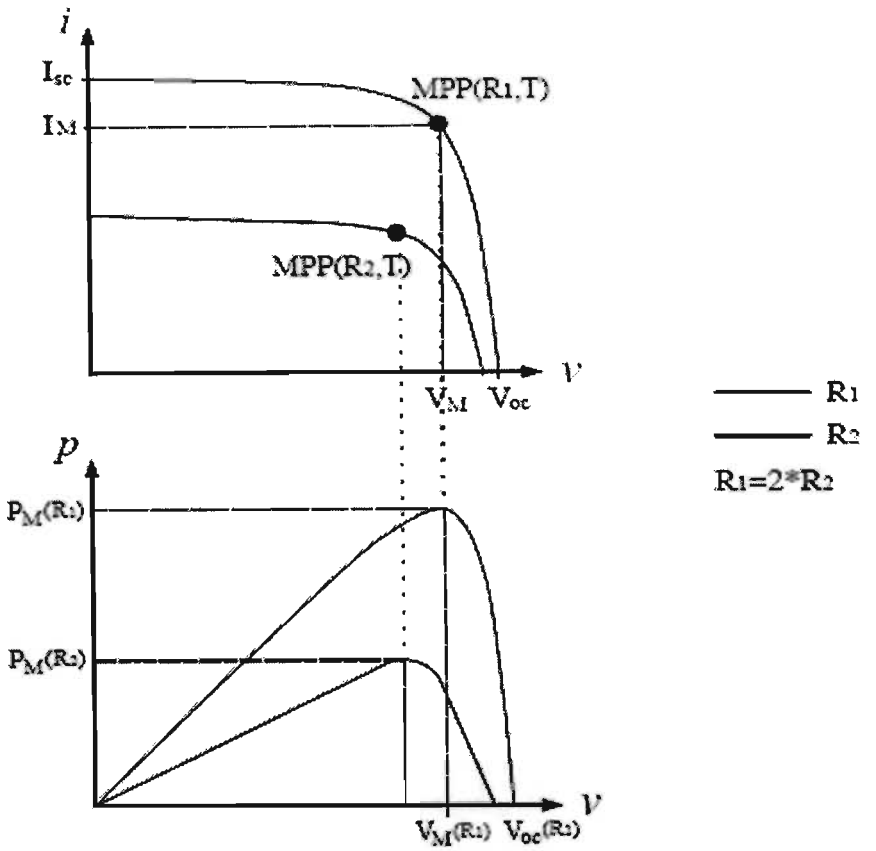

Figure 5-26: Variation of I-V curves with insolation [70].

The MPP locus varies with temperature, insolation intensity and shading conditions such as cell and also with the PV cells ageing. Thus, if directly connected to the load, operation of the PV array at the MPP can not be ensured even for constant loads. Moreover, practical load electrical characteristics might vary, due to parameters such as the charge condition of batteries and its aging or the loading and speed of dc motors powered by the PV array [70]. Figure 5-27 shows the graphical implementation of different maximum power points for different insolation intensities in the I-V plane for a resistive load.

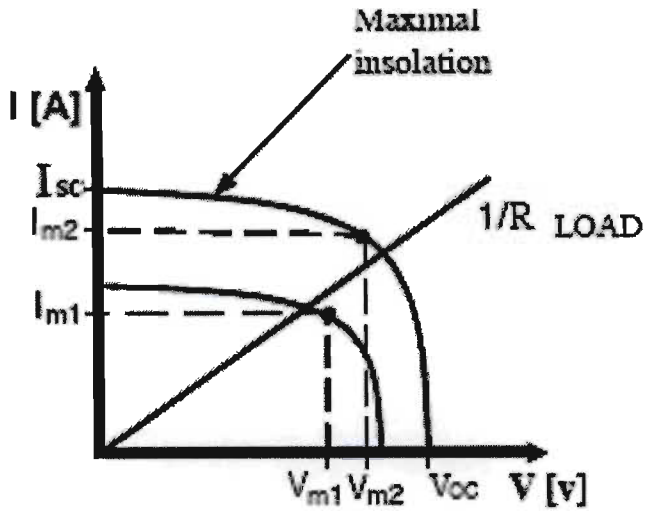

Figure 5-27: Different MPPs for different insolation intensities in the I-V plane [70].

5.6.1 Maximum Power Point of a PV with a DC Motor as the Load.

The fractional horse power dc machine finds great utility in such loads as mobile hydraulic pumps, mobile hoists and lifts, exercise equipment, office machines and many solar powered applications due to its high-starting torque since no current is needed to excite the magnetic field [47]. Apart from being used in control schemes, permanent magnet DC motors are commonly used in applications which require high starting torque or predictable torque throughout the speed range. They use less energy than other types of DC motors, because no current is needed to excite the field, as in field-wound types of DC motors. Figure 5-28 shows the schematic diagram of a DC motor connected to a load and the equivalent circuit diagram is shown in figure 5-29.

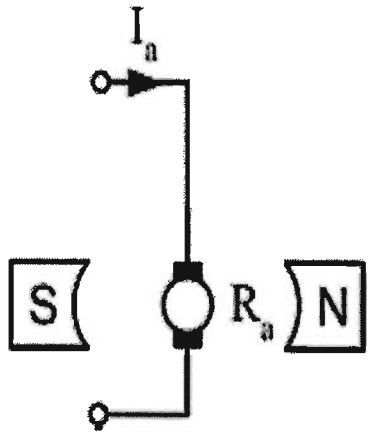

Figure 5-28: Schematic diagram of a DC motor (with permanent magnets) connected to a load [71].

The rotor (armature) rotates with rotational speed ***n***.

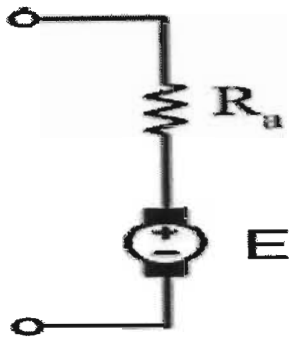

Figure 5-29: Equivalent circuit of a DC motor connected to a load [71].

$$V = E + R_a I_a \quad (5.4);$$

and

$$E = ken \quad (5.5)$$

Substituting equation 5.4 into 5.5, we have;

$$V = ken + I R_a \quad (5.6)$$

Where; E – Electromotive force induced in the rotor and R_a – Rotor resistance, n – rotor speed, Ke is a constant.

To start up a motor, the figure 5-30 below explains the equivalent circuit of a PV array connected directly to a DC motor without MPPT.

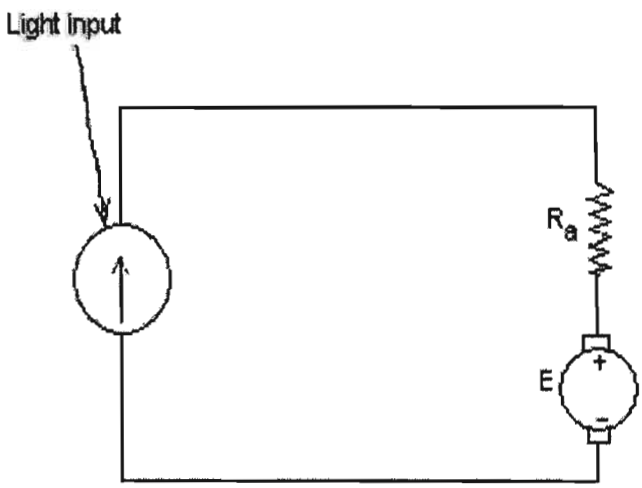

Figure 5-30: Equivalent circuit of a PV array connected directly to a DC motor [71]

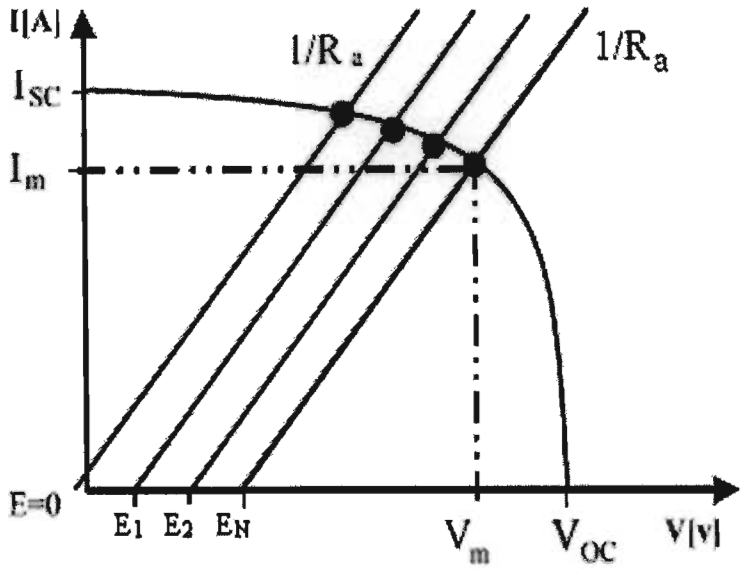

Figure 5-31: I-V Curve of a DC motor powered by a PV array [71].

At start instance n = 0, then E = 0. Therefore the motor appears like a resistive load. During acceleration the motor does not operate at MPP. As a result the acceleration takes long or might not be possible at all due to the reduced starting torque.

When a MPPT is now introduced, the equivalent circuit to illustrate this is shown in figure 5.32 below.

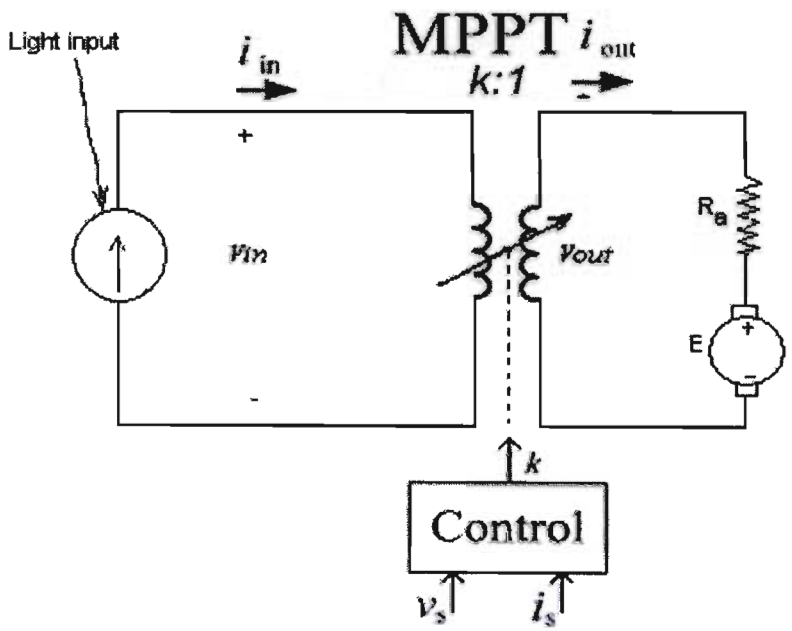

Figure 5-32: Equivalent circuit of a PV array connected directly to a DC motor controlled with MPPT [72].

The ideal matching network in a time variable DC transformer with transfer ratio k (t) [71, 72]. This transformer is controlled so as to operate the PV generator at MPP, regardless of the load type. The controller transfer ration is *k*

The transformer model implies:

$$\begin{pmatrix} V_{out} \\ i_{out} \end{pmatrix} = \begin{pmatrix} k^{-1} 0 \\ 0 \;\; k \end{pmatrix} \begin{pmatrix} v_{in} \\ i_{in} \end{pmatrix} \tag{5.7}$$

The controller sets the transfer ratio, k, based on the sensed parameters, v_s and i_s (which are, traditionally the MPPT's input voltage, and current v_{in} and i_{in}). Consider a load typically applied in PV systems, which may be represented as a series connected voltage source E and a resistor R:

$$V_{out} = \mathrm{E} + i_{out}.R \tag{5.8}$$

This load has as a linear load line in the V_{in} - i_{in} plane, determined by the transformer turns ratio.

$$V_{in} = k\mathrm{E} + i_{in}.k^2 R \tag{5.9}$$

5.6.2 Transferred load characteristics for different values of *k*. transfer ratio

For different values of k, the shape of the graph will look like what is presented in figure 5-33 [73]

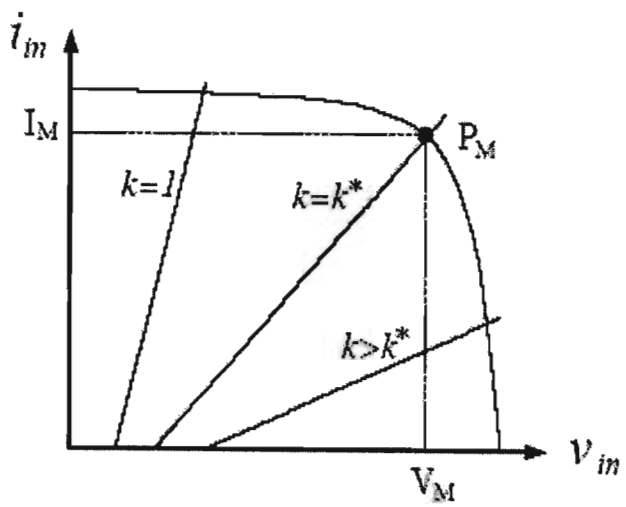

Figure 5-33: I-V Curve of a PV array connected directly to a DC motor using k ratio [73].

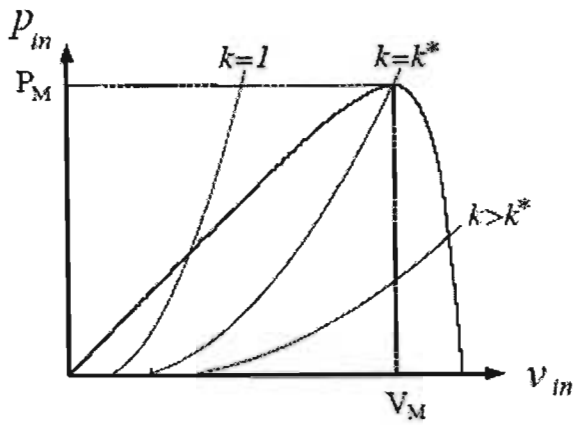

Figure 5-34: I-V Curve of a PV array connected directly to a DC motor using k ratio for MPPT calculation [73]

$$p_{in} = \frac{v_{in}^2 - k \cdot E \cdot v_{in}}{k^2 \cdot R} \qquad [73] \quad (5.10)$$

$$k^* = \frac{\sqrt{E^2 + 4 \cdot P_M \cdot R}}{2 \cdot I_M \cdot R} \qquad [73] \quad (5.11)$$

Where k^* is the new control ration. In practice, the above equations cannot be used to set k because P_M, I_M and E are not constants and R might be unknown. Thus a control algorithm is iteratively applied until maximum available power is obtained. Therefore, P_{in} must be successively calculated by multiplying i_{in} and v_{in}.

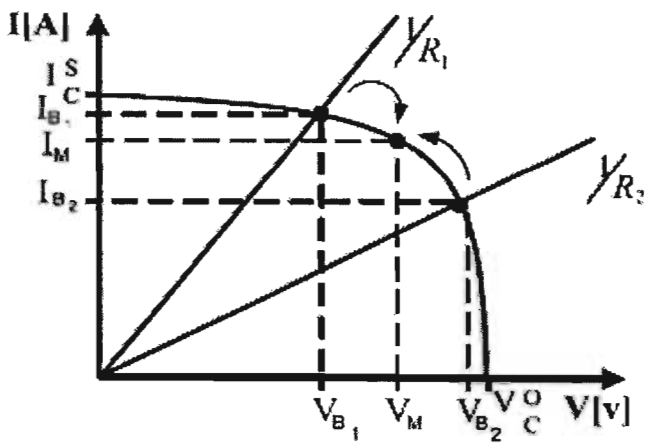

Figure 5-35: I-V Curve of a PV array connected directly to a load under load variation [73].

Under load variation, the matching network transfers the operation point of any load to the PV source MPP.

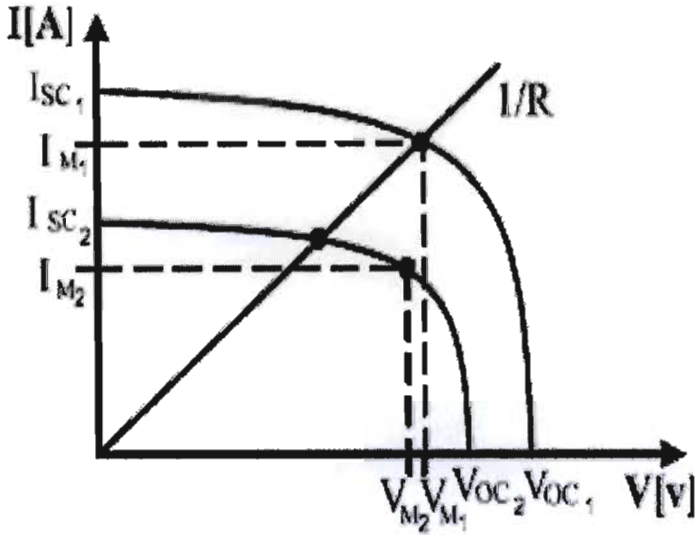

Figure 5-36: I-V Curve of a PV array connected directly to a load under varying conditions. (e.g. insolation, shading, temperature, etc.). [73]

The matching network varies so as to always extract the PV source available power (by setting the operation point at the MPP).

5.6.3 Starting a DC motor using an MPPT

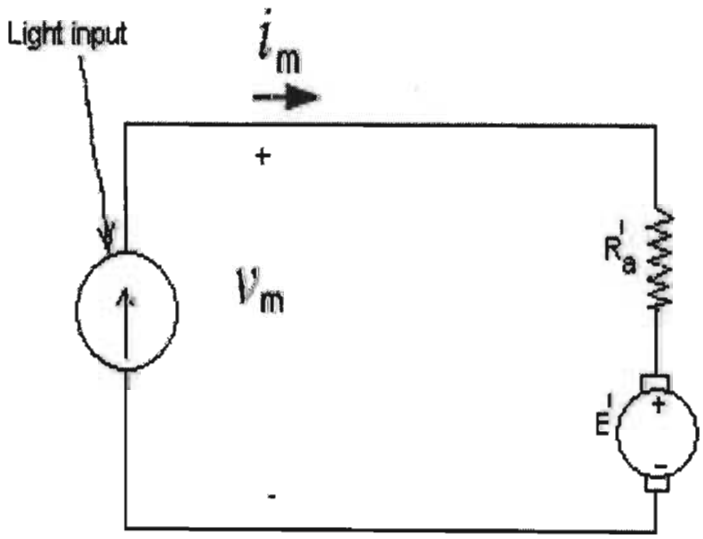

Figure 5-37: Equivalent circuit of a PV array used for starting a DC motor controlled using MPPT [73].

Recall from Figure 5-29 (equivalent circuit of a motor) and equations 5.4 and 5.6.

$$R_a' = k^2(t)R_a \tag{5.12}$$

$$E' = k(t)E \tag{5.13}$$

So, higher start current can be obtained by employing maximum an MPPT matching network which results in start torque.

5.6.4 MPPT implied motor start process

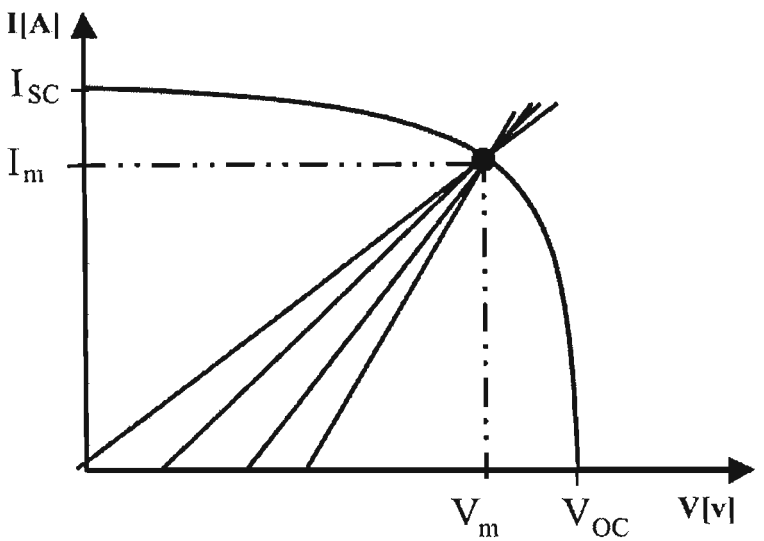

Fig 5-38: I-V Curve of a PV array connected directly to a DC motor controlled with MPPT [71].

From figure 5-38, both the current and voltage of the system are at their maximum values to allow the motor draw enough current to allow it run smoothly at the start up process.

CHAPTER SIX

LIFE CYCLE COSTING AND ECONOMIC ANALYSIS OF THE PV SYSTEM

The economic evaluation of an energy system investment generally includes an assessment of the projected benefits compared to the estimated cost of the system [74]. The direct financial benefit of a PV system is primarily the value of the energy generated and environmental impact. These benefits and direct economic costs may be viewed as the projected benefits and estimated costs. The projected benefits as stated above is the value of electricity generated while the estimated costs are the capital, maintenance, life cycle, replacement costs and decommissioning costs [75].
The life cycle cost analysis of the PVG system was carried out using an iterative process to establish the systems' cost effectiveness.

6.1 Product Life Cycle

Life Cycle Analysis (LCA) provides a systematic approach to measuring resource consumption and environmental releases associated with different electric power generation technologies. This can be done by quantifying and comparing the environmental effects produced by different stages within the process, allowing assessment of the overall, cumulative environmental impact. It also provides useful information on the environmental impacts of such technologies [76]. Life cycle analysis can also be said to be an appropriate method to evaluate the energy and green house gases (GHG) emissions embodied in the life cycle of products and services [77]. LCA is a framework for describing the possible lifespan environmental impacts of material/energy inputs and outputs of a product or process [78].

In life cycle cost analysis, all relevant, present and future costs associated with an energy system are summed in present or annual value during a given study period. Amongst others, these costs include energy, acquisition, installation, operations and maintenance, repair, replacement, inflation and discount rate for the life of the investment. The running cost may include operation and maintenance, general replacement costs, insurance etc. The most common cost element of operation and maintenance of a PV system is the cleaning of the PV modules to reduce dirt build-up and maintain optimal generation. Although accumulated dust

can decrease efficiency and performance of a PV array, for tilted panels, cleaning may not be necessary during rainy seasons, as normal rainfall is usually sufficient to wash off dust and dirt [79].

6.2 Environmental Effects of Energy Resource Processing

The generation of electricity, and the consumption of energy in general, result in consequences to the environment. Material and energy balances can be used to quantify the emissions, energy use, and resource consumption of each process required for any power plant to operate. These include feedstock procurement (mining coal, natural gas extraction, biomass accumulation, collecting residue biomass), transportation; manufacturing of equipment and intermediate materials (e.g., fertilizers, limestone), construction of the power plant, decommissioning, and waste disposal. However, all these activities have adverse environmental effects. Table 6-1 shows a matrix complied by Baumann and Hill [80] on the negative effects of 12 different energy sources with relative significances indicated.

Table 6-1: Relative environmental effects of a variety of renewable energy and non-renewable energy sources.[80]

Negligible/significant=1 Significant=2 Significant / large=3 Large = 4	SO_x and NO_x	CO_2	CH_4	Health	Particulates	Heavy metals	catastrophes	Waste disposal	Visual Intrusion	Noise	Land requirements
Passive solar energy									1		
Photovoltaics					1	1		1	1		1
Wind									3	1	1
Biomass	1		3	1	1	1		1	1	1	3
Geothermal	1	1	1	1		1		2	1	1	
Hydro							2		3		3
Tidal							1		3		1
Water waves							1		1		
Coal	4	4	2	1	2	2	1	2	2	1	3
Oil	3	4	1	1	2	1	2	1	1		1
Natural gas	1	4	3	1			2		1		1
Nuclear	1	1		1			2	3	2		1

Most energy sources with an exception of passive solar energy and photovoltaic energy systems produces pollution one way or the other. Most investors consider PV systems to be very expensive; but on the long run, they are a very cheap source of clean energy.

6.3 Load Management Control

The purpose of load management control in a PV system is to coordinate the interaction between system components and to control the energy flows between the various energy resource units, energy storage units and the users [81]. The end use of electricity is an important parameter for any power distribution system. In order to manage and control the load delivered from a PV system, two models are proposed. The first is to model the demand level of individual households. In order to model the demand on the level of the individual households, each load is modeled based on the statistics of household appliances in individual homes. Using the statistical information of the domestic appliance in individual households, the appliance compositions of individual households can be approximately modeled. The utilization frequency of each type of appliances can be computed. The total demand of individual customer is defined by summing up the total power demand of their individual domestic appliances, including the stand-by power consumption and the extra demand from the small appliances not identified in the statistics.

The mathematical modeling of the loads is done based on the following analysis [82]. Each appliance A has a defined weekly working frequency $f(A)$. The probability for the appliance to begin working for each hour H of the day is $P_{hour}(A,H)$. The modeled hour is divided into S steps, and thus the probability for each step is scaled with the factor P_{step}. Their product is still scaled with a seasonal working probability $P_{season}(A,W)$, where W refers to the week of the year. Thus the total probability for the appliance to start working during any one step is

$$P_{appl}(A,H,W) = P_{season}(A,W).P_{hour}(A,H).P_{step}.f(A). \tag{6.1}$$

When we consider, that the probability parameters have the following characteristics

$$S.P_{step} = 1.0, \sum_{H=1}^{24} P_{hour}(A,H) = 1.0, \frac{\sum_{W=1}^{52} P_{year}(A,W)}{52} = 1.0 \tag{6.2}$$

Thus the average yearly amount of starting the appliance is

$$N_{year,ave} = \sum_{W=1}^{52} \sum_{H=1}^{24} \sum_{steps} P_{appl}(A,H,W) = \sum_{W=1}^{52} \sum_{H=1}^{24} S.P_{season}(A,W).P_{hour}(A,H).P_{step}.f(A) \tag{6.3}$$

$$N_{year,ave} = \sum_{W=1}^{52} P_{season}(A,W).\sum_{H=1}^{24} P_{hour}(A,H).f(H) = 52.f(A) \tag{6.4}$$

The second approach is to model the power feeding the load in the PV system. However, to maximize the load energy, there are two main constraints such as battery limitation and daily allowable load from the battery bank. This is represented mathematically as:

$$P_a = P_d + P_u = P_L + P_b \tag{6.5}$$

where P_a is the total power available, P_d is the power delivered, P_u is unused power, P_L is the load power and P_b is the battery bank power.

The state of charge (SOC) of the battery can be represented at different levels:

SOC high (SOC>95%)

SOC medium ($50 < SOC \leq 95\%$)

SOC low ($SOC \leq 50\%$)

Table 6-2: Soc Analysis

State 1	State2	State3
SOC High	SOC medium	SOC Low

Some domestic loads such as a fractional blender, cooker can be controlled during usage in the house. Domestic chores such as cooking can be performed while putting off other loads such as lighting. This eliminates the premature ageing and minimal consumption of the back-up energy of the battery. It also leads to an effective use of the generated electricity and extends the life time system operation of the PV generator.

6.4 Life Cycle Cost and Economic analysis of the PV System

To perform a levelized cost analysis, all capital and operating expenditures incurred over the span of the evaluation period must be taken into account. The expenditure stream includes generation equipment costs, BOS component costs, and annual operating and maintenance (O&M) expenses [83]. Generation equipment costs include hardware costs and cost for delivery and installation of the PV array and generator set. The BOS component costs reflect the costs of purchasing, delivering and installing the power conditioning systems. Both the electricity generation equipment and BOS component cost streams include initial and replacement costs. The O&M expenses cover regular service, maintenance and repair costs (e.g., lubrication and bushing repairs are included for gen-sets and array surface washing and electrical connection inspection are included for PV systems). For gen-sets powered by

diesel, the O&M costs also include the delivered fuel costs. This is based on fuel prices in the local market and the average cost per unit of delivered fuel to the site [84].

Table 6-3 shows the economic parameters for the life cycle cost comparing a PV system and a system fed from a diesel powered generator. Prices for all system components are based on the actual cost index of all the materials used for the test facility in the laboratory.

Table 6-3: illustrating the economic parameters [85]

Load System Life	25years
550W array @ $3.50 / W	$1925
500W gasoline generator @ $250	$250
Inflation rate	3%
Discount rate	10%

For the PV system and generator, the present worth factor of the batteries and generators can be calculated using;

$$P_r = \left(\frac{1+i}{1+d}\right)^n \tag{6.6}$$

Where n is the number of years i is the inflation rate and d is the discount rate;
For the generator, the present worth factor of the fuel and maintenance cost can be calculated using

$$P_r = \left(\frac{1-x^n}{1-x}\right) \tag{6.7}$$

where n is the number of years, and

$$x = \left(\frac{1+i}{1+d}\right) \tag{6.8}$$

The cumulative present worth factor needed for the maintenance cost of the PV system can be calculated using

$$P_{al} = xP_a \tag{6.9}$$

Using the inflation rate and discount rates given above,

$x = 0.9364$,

$P_a = 11.50$ and

$P_{a1} = 10.77$.

The system is assumed to operate for 24hr per day with minimal down time. A load coupled to the system uses 2Kwh per day with a 25years life time.

Table 6-4: Comparison of life cycle costs (LCC) for PV system and generator system for a typical load.

PV SYSTEM			**DIESEL POWERED GENERATOR SYSTEM**			
Component	IC($)	PW ($)	Component	I.C. ($)	AC ($)	PW ($)
Photovoltaic	1925	1925	Generator	250		250
Charge Controller.	150	150				
Battery.	900	900	Fuel		469	5394
Battery. 5year	900	648	Generator 5yr	250		180
Battery. 10year	900	466	Generator 10yr	250		130
Battery 15year	900	336	Generator 15yr	250		93
Battery 20year	900	242	Generator 20yr	250		67
Battery 25year	900	174	Generator 25yr	250		48
Annual Maintenance	100	1077	Annual Maintenance		500	5750
Array Mount / Installation	100	100	Installation Cost	100		100
Inverter	100	100	Other Items	50		50
Protection switch fuse	20	20	Isolator	20		20
Wiring cables	50	50	Wiring Cables	50		50
LCC		**6188**	L.C.C			**12132**
Total System Cost	**7845**					

[PW is present worth; IC is initial cost; AC is annual cost; and yr. is year.]

6.4.1 Costs Analysis

In life cycle cost analysis, all relevant, present and future costs associated with an energy system are summed in present or annual value during a given study period. These costs include energy, acquisition, installation, operations and maintenance, repair, replacement, inflation and discount rate for the life of the investment. PV technology, when used for localized rural, semi-urban and urban areas, has economic costs and benefits that may be shared between the consumers and the electric utility [85]. This brings a significant return on investment for both the electric utility and the consumer

Table 6-4 shows the costs of principal components and the annual operation and maintenance costs of the total systems. The total investment of US$7845 for the PV System;

includes the cost of the PV array (US$ 1925). The cost of the power converters (charge controller) is estimated of US$ 150 and the cost of storage batteries is US$900 which has to be replaced after 5years. The diesel generator was US$250. In the LCC from table 6-4, the system is capable of 24-hour per day operation with minimal down time. The average power requirement of the load is less than 80watts. In this case, the generator would be running at an under rated load, it will produce about 2.5 kWh per gallon. The fuel consumed is ±300galoons per annum and the annual maintenance cost is estimated at US$500.

The economic analyses assess the 25-year LCC of the PV system actually installed. The LCC estimate projects a net savings associated with the PV system of $5844 over the 25-year service life. In addition, the PV system will save over 7,500 gallons of propane fuel, during a 25-year service life. The strength of this analysis is its use of actual load, PV production, and generator run-time data was calculated. O&M and replacement schedules were also developed for all major components. For the generator sets, O&M comprises: oil change; valve adjustment and replacement costs (every 5yrs). Due to high usage, the generator has an average lifespan of 5yrs and must be replaced. The PV system will allow it to serve for the full 25 years without replacement.

The analyses above simply conclude that the PV system is relatively cheaper to use when compared to a generator system. The cost effectiveness of this PV system is due to the combined effects of active load management, load segmentation, and effective system design. Our cost analysis suggests that PV systems can meet increased energy demand at relatively stable costs to the user, improving this system's competitive standing over gen-sets, which can suffer long down-times as maintenance needs, parts failures and fuel shortfalls interrupt service.

6.5 Cost of Electricity from the PV System

The total life expectancy of the PV systems is assumed to be 25 years, while the lifespan of the storage batteries are 5years respectively. The capacity of the unit considered is a 0.55kW solar panel. The system is designed to work during the availability of insolation, which is considered to be 8hrs daily. If the insolation is less than 8hrs (e.g. during winter), a battery is used as a storage element to power the system. However, a maintenance plan of 5hrs is considered yearly for PV system cleaning, connections and cable checking.

The plant/ unit availability can be calculated as:

Total available hours of operation/day per total number of hours/day, A_v

$$A_v = \frac{8\,hrs}{24\,hrs} = 33\,\%$$

Total on- time per year would be:

$$ontime(hrs) = availablity * hrs(days) * days(yrs) * lifespan \qquad (6.10)$$

$$\text{On-time (hrs)} = 0.33 * 24 * 360 * 25 \text{ hrs}$$

$$\text{Down time (hrs) would be} = 5 * 25 = 125 \text{ hrs}$$

Total available time of the system is $= ontime(hrs) = 71280 - 125 = 71155$ hrs.

Total life span plant capacity is $= Capacity(kW) * Ontime(Hrs) =$

$$0.55 * 71155 = 39135.25 \text{ kwhr}$$

To calculate the unit electricity cost, the total plant cost is divided by the total plant capacity

Unit Electricity cost is

$$\frac{7845}{39135.25} = 20 cents / Kwh$$

The following assumptions were made: In the above energy cost, the unit cost derived was based on a 0% on interest, inflation and depreciation.

6.6 Comparison of Energy Sources

Table 6-5 shows the unit electricity cost from various energy sources [86-88]

Table 6-5: Comparison of the Costs of Electricity Generation Using Different Power Plants

Energy Power Type	Capacity kW	Capital Cost $/kW	Fuel Cost $/kWh	O&M Cost $/kWh	Service Life Years	Unit cost (Cents/Kwh)
Microturbine-CHP & Power	100	1485	0.075	0.015	12.5	4
Gas ICE—Power & CHP	100	1030	0.067	0.018	12.5	3.21
Fuel Cell--CHP	200	3674	0.029	0.01	12.5	7
Solar Photovoltaic	100	6675	0	0.005	20	20
Wind Turbine	1000	1500	0	0.005	20	3.5
Combustion Turbine—Power & CHP	10000	715	0.067	0.006	20	3.25
Combined-Cycle System	100000	690	0.032	0.006	20	3.18
Nuclear	100000	2500	0.035	0.25	20	2.4

From Table 6-5, it shows that the unit cost of solar photovoltaic systems has the highest unit cost. Renewable sources of energy generation are generally more expensive than conventional generation technologies [89]. This is due in part to the immaturity of the technology and the more limited opportunity to take advantage of cost savings brought about by economies of scale usually associated with more traditional fossil-fuel types of generation.

In the calculation of the unit electricity cost of the PV system, the unit cost derived was based on a 0% on interest, inflation and depreciation. If these factors were considered, trade offs is the basis of elimination when it comes to the choice of a power generating system. For example, in a comparison between coal and nuclear energy, nuclear energy generally has much lower fuel costs but higher capital costs. This makes an economic choice dependent to a large extent on the expected capacity factor (or equivalent full-load hours of operation expected per year) for the unit. Coal and nuclear-energy systems have, however, significant but vastly different environmental impacts. It may well turn out that one system is chosen

over another largely on the basis of a subjective perception of the risks or of the environmental impacts of the two systems.

Similarly, a seemingly desirable and economically justified hydroelectric project (which has the additional attractive features of using a renewable energy source and in general having high system availability and reliability) may not be undertaken because of the adverse environmental impacts associated with the construction of a dam required for the project. The adverse environmental impacts might include the effects that the dam would have on the aquatic life in the river, or the need to permanently flood land above the dam that is currently being farmed, or is inhabited by people who do not wish to be displaced.

It can also be found out that the decommissioning costs of most power generating plants are not considered in the design cost analysis [74]. Hence, if this is included in the cost analysis, it would be obvious that the PV system advantages out weighs the disadvantages. Apart from these, the present large price swings in the demand and supply of oil has made coal, oil and gas fire plants very expensive to run and maintain [90]. Generally, plant choice is likely to depend on a country's international balance of payments situation but the issue of global warming is highly considered lately [91]. However, when the decommissioning costs, environmental impact or pollution cost, and overall system on-time factor, are all included, the unit cost for all the corresponding generating systems will be higher.

The table below shows the Levelized Cost of Solar Photovoltaic Electricity, 1980 to 2020 [92].

Table 6-6: illustrates a projected cost of the unit cost of PV systems in years to come [92].

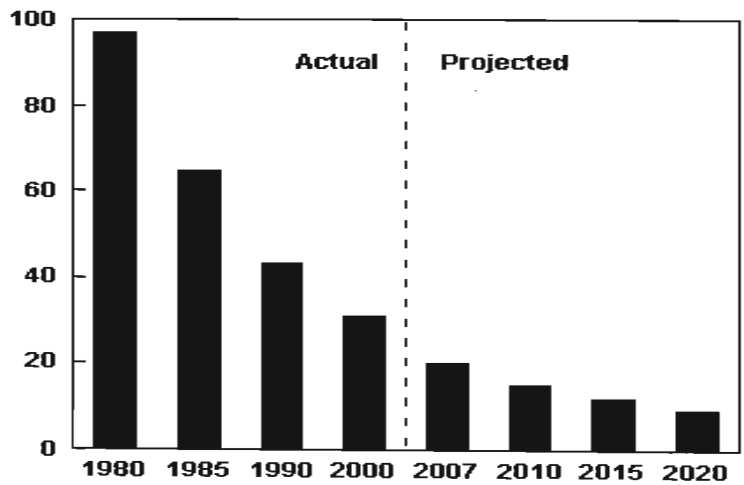

The coupling of a Photovoltaic system to a battery allows converting at, high efficiency, and renewable electricity into time-stable storage using a battery as a backup energy storage system. Using a battery to get back to electricity allows building a noiseless energy generator. The PV generators operate with excellent availability and reliability. In addition, over its life span, the PV system will consume no fuel and avoid the emissions of tons of pollutants [85]. The cost effectiveness of this PV system is due to the combined effects of active load management, load segmentation, and effective system design. The PV system is currently very expensive but in the future, the investment should become competitive to the other stand-alone systems. Although the presented system does not show high efficiency and very low forecasted price, much progress is expected and necessary.

CHAPTER SEVEN

DISCUSSION, CONCLUSION AND RECOMMENDATIONS

7.1 Discussion

Optimal Operation of Energy Delivery and PV System

Solar powered photovoltaic (PV) systems have numerous applications and can be designed to provide energy demands from a few watts to kilo- or megawatts. Some typical PV applications are: communication, monitoring and sensing, water pumping, corrosion protection, lighting, and refrigeration, to name a few. Solar energy is seasonal, varied and intermittent. Therefore, energy storage, conversion and delivery to satisfy application loads are key system design criteria for specific PV applications [93-94]. The satisfactory dynamic responses of the PV system were also analyzed but the transient stability analysis of the system was not considered. The conversion of dc power to ac in the PV system setup is made by controlling switching schemes using a 3KW inverter. Thus the system power system can achieve more real versatile and reactive power control than the conventional power sources because the former does not contain any rotating masses.

Error Estimation in Measurement and Analysis

The performance ratio of any PV system can be influenced by the mean intensity of the solar irradiance, the system size and the system layout. The average efficiency of the PV panel is a function of the irradiance, the power efficiency of the inverter depends normally on the size [95]. High voltage arrays involve low currents, which lead to increasing mismatch, increasing inverter efficiency and decreasing resistance losses. In order to have limited errors in the system and for a good analysis of the system behaviour we used a data-acquisition system (based on a PC) with an average sampling period of only 5 minutes. This also helped to identify improperly functioning components in the system. However, to make a complete overview of the system behaviour, we compared the measured values with the expected ones and also the calculated parameters. The error margin was close to zero. The system however still experienced some losses due to the inverter switching, ohmic loses, temperature losses, Low irradiance losses and String losses.

Efficiency of PV System

The efficiency of the solar cell is defined as [41]:

$$\eta = \frac{P_{out}}{P_{in}} = \frac{P_{max}}{P_{in}} \qquad (7.1)$$

The maximum solar energy conversion efficiency depends mainly upon the solar cell internal construction, dimension, active area, specific materials properties, photovoltaic junction characteristics, anti-reflective coating, surface texture, illumination level, cell operating temperature, particular irradiation damage, temperature cycling.

The fill factor is the term used to describe the sharpness of the I-V curve. The sharper the I-V curve is, the greater the maximum power output. It can be represented as the ratio of the maximum power can be delivered to the load and the product of I_{SC} and I_{OC}

$$FF = \frac{P_{max}}{V_{OC} I_{SC}} = \frac{V_{max} I_{max}}{V_{OC} I_{SC}} \qquad (7.2)$$

Where V_{OC} is the open circuit voltage, V_{Se} is the short circuit voltage [5].

The fill factor is also a measure of the real $I-V$ Characteristic. Its value is between 0.75 and 0.8 for a typical solar cell. The efficiency of the solar cell used in this research is 17% [33].

Applications of the PV System

Lately, many people are familiar with PV-powered calculators and watches, the most common small-scale applications of PV. However, there are numerous large- scale, cost-effective PV applications [96]. PV systems applications vary from need to areas. Some are used as autonomous systems; where they are used alone without a backup or auxiliary power source. Hybrid systems are situations in which the PV is used alongside other power generating sources such as diesel generating set, wind power system. A grid connected PV system as the name implies is used to supply electricity directly into a regional or community power grid. They can also be used as standalone systems in areas where the community is highly remote and don't have access to the electrical grid. [22]

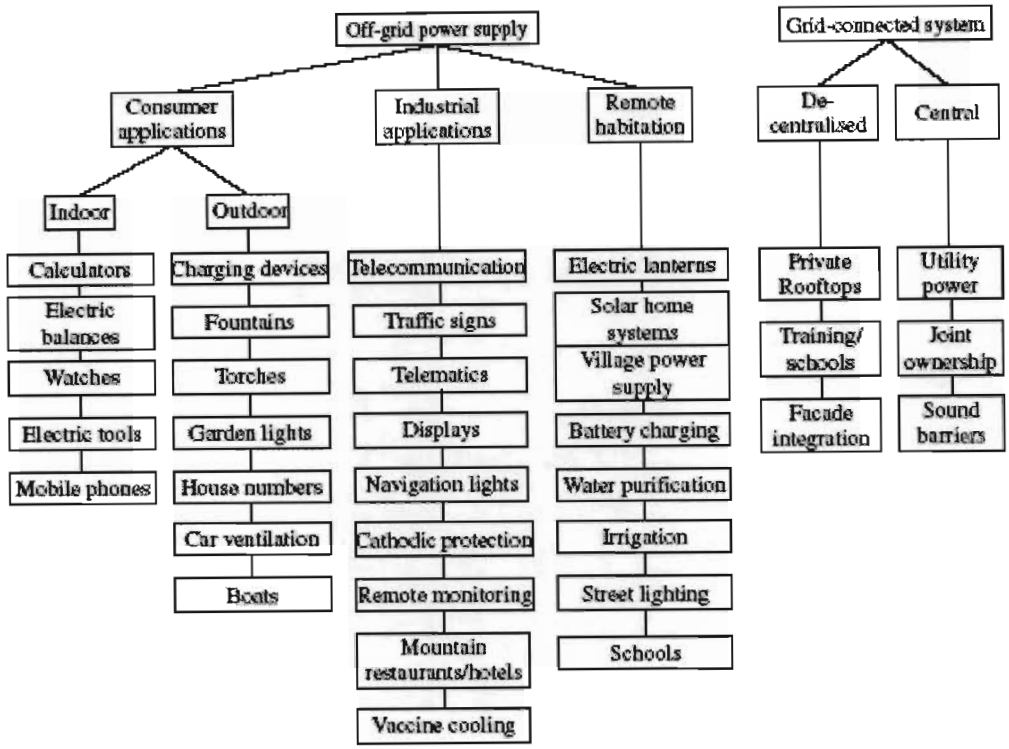

Figure 7-1: showing the application areas of photovoltaic systems

Grid-independent Photovoltaic Systems for Small Devices and Appliances

Solar electric power supplies for appliances and small loads in the power range from several milliwatts to several hundred watts are being applied generally because of its cost-effectiveness against a grid connection, in many cases even when the consumer is situated very near to the next grid connection point. [97]. Advantages include: their reliability, portability and their environmentally benign production of energy. In very small systems such as wristwatches or scientific calculators, the solar generator consists of one or only a few solar cells. When more power is needed, the individual solar cells are connected together to form solar modules. Pocket Calculators, fans and electric letter balances are examples of such applications [98]

- Solar home systems [99,100]
- Solar lantern for rural households in developing countries
- Photovoltaically powered intelligent emergency telephone [101]
- Consumer applications

Photovoltaic Systems for Remote Consumers of Medium and Large Size

Electricity also helps solves other material supply problems. Workshops, food storage and processing, telecommunication, health services and tourism normally demand higher daily

amounts of energy and power than can be supplied by a Solar Home System. Small stand-alone grids that are supplied by various electricity generators are the next step in remote area power supply. With increasing demands, the connection to the public electricity grids makes good sense.

- Photovoltaically powered telecommunication system
- PV powered battery-charging stations[102]
- Photovoltaic hybrid systems
- Village power supply systems
- Photovoltaic pumping systems[103]
- Photovoltaically powered water purification[104]
- Social aspects in off-grid rural electrification [105]

Decentralized Grid-connected Photovoltaic Systems

Photovoltaic systems can be connected to the public electricity grid via a suitable inverter. Energy storage is not necessary in this case. On sunny days, the solar generator provides power for the electrical appliances in a house. Excess energy is supplied to the public grid. During the night and overcast days, the house draws its power from the grid [106]. Photovoltaic systems operating parallel to the grid have a great technological potential [107]. Examples of grid connected PV systems include:

- Rooftop PV generators
- Building integration

Central Grid-connected Photovoltaic Systems

The photovoltaic systems discussed are usually small decentralized systems in the lower kilowatt range; it is also possible to build large central photovoltaic power stations in the higher kilowatt to megawatt range. It is then possible to feed directly into the medium- or high-voltage grid.

- Utility systems
- Joint ownership

Space Application

The general uses of the PV systems include [22]:

Water pumping for small-scale remote irrigation, stock watering, residential uses, remote villages, and marine sump pumps;

Lighting for residential needs, billboards, security, highway signs, streets and parking lots, pathways, recreational vehicles, remote villages and schools, and marine navigational buoys;

Communications by remote relay stations, emergency radios, orbiting satellites, and Cellular telephones

Refrigeration for medical and recreational uses;
Corrosion protection for pipelines, docks, petroleum, water wells and underground tanks;
Utility grids that produce utility- or commercial-scale electricity;
Household appliances such as ventilation fans, swamp coolers, televisions, blenders, stereos, and other appliances
Disaster and energy security applications [22]

From the result of this investigation, the PV system can be used as building energy supply, energy management and as building services technologies.

7.2 Conclusion

This study has demonstrated the performance analysis of PV systems and highlights the economic evaluation of the system for a Standalone power system. This is contributive to solving household problems of many domestic homes that do not have an access to electricity supply. The backup system used in this study is a battery bank and it has nice characteristics such as fast load-response capability, modularity in production, highly reliable power sources and environmentally acceptability. Time-domain simulation results showed effectiveness of the developed model. The PV system responded very well to PV power changes so that the system can maintain the standalone real and reactive power demand commands. The conversion of dc power to ac in the PV system setup is made by controlling switching schemes using a 3.0kW inverter. Thus the power system can achieve more real versatile and reactive power control than the conventional power sources because the former does not contain any rotating masses.

From the experimental results obtained during this project, it is clear that the photovoltaic generator (PVG) is an efficient source of energy. The different loads which were connected to the system responded satisfactorily. The results from the mathematical models obtained from the MATLAB, Digital Visual Fortran and C++ for the solar panels serve to verify the theoretical I-V characteristic drawn from the SHELL SM110-24 product datasheet. A complete model for the power, voltage and the current characteristics was developed for the mathematical model of this work. The developed models of the system for the power-voltage, and the voltage-current characteristics proved to be similar to the same characteristics shown on the product data sheet. Hence the modeling for the PV generator proved to be successful.

The PV generator is a socially acceptable technology by people, who are concerned about a degradation of the environment. The only major impediment to expand the PV generator system for standalone application is the high production cost of PV modules. The price of PV modules continues to decline as efficiency continues to rise. It has been observed that the yearly prices declined from $6/W in 1983 to less than $3.5/W in 2005 and it is projected to continue to decrease in future. However, the running cost and decommissioning cost of the PV system is negligible compared to the conventional power sources.

However, the PV is less appealing due to the significant feature of its intermittent power output on fluctuating weather condition. Thus, a PV power generation should be integrated with other power sources. Combining a battery power with a PV power plant had been proven to be a feasible technology for alleviating such a PV power's inherent problem.

New processes for manufacturing photovoltaic cells and for enhancing their conversion efficiency are currently being explored and are aimed at reducing the cost per peak watt. The technology for the commercial applications of PV generation will reduce in the near future since the dependence on fossil fuel and the environmental impact of fossil fuel has been a major endangering factor human existence-global warming. Recent price increases in oil and gas in the global market has strengthened a case for further PV resources development and utilization.

At the end of this investigation, the following tasks have been achieved;

- Successful modeling of the PV generator system using MATLAB, DVF and C++,
- Performance analyses of the PV generator system under different loads and the outcomes have been satisfactory because the research carried out showed that the systems being tested showed clear similarities between the experimental and simulation results.
- As a result of the experimental tests carried out, the PV generator system backed up with an energy storage system is a reliable alternative power supply for low energy consumers.
- An economic analysis of the whole system was carried out and it was discovered that it is an expensive mode of energy generation hence it needs state subsidy to be viable.

7.3 Recommendations

Extra efforts need to be made on increasing the efficiency of the PV modules and control systems should be developed to measure and regulate the transient and steady state analysis of the PV systems.

Government policies should discourage the use of kerosene lamps, diesel generators as this will have a significant reduction in green house gas emission.

A procedure for quantifying energy losses in stand alone systems due to the random inverter failures should be analyzed. In addition, an inverter control strategy to improve the system efficiency during periods of low insolation should be developed. Finally, a cost/benefit analysis to determine the optimal system configuration that yields minimal system life–cycle costs should be researched on considering the environmental impacts of the conventional energy sources.

APPENDIX A

MATLAB M-FILE OF THE MATHEMATICAL MODEL OF THE PV SYSTEM.

```
% The programme below shows the MATLAB Model of the PV System
clear
clc
pmpp=110;% maximum power point of PV module power
vmpp=35;%maximum power point of PV module voltage
impp=pmpp./vmpp;
%impp=3.14;%maximum power point of PV module Current
isc=3.45;% Short circuit current
voc=43.5;%Open circuit Current
%i= (isc.*(1-(c3.*(exp((c4.*(v.^m))-1)))) );main Current equation for a Pv
%module
%because there would be five(5) unknowns in the equation, declare voltages
%(V) as array

v1= linspace(0,46.2);% first voltage from PV module
v2= linspace(0.0009,42.8);%second voltage from PV module
v3= linspace(0.0009,42.1);%third voltage from PV module
v4= linspace(0.0009,41.3);%fourth voltage from PV module
v5= linspace(0.0009,39.5);% fifth voltage from PV module

% give values to all the constants in the main Current equation for a PV
% module

  %c3=0.01175;
  %c6=(log((1+c3)./c3) );
  %c5=(log((isc.*(1+c3)-impp)./(c3.*isc)) );
  %m=(log(c5./c6) ./log(vmpp./voc)    );
  %c4=( (c6./(voc.^m)) );

  % rewrite all constant evaluation equations in matlab format

  c3=0.01175;
  c6=real(log((1+c3)./c3) );
  %c6=4.46;
  c5=real(log((isc.*(1+c3)-impp)./(c3.*isc)) );
  %c5=real(log((1.01175.*isc)))
  m=real(log(c5./c6) ./log(vmpp./voc)    );
  c4=real( (c6./(voc.^m)) );

  % write main current equation in matlab format indicating the voltage as an
  % array as stated above
  % find the differnt values of currents at percentages ranging from 20 to
  % 80%
  i= real(isc.*(1-(c3.*(exp((c4.*(v1.^m))-1)))) );
  i1=real((0.8.*i));
  i2=real((0.6.*i));
```

```
i3=real((0.4.*i));
i4=real((0.2.*i));

% find the power generated by the PV
% note that power(P) = current(I) * Voltage (V)
%p=v*i
% find power in all corresponding five places just as solved above
p1=real(v1.*i);
p2=real(v2.*i);
p3=real(v3.*i);
p4=real(v4.*i);
p5=real(v5.*i);

%Plot the Current-Voltage(I-V) curve of the solar cell
%subplot(2,2,1)
plot(v1,i,v2,i1,v3,i2,v4,i3,v5,i4)
AXIS([0 47 0 4])
grid on
xlabel('Voltage[V]')
ylabel('Current[I]')
title(' Current- Voltage(I-V) Characteristics of the PV Generator')

%Plot the Power-Voltage (P-V) curve of the solar cell
%subplot(2,2,2)
figure
plot(v1,p1,v2,p2,v3,p3,v4,p4,v5,p5)
AXIS([0 50 0 125])
grid on
xlabel('Voltage - V')
ylabel('Power - W')
title(' Power - Voltage(P-V) Characteristics of the PV Generator')
```

APPENDIX B1

DIGITAL VISUAL FORTRAN CODES OF THE MATHEMATICAL MODEL OF THE PV SYSTEM.

```
!!This Program is used for simulating the mathematical model of a
!!Photovoltaic generator  It derives the current and voltage and Power and
!!Voltage equations and gets all the values needed.

PROGRAM  mathematicalmodel
IMPLICIT  NONE
!! the constants and variables are defined in this section.


REAL                          :: k2,k3,k4,m,k3temp,k3k4temp,vmpptemp     !derived constants
Integer                       :: j              !iteration integer

!!!!!!---! ASSIGNMENT OF CONSTANTS

REAL,parameter                :: k1   = 0.01175 ! Conversion constant
REAL,parameter                :: vmpp = 35.0    ! voltage at maximum power point
REAL,parameter                :: voc  = 43.5    ! open circuit voltage
REAL,parameter                :: impp = 3.14    ! current at maximum power point
REAL,parameter                :: isc  = 3.45    ! short circuit current

!!!!declare array value for voltage, current and power
integer, parameter            :: max  = 50      ! Maximum voltage value in array
integer, dimension (0:max)    :: v              ! Declare voltage an array
real, dimension (0:max)       :: vtemp,r,x,i,p


!!This section computes the value of one of the conversion constants.
k4 = log((1+k1)/k1)                                  ! transformation factor

!! Write out the value of constant k4
WRITE(*,*)  'the value of k4 is:'

!!Compute the temporary value of k3
k3temp = ((isc*(1+k1))-impp)

!!Compute constant k3
k3 = log((k3temp)/(k1*isc))


!!Compute the value of "m"
WRITE(*,*)  'the value of k3 is:'
k3k4temp =  log(k3/k4)
vmpptemp = log(vmpp/voc)
m =  (k3k4temp/vmpptemp)


write(*,*) ' the value of m is:'
!!Compute the value of k2
k2 = k4/(voc**m)

write (*,*) ' the value of k2 is:'

!!Write out the voltage values declared in array above
write(*,*) 'input voltages are '
write(*,*) '(v(j),j=0,max) '

!!Start iteration loop for various values of voltage to get the
```

```
!!corresponding current values

x = 0.0          !

    do j=0,max
        if(v(j)<50)then
        vtemp=  (v**m)
        x = ((vtemp*k2)-1)
        r = exp(x)
        else
        write(*,*) 'out of voltage limits'
        end if
    end do
!!Compute the current values
i(v)=isc*(1-k1*(r))

!!Compute the power values
p(v)=i(v)*v

!!Write out computed values of Currents and Powers


END PROGRAM  Mathematicalmodel


!!Plot results.
!!The graphs of Current Vs Voltage i.e. I-V Curve
!!And the graph of Power Vs Voltage i.e. P-V Curve.
```

APPENDIX B2

C++ CODES OF THE MATHEMATICAL MODEL OF THE PV SYSTEM.

```
#include <stdio.h>

#pragma hdrstop
#include <condefs.h>
#include <iostream.h>
# include <complex.h>
#include <math.h>
//---------------------------------------------------------------------------
#pragma argsused

// This program runs the simulation of the mathematical model of a PV
// Generator using C++.
// This section defines att the constants as complex vectors
// the complex vectors in the transformation and multiplying factors.
int main(int argc, char* argv[])

{
   double K1;       // transformation factor
   double K2,K3,K4,m;  // multiplying factor
   double Vmpp,Voc;    // the voltage at maximum point and open circuit voltage
   double Impp,Isc;  // the current at maximum point and open circuit current

  // Assign values to the constants as provided in the manufacturers data sheet
   K1 = 0.01175;
   Vmpp = 35;
   Voc = 43.5;
   Impp = 3.14;
   Isc = 3.45;

   // Equations

   K4 = log((1 + K1)/K1);
   cout<<" The Value of K4 = "<<K4<<endl;

   double K3temp;
   // start solving for main Current equation
```

```
 // start solving for main Current equation
 K3temp =((Isc*(1 + K1)) - Impp);

 K3 = log((K3temp)/(K1*Isc));

 cout<<" The Value of K3 = "<<K3<<endl;

 double K3K4temp;
 K3K4temp = log(K3/K4);
 double Vmpptemp;
 Vmpptemp = log(Vmpp/Voc);

 m = (K3K4temp/Vmpptemp);

 cout<<" The Value of m = "<<m<<endl;

 K2 = K4/(pow(Voc,m));

 cout<<" The Value of K2 = "<<K2<<endl;

 //Declare voltage as an array and compute the corresponding values
 // of currents and power
 double *I;
 double *P;
 I = new double [100];
 P = new double [100];
 int v;  double Vtemp;  double expvalue=0;

 double result;
 double x = 0.0;


cout<<"The values of I are as follows"<<endl;
//start array iteration
 for (v=0; v<50; v++)
 {
     Vtemp = pow(v,m);
     x = ((Vtemp*K2) - 1);
     result = exp(x);
     //cout<<result;

       //cout<<result;
       I[v] = Isc*(1 - K1*(result));
       P[v] = I[v]*v;
       cout<<I[v]<<endl;
   }
   cout<<" The Power Values are as follows "<<endl;
   for (v=0; v<50; v++)
   {  cout<<P[v]<<endl;}




        getchar();
        return 0;
}

 //plot the value of current and power
```

APPENDIX C1

MATLAB M-FILES OF THE BATTERY DISCHARGE TESTS ON THE PV SYSTEM.

```
% battery discharge tests
clear;
clc
% battery discharge tests using a single unit of 12Ah battery
time=[0,5,10,15,20,25,30,35,40,45,50,55,60,65,70,75,80,85,90,95,100,105,110,115,120,125,1
v1=[12.23,12.21,12.19,12.16,12.15,12.13,12.12,12.10,12.08,12.06,12.04,12.02,12.01,12.00,1
i1=[10,10,10,10,10,9.91,9.91,9.91,9.81,9.81,9.81,9.81,9.76,9.76,9.76,9.71,9.71,9.71,9.61,
p1=[122.28,122.1,121.87,121.6,121.47,120.21,120.09,119.91,118.54,118.31,118.11,117.92,117
v2=[12.23,12.22,12.22,12.22,12.21,12.21,12.21,12.2,12.2,12.2,12.2,12.19,12.19,12.19,12.19,
i2=[10,10,10,10,10,9.91,9.91,9.91,9.81,9.81,9.81,9.81,9.76,9.76,9.76,9.71,9.71,9.71,9.61,
p2=[122.3,122.2,122.2,122.2,122.1,121.0,121.0,120.9,119.7,119.7,119.7,119.6,119.0,119.0,1

% battery discharge tests using a single Unit of 12Ah battery
plot(time,p1);
grid on
xlabel('time - min')
ylabel('power - watts')
title(' p-t graph')
figure

plot(time,v1);
grid on
xlabel('time - mins')
ylabel('voltage - volts')
title(' v-t graph')
figure

plot(time,i1);
grid on
xlabel('time - min')
ylabel('Current - Amps')
title(' I-t graph')
figure
% battery discharge tests using 10 Units of 12Ah connected in parallel
plot(time,p2);
grid on
xlabel('time - min')
ylabel('power - watts')
title(' p-t graph of 10 units of batteries')
figure

plot(time,v2);
grid on
xlabel('time - mins')
ylabel('voltage - volts')
title(' v-t graph of 10 units of batteries')
figure

plot(time,i2);
grid on
xlabel('time - min')
ylabel('Current - Amps')
title(' I-t graph of 10 units of batteries')
```

APPENDIX C2

MATLAB M-FILES OF THE MODELING OF THE PV SYSTEM WITH A LOAD.

```
% modelling the PVG with a load
clear
clc
pmpp=110;
% maximum power point of PV module power
vmpp=35;
%maximum power point of PV module voltage
%impp=pmpp./vmpp;
impp=3.14;
%maximum power point of PV module Current
isc=3.45;
% Short circuit current
voc=43.5;
%Open circuit Current
km=0.0621;
ki=0.386;
k=ki.*km;
b=0.00025;
ra=2.2;
flux=100;
%i= (isc.*(1-(c3.*(exp((c4.*(v.^m))-1))) );main Current equation for a Pv
%module
%because there would be five(5) unknowns in the equation, declare voltages
%(V) as array

v1= linspace(0,46.5);
% first voltage from PV module
v2= linspace(0.0009,42.8);
%second voltage from PV module
v3= linspace(0.0009,42.1);
%third voltage from PV module
v4= linspace(0.0009,41.3);
%fourth voltage from PV module
v5= linspace(0.0009,39.5);
% fifth voltage from PV module

% give values to all the constants in the main Current equation for a PV
% module

%c3=0.01175;
%c6=(log((1+c3)./c3) );
%c5=(log((isc.*(1+c3)-impp)./(c3.*isc)) );
%m=(log(c5./c6) ./log(vmpp./voc)    );
%c4=( (c6./(voc.^m)) );

% rewrite all constant evaluation equations in matlab format
```

```
c3=0.01;
%c6=real(log((1+c3)./c3) );
c6=4.46;
c5=real(log((isc.*(1+c3)-impp)./(c3.*isc)) );
m=real(log(c5./c6) ./log(vmpp./voc)   );
c4=real( (c6./(voc.^m)) );

% write main current equation in matlab format indicating the voltage as an
% array as stated above
% find the differnt values of currents at percentages ranging from 20 to
% 80%
i= real(isc.*(1-(c3.*(exp((c4.*(v1.^m))-1)))) );
i1=real((0.8.*i));
i2=real((0.6.*i));
i3=real((0.4.*i));
i4=real((0.2.*i));

% find the power generated by the PV
% note that power(P) = current(I) * Voltage (V)
%p=v*i
% find power in all corresponding five places just as solved above
p1=real(v1.*i);
p2=real(v2.*i);
p3=real(v3.*i);
p4=real(v4.*i);
p5=real(v5.*i);

%%%%%%%%%%%%%%%%%%%%%%%%%%%%%%%%%%%%%%%%%%%%%%%%%%%%%%%%%%%%
%t1=i.km*flux
t1=ki.*(i.^2);
t2=ki.*(i1.^2);
t3=ki.*(i2.^2);
t4=ki.*(i3.^2);
t5=ki.*(i4.^2);


%%%%%%%%%%%%%%%%%%%%%%%%%%%%%%%%%%%%%%%%%%%%%%%%%%%%%%%%%%%%
%w=(v1-ra*i)/k
w=(v1-ra*i)./km;
w1=(v2-ra*i1)./km;
w2=(v3-ra*i2)./km;
w3=(v4-ra*i3)./km;
w4=(v5-ra*i4)./km;

%Plot the Current-Voltage(I-V) curve of the solar cell
plot(v1,i,v2,i1,v3,i2,v4,i3,v5,i4);
```

```
AXIS([0 47 0 4])
grid on
xlabel('Solar Cell Generator Voltage - V')
ylabel('Solar cell Generator Current - I')
title(' I-V Characteristics of a Solar Cell')


%Plot the Power-Voltage (P-V) curve of the solar cell
figure
plot(v1,p1,v2,p2,v3,p3,v4,p4,v5,p5);
AXIS([0 50 0 125])
grid on
xlabel('Solar Cell Generator Voltage - V')
ylabel('Solar cell Generator Power - W')
title(' Power Relationship of Solar Cell')


%Plot the speed-torque (w-T) curve of the PVG coupled to a Universal
%motor
figure
plot(t1,w,t2,w1,t3,w2,t4,w3,t5,w4);
AXIS([0 5 0 1000])
grid on
xlabel('Electromagnetic Torque - T (N.m)')
ylabel('Speed- w (rad/sec)')
title(' Torque -Speed Curve of a Universal Motor driven by a PVG')
```

APPENDIX C3

MATLAB M-FILES OF THE DC AND AC EXCITATION TESTS ON THE PV SYSTEM.

```
% AC and DC Excitation tests for the PV System
clear;
clc

voltage=[0,0,0,50,60,70,80,90,100,110,120,130,140,150,160,170,180,190,200,210,220];
accurrent=[0,0,0,0.175,0.200,0.230,0.245,0.255,0.258,0.290,0.315,0.335,0.355,0.370,0.395,0
acspeed=[0,0,0,979,2065,3310,3495,4350,4780,5316,5841,6490,6860,7850,8250,8465,9680,10540,
acspeedradsec=[102.5339333,216.2743333,346.6673333,366.043,455.59,500.6253333,556.7624,611
dccurrent=[0.14,0.17,0.18,0.19,0.21,0.23,0.25,0.27,0.29,0.31,0.315,0.315,0.32,0.33,0.34,0.
dcspeed=[365,1650,2615,3645,4535,5504,5815,6005,6634,7056,8290,8874,9610,10319,10885,11351
dcspeedradsec=[38.22766667,172.81,273.8776667,381.753,474.9656667,576.4522667,609.0243333,
pvvoltage=[80,75,70,65,60,55,50,45,40,35,30];
pvcurrent=[0.29,0.25,0.23,0.23,0.225,0.22,0.21,0.2,0.19,0.15,0.14];
pvspeed=[6425,6001,5646,5135,4420,4020,3640,3220,2878,2165,1600];
pvspeedradsec=[672.9116667,628.5047333,591.3244,537.8056667,462.9213333,421.028,381.229333


plot(voltage,acspeed,'-',voltage,dcspeed,'-*');
grid on
xlabel('voltage - v')
ylabel('speed - rpm')
title('n-v graph')
figure
plot(voltage,accurrent,'-',voltage,dccurrent,'-*');
grid on
xlabel('voltage - volts')
ylabel('current - amps')
title(' Ac and Dc Currents-v graph')
figure

plot(pvvoltage,pvcurrent);
grid on
xlabel('voltage - v')
ylabel('pvcurrent - amps')
title(' n-v graph')
figure

plot(pvvoltage,pvspeed);
grid on
xlabel('voltage - v')
ylabel('pvspeed - rpm')
title(' PV n-v graph')
```

APPENDIX C4

MATLAB M-FILES OF THE OPTIMUM PERFORMANCE TESTS USING A 0.37KW INDUCTION MOTOR ON THE PV SYSTEM .

```
% Optimum performance tests using a 0.37kw induction motor
clear;
clc

Current=[2.05,1.8,1.65,1.50,1.35,1.25,1.15,1.05,0.85,0.75];
voltage=[220,210,200,190,180,170,160,150,140,130];
power=[195,170,150,130,115,100,90,80,73,65];
speed=[1500,1500,1500,1500,1500,1500,1500,1500,1450,1300];

plot(voltage,Current);
grid on
xlabel('Voltage - V')
ylabel('Current - Amps')
title(' I-V graph')
figure

plot(voltage,speed);
grid on
xlabel('Voltage - V')
ylabel('Speed - rpm')
title(' w-V graph')
figure
plot(voltage,power);
grid on
xlabel('Voltage - V')
ylabel('Power - Watts')
title(' P-V graph')
```

APPENDIX D

RESEARCH PUBLICATIONS.

Parts of this thesis have been presented at international and local conferences and journals. Some have been published already, while others are still awaiting review. They include the following;

i. M.M. Bello and I.E. Davidson, "Economic Analysis Of A Photovoltaic Fuel Cell Generator As A Power Supply System", *Proceedings of the 15th International Photovoltaic Science and Engineering Conference and Solar Energy Exhibition (PVSEC-15)*, Shanghai City, China, October 10 -15, pp. 275-276, 2005.

ii. M.M. Bello and I.E. Davidson, "Dynamics Of A PV-Powered Fractional Horsepower Motor", *Proceedings of the 2nd International Conference on Electrical and Electronics Engineering (ICEEE) and XI conference on Electrical Engineering (CIE 2005)*, Mexico City, Mexico, September 7-9, pp. 273-277, 2005.

iii. M.M. Bello and I.E. Davidson, "Spatial Modeling and Dynamics of a PV-Powered Fuel Cell Generator for Renewable Energy Application" *Proceedings of the IEEE-PES 2005 Inaugural Conference and Exposition in Africa*, Durban, South Africa, July 11-15, pp. 125-131, 2005.

iv. M.M. Bello and I.E. Davidson, "Photovoltaic Fuel Cell Generators: Economic Overview", *Proceedings of Electric Power 2006 Conference*, Atlanta, Georgia; U.S.A. May 2-4, 2006. **Paper accepted for publication.**

v. M.M. Bello and I.E. Davidson, "Performance Analysis Of A Photovoltaic System Coupled To A Universal Motor Using MATLAB Tool." *Proceedings of IEEE Power Engineering Society (PES) 2006 General Meeting*, Montréal, Quebec Canada, June 18 - 22, 2006. **Paper accepted for publication.**

vi. M.M. Bello and I.E. Davidson, "An Effective Load Management Control Of A Photovoltaic Fuel Cell Generator." *Proceedings of 41st International Universities Power Engineering Conference, UPEC 2006*, Newcastle-Upon-Tyne, United Kingdom, Sept 6-8, 2006. **Paper accepted for publication.**

vii. M.M. Bello and I.E. Davidson, "Performance Analysis Of A 550w, 220v VSD Fed From A PV-Generator Using MATLAB And DVF Tools.' *IEEE Transaction on Energy Conversion,* New Jersey, U. S.A, 2006. **Paper submitted for Review.**

viii. M.M. Bello and I.E. Davidson, "Life Cycle Costing and Economic analysis of a PVFC Generator." *ASCE Journal of Energy Engineering*, Reson, VA, U.S.A. 2006. **Paper submitted for Review.**

ix. M.M. Bello and I.E. Davidson, "Modeling and Dynamics of a standalone PVFC Generator" *Journal of Engineering, Design and Technology*, South Africa. 2006. **Paper submitted for Review.**

REFERENCES

[1] A. Pregelj, "Impact of Distributed Generation on Power Network Operation," Ph.D. thesis, School of Electrical and Computer Engineering, Georgia Institute of Technology, Atlanta, December, 2003.

[2] M. Kennedy, "Distributed Generation: harder than it looks," *IEE Power Engineer Journal*, Vol. 17, issue 1, pp. 8-9, February, 2003.

[3] D. Vincent, "A Low Carbon Trust," *IEE Power Engineer Journal*, Vol. 17, issue 3, pp. 37-39, June/ July, 2003.

[4] M. Newton, "Recent development of Sustainable development in the UK," *IEE Power Engineer Journal*, Vol. 17, issue 6, pp. 8-9, December/ January, 2003/04.

[5] A.M. Borbely and J.F. Kreider, "Distributed Generation, the paradigm for the new millennium," CRC Press, Florida, 2001.

[6] B.M. Jatzeck, "The Application Of The Luus-Jaakola Direct Search Method To The Optimization Of A Hybrid -Renewable Energy System," M.Sc. thesis, Dept of Electrical and Computer Engineering, University Of Alberta, Fall 2000.

[7] R. Karki, "Reliability and Cost Evaluation of Small Isolated Power Systems Containing Photovoltaic and Wind Energy," PhD thesis, Dept of Electrical Engineering, University of Saskatchewan, Saskatoon, Saskatchewan, Canada, April, 2000.

[8] L.G. Leslie, "Design and analysis of a grid connected photovoltaic generator system with active filtering function," M.Sc. thesis, Dept of EE, Polytechnic Institute and State University Virginia, USA. 2003.

[9] M. Gustafsson and N. Krantz "Voltage Collapse in Power Systems Analysis of Component Related Phenomena using a Power System Model," M.Sc thesis at the School of Electrical and Computer Engineering, Chalmers University of Technology, Göteborg, Sweden, Dec. 1995.

[10] J.N. Wolete "An Interactive Menu-Driven Design Tool For Stand-Alone photovoltaic Systems," M.Sc. thesis, Virginia Polytechnic Institute and State University Blacksburg, Virginia. January, 1998.

[11] D.C. Cherus, "Modeling, Simulation and performance analysis of a hybrid Power system for mobile medical clinic," Ph.D. thesis, Dept of Electrical Engineering, Universitat Kassel, Germany, June 2004.

[12] "Photovoltaics and Distributed Generation," Available in: http://www.fsec.ucf.edu/pvt/pvbasics/index.htm on 12th June, 2005

[13] A. Luque and S. Hegedus, "Handbook Of Photovoltaic Science And Engineering," John Wiley & Sons Ltd., 2002.

[14] P. Kay, P. Buttery, S. DeAngelis, W. Carwardine, S. Sheridan, and K. Siren, "The Feasibility Of Implementing A Solar Energy System On Environmental Studies Two. Ers 250," University of Waterloo, Canada, Autumn 2004.

[15] J.W. Twidell and A.D. Weir, "Renewable Energy Resources," University Press, Cambridge, 1990.

[16] J. Stoke, "Regression Analysis Program for the Characterization of Photovoltaic Devices," Fellowship Report, Colorado State University, National Renewable Energy Laboratory, Golden, Colorado, August 17, 2001.

[17] H. Schmidt, D.W. Sauer and H.G. Plus, "36 Cells For A Standard Module," In the *Proceedings of 2nd World Conference and Exhibition on PV Solar Energy Conversion,* Vienna, Austria, pp. 2203, 1998.

[18] Extract from "Postgraduate Distance Learning Series in Renewable Energy Systems Technology Solar Power Unit 7," CREST Publishers, United Kingdom, 2000.

[19] P.L. Auer, P.B. Bos, V.W. Roberts, and W.C. Gough, "Renewable Energy Resources-Unconventional Energy Resources," *World Energy Conference*, IPC Science and Technology Press, Surrey, pp. 35, 1978.

[20] J.H. Harker and J.R. Brackhurst, "Fuel and Energy" Academic Press Inc. London Ltd., pp. 216, 1981.

[21] E.S. Cassedy, "Prospects for sustainable Energy" Cambridge University press, pp. 53, 2000.

[22] Extract from "Photovoltaics: Basic design Principles and Components," Version; DOE/GO-10097-377 FS 231, New York, March 1997

[23] C.A. Vincent, "Modern Batteries: An Introduction to Electrochemical Power Sources," Edward Arnold (Publishers) Ltd., London, pp. 1, 1984.

[24] "Determining your solar power requirements and planning the number of components," Available in: www.solar4power.com/solar-power-sizing.html. On 14th March, 2005.

[25] Extract from "Photovoltaic Systems Design Manual," Canada Centre for Mineral and Energy Technology, March, 1989.

[26]. B.H. Chowdhury and S. Rahman, "Analysis Of Interrelationships Between Photovoltaic Power And Battery Storage For Electric Utility Load Management," *IEEE Transactions on Power Systems*, Vol. 3, No. 3, pp. 900 -907, August 1988.

[27] R. Messenger and J Ventre, "Photovoltaic Systems Engineering," CRC Press, 2000.

[28] S. Roberts, "Solar Electricity: A Practical Guide to Designing and Installing Small Photovoltaic Systems," Prentice Hall, NJ, 1991.

[29] W. S. Fyfe, M. A. Powell, B. R. Hart and B. Ratanasthien, "A Global Crisis: Energy in the Future, Nonrenewable Resources," pp. 187-195, 1993.

[30] Extract from "Fuel Cell Handbook (Fifth Edition)," EG&G Services Parsons, Inc. Science Applications International Corporation, United States Dept. of Energy, Virginia. October, 2000.

[31] Shell, SM 110-24 product data sheet and manufacturers manual, Available in: http://www.alternative-power.ca/products/Solar%20Modules/Shell/SM110-24.pdf on 14th February, 2005.

[32] P.C Sen, "Principles of Electric Machines and Power Electronics," John Wiley & Sons, New York, Second Edition, January, 1989.

[33] M.H Rashid, "Power Electronics: Circuits, Devices and Applications," Prentice Hall, Englewood Cliffs, 1988.

[34] N Mohan, "Power Electronics: Converters, Applications and Design," John Wiley and Sons, Inc. Second Edition, January, 1995.

[35] J. Vithayathil, "Power Electronics: Principles and Applications," McGraw – Hill, Inc. 1995.

[36] M.R Vervaart, F.D.J Nieuwenhout, "Manual for the Design and Modification of Solar home System Components," ECN – Netherlands Energy Research Foundation Petten, The Netherlands, 1998.

[37] Designer Heat Sinks, Electronics World, pp. 1036 – 1037, December 1997.

[38] I.E. Davidson, "Spatial Modelling Of A Photovoltaic Fuel-Cell Generator For Localised Load Management," University of KwaZulu-Natal, Durban, South Africa, Eskom Research Project Proposal Report, Vol. 9, Project Code: 11003799, April, 2004.

[39] J. Appelbaum and J. Bany, "Performance analysis of a DC Motor photovoltaic Converter System-I-Separately excited motor," *Solar Energy Magazine*, Vol. 22, pp. 439-445, 1979.

[40] J. Appelbaum, "Staring and Steady State Characteristics of DC Motors powered by Solar Cell Generators," *IEEE Transactions on Energy Conversion*, Vol.EC-1, No. 1, pp. 17-25, March 1986.

[41] S. Rauschenbach, "Solar Cell Array Design Handbook," Van Nostrand Reinhold Company, pp 55-59, 1980.

[42] C.E. Backus, "Solar Cells," IEEE Press Inc. New York, 1976

[43] S.W. Augrist, "Direct Energy Conversion," 3rd Edition, Allyn and Bacon, Boston, 1976.

[44] M.A.Green, "Solar Cells-Operating Principles, Technology and Systems applications," Prentice Hall Inc., Englewood Cliffs, N.J. 07632, 1982.

[45] S. Rahman, M.A. Khallat, "A Probabilistic approach to Photovoltaic Generator performance Prediction," *IEEE Transactions On Energy Conversion*, Vol. EC-1, **No.** 3 pp. 34-40, Sept., 1986.

[46] A. Hoque, "A Methodology for Analyzing Electrical Energy Options for Isolated Areas," Ph.D. Thesis, (Chapter 6 & 7), Dept. EEE, BUET, Dhaka, Bangladesh, 1990.

[47] M.M. Bello and I.E. Davidson, "Dynamics Of A PV-Powered Fractional Horsepower Motor," in the *Proceedings of the 2nd International Conference on Electrical and Electronics Engineering (ICEEE) and XI conference on Electrical Engineering (CIE 2005)*, Mexico City, Mexico, pp 273-277, September 7-9, 2005.

[48] J. A. Gow and C. D. Manning "Development of a photovoltaic array model for use in power electronics simulation studies," *IEE Proceedings on Electric Power Applications*, vol. 146, no. 2, pp. 193-200, March 1999.

[49] R.P. Mukund, "Wind and Solar Power Systems," CRC Press, 1999.

[50] MathWorks. (2001). Introduction to MATLAB. The MathWorks, Inc. Available in: http://www.mathworks.com/access/helpdesk/help/techdoc/learn_MATLAB/ch1intro.shtml#12671. on 18th August, 2001

[51] D.M Etter, "Introduction to MATLAB for Engineers and Scientists," Prentice-Hall, Inc., 1996.

[52] J.H. Mathews and K.D. Fink, "Numerical Methods: Using MATLAB: (International Edition), Fourth Edition," Pearson Education Pearson Shared Services UK and International, 2004.

[53] M. Etzel and K. Dickinson, "Digital Visual Fortran programmer's guide.", Butterworth-Heinemann, 1999.

[54] Compaq Fortran: Language reference manual, Digital equipment Corporation, Sept., 1999.

[55] D.M Etter, "Introduction to C++ for Engineers and Scientists.", Prentice-Hall, Inc., 1996.

[56] D. Brendt, "Maintenance free batteries-A Handbook of battery technology," John Wiley & Sons, Chichester, UK, 1993.

[57] S. McCarthy, A. Kovach and G. Wrixon, " Operational Experience with batteries in the 16PV Pilot Plants," in the *proceedings of 9th European Photovoltaic Solar Energy Conference*, Freiburg, Germany, pp. 1142-1145, 1989.

[58] "Universal Motors," Available in : http://www.freescale.com/webapp/sps/site/overview.jsp?nodeId=02nQXGrrlPbFqM&tid=tMfp on 12th Sept., 2005.

[59] I.E. Davidson, "Performance Analysis of a Fractional Horse power Universal Motor," In the *Proceedings of 7th IEEE Africon Conference*, pp. 1179 – 1184, 15-17 Sept, 2004,

[60] Data sheet of "Banshee 85, 220V, 0.6A universal motor," .

[61] I.E. Davidson, "Spatial Modelling Of A Photovoltaic Fuel-Cell Generator For Localised Load Management," University of KwaZulu-Natal, Durban, South Africa, Eskom Research Project Proposal Report, Vol. 9, Project Code: 11003799, April, 2004.

[62] K. Agbossuo, J.Hamelin, A. Laperriere, & F. Laurencelle, "Load commutation for stand alone wind and PV hydrogen energy system," in the *Proceedings of Canadian conference of electrical and computer engineering (CCECE)*, pp. 555-558, January, 2000.

[63] L.M Leander and J.D. Morgan, "Electromagnetic and Electromechanical machines," John Wiley & Sons, pp. 404-405, 1987.

[64] "Standby Service to Distributed Generation Projects: The Wrong Tools for Subsidies," the *Electricity Journal*, Elsevier Inc., 1040-6190, pp. 85-92, 2003.

[65] R.A. Bruns and R.M. Saunders, "Analysis of Feedback control systems: Servomechanisms and Automatic regulators," New York, McGraw-Hill,1955.

[66] J.A. Edminister and M.Nahvi, "Schaum's series outline of theory and problems of Electric Circuits," The Mc-Graw Hill Companies Inc., pp. 42-43, 1997.

[67] Maximum Power Trackers, Available in: http://www.windsun.com/ChargeControls/PPT.htm on 19th February, 2005.

[68] What is Maximum power tracking and how does it work? Available in: http://www.blueskyenergyinc.com/pdf/Blue%20Sky_What%20is%20MPPT.pdf on 19th October, 2005.

[69] How Maximum power trackers work. Available in: http://www.aesltd.com.au/whatwedo/docs/mppt.htm. on 17th April, 2005.

[70] D. Shmilovitz, "On the control of photovoltaic maximum power point tracker via output parameters," *IEE Proceedings of Electric Power Applications*, Vol. 152. Issue 2, pp. 239-248, March, 2005.

[71] D. Shmilovitz, "Time variable transformers operating at near unity transfer ratio and some possible applications," *IEE Trans. on Power applications*, vol. 151, issue 2, pp. 161-168, March 2004.

[72] R. W. Newcomb, "The Semistate Description of non linear Time-Variable Circuits," *IEEE Trans. Circuits and systems*, vol. 28, pp. 62-71, Feb. 1981.

[73] D. Shmilovitz, "Maximum Power Points: Converters and Control," Seminar presented at Tel Avil University, Israel, 2005, unpublished

[74] M.M. Bello and I. E Davidson, "Spatial Modeling and Dynamics of a PV-Powered Fuel Cell Generator for Renewable Energy Applicationr". In the *Proceedings of the Inaugural IEEE-PES Conference and Exposition in Africa*, Durban, South Africa, pp. 125-131, 11-15 July 2005.

[75] International Energy Agency, "Photovoltaic Power Systems: Guidelines for Economic Evaluation," Report of the International Energy Agency, IEA PVPS T7-05:2002, pp. 3-49

[76] IEA Coal Clean Centre, Coal full Cycles Analysis, Available in: http://www.iea-coal.org.uk/templates/ieaccc/report_detail.asp?LogDocId=81332&PageId=323 on 12th Sept.,2005.

[77] Frankl, P., A. Masini, M. Gamberale, and D. Toccaceli. "Simplified life-cycle analysis of pv systems in buildings – present situation and future trends," Progress in Photovoltaics: Research and Applications 6(2), pp. 137-146. 1998.

[78] V.M. Fthenakis, E.A. Alsema, and M.J. de Wild-Scholten, "Life Cycle Assessment Of Photovoltaics: Perceptions, Needs, And Challenges," in the *Proceedings of 31st IEEE Photovoltaic Specialists Conference*, Orlando, FL. Jan. 3-7, 2005.

[79] S.B. Riffat, S.A. Omer and R. Wison., "Monitoring PV systems at the centre for renewable energy and eco-energy house," University of Nottingham, 2001

[80] A.Baumann, and R. Hill, "Environmental Effects of Energy Sources," in the *Proceedings of 10th EC Photovoltaic Solar Energy Conference*, Kleuwer, Dordrecht, pp. 834-837, 1991.

[81] R. Kaiser , D.U. Sauer, A. Armbruster, G. Bopp, H.-G. Puls, "New Concepts for System Design and Operation Control of Photovoltaic Systems," In the *Proceedings of 14th European Photovoltaic Solar Energy Conference*, Barcelona, June, 1997

[82] J. Paatero, T. Sevòn, A. Lehtolainen and P. Lund, "Distributed Power System Topology and Control Studies by Numerical Simulation," in the *Proceedings of Second International Symposium on Distributed Generation: Power System and Market Aspects* Stockholm, October 2002.

[83] M. Thomas and H. Post, "Economic Analysis Of Pv Hybrid Power System: Pinnacles National Monument," In the *Proceedings of the 26th IEEE Photovoltaic Specialists Conference*, Anaheim, California. September 29-October 3, 1997.

[84] J. Byrne, B. Shen and W. Wallace, "The Economics of Sustainable Energy for Rural Development: A Study of Renewable Energy in Rural China," Published in the *Energy Policy Magazine*, Vol.26 (1) pp. 45-54, 1998.

[85] M.M. Bello and I.E. Davidson, "Economic analysis of a photovoltaic fuel cell generator as a power supply system," in the *Proceedings of the 15th International*

Photovoltaic Science and Engineering Conference and Solar Energy Exhibition (PVSEC-15), Shanghai City, China, pp. 275-276, October 10-15, 2005.

[86] "Electricity Demand and Generation," Available in: http://www.med.govt.nz/ers/electric/fossilfuel/fossilfuel-12.html#P587_19410 on 20th November, 2005;

[87] "Comparative Costs Of Electricity Generation: A Canadian Perspective," Available in: http://www2.nrcan.gc.ca/es/erb/erb/english/View.asp?x=454&oid=779#1 on 19th Nov., 2005;

[88] "UK Policy Report," Available in: http://www.raeng.org.uk/policy/pdfs/ResponseV3.pdf on 20th Nov., 2005

[89] A. Dennis and A Kulsum, "The Case for Solar Energy Investments", World Bank technical paper, WTP 279. *Energy Serie,* 2002.

[90] The OECD/ IEA NEA 2005 technical paper, "Projected Costs of Generating Electricity- update", October 2005.

[91] "Prospects for Distributed Electricity Generation," Available on: http://www.cbo.gov/ftpdoc.cfm?index=4552&type=1 On 7th October 2005.

[92] "IPRO Project, Solar Sign," Available in: http://www.iit.edu/~ipro301f04/dist/description.html on 16th March, 2005.

[93] S. Rahman and M.A. Khallat, "A Model For Capacity Credit Evaluation Of Grid-Connected Photovoltaic Systems With Fuel Cell Support.", *IEEE Transactions On Power Systems*, Vol. 3, No. 3, pp. 1270-1276, August 1988.

[94] R. Acker and D.M. Kammen, "The quiet (Energy) revolution: the diffusion of photovoltaic power systems in Kenya," *Energy Policy*, 24, pp. 81-111, 1996

[95] C.E. Mortimer, "Chemistry: A Conceptual approach," Second edition, D. Van Nostrand Company, New York, 1971.

[96] J. Amann et al., Produkte mit integrierter photovoltaischer Energieversorgung, BMBFStatusseminar Photovoltaik, Bad Breisig, pp. 23.-25, April, 1996.

[97] W. Roth, H. Lemmel, "Elektronik Fachzeitschrift f¨ur industrielle Anwender und Entwickler," pp. 43-20, 1996

[98] G. Foley, "Electricity for Rural People," Panos Publication Ltd., London N1 9PD, UK 1990.

[99] G. Foley, "Photovoltaic Applications in Rural Areas of the Developing World," World Bank Technical Paper, Number 304, 1995.

[100] N. Pfanner, W. Roth and A. Steinh¨user, "Application of Photovoltaics in the Stationary Sector of Road Traffic," in the *Proceedings of 12th European PV Solar Energy Conference*, Amsterdam, pp. 11-15, April 1995.

[101] B. Wiengmoon, R. Wattanapong, O. Parodi and E. Wiemken, "PV-Battery Charging in the Huay Dua Village, Thailand," in the *proceedings of South-East Asia PV Conference* Phuket, Thailand, 1997.

[102] W. Roth and H. Schmidt, "PV Systems, Seminar Handbook," Fraunhofer ISE, Freiburg, Germany , 1995.

[103] O. Parodi, M. Preikschat and K. Preiser, "PV Contra Coli-Bacteria – Suitability of UV-Water Purifi-cation Devices for PV Systems," in the *Proceedings of 14th EU PV Solar Energy Conference* , Barcelona, Spain, 1997.

[104] Erge Th et al., "The German 1000-Roofs-PV-Programme – a R´esum´ee of the 5 Years Pioneer Project for Small Grid-Connected PV Systems," in the *Proceedings of 2nd World Conference and Exhibition on Solar Energy Conversion,* Wien, ¨ Osterreich, pp. 2649-2651, 6^{th} -10^{th} July,1998.

[105] W. Heydenreich, E. Wiemken, H. Gabler and K. Kiefer, "Correlation Between Photovoltaic Energy Production and Household Electricity Consumption – Evaluation of Data from the German Thousand Roofs Programme," in the *Proceedings of EuroSun '96,* Freiburg, Germany, 1996.

[106] T.H. Erge, K. Kiefer and V. Hoffmann , *Solar Energy Journal.* Vol **70 No.** 6,pp. 479–487, 2001.